THE INFLUENCE OF THE RANDOM METAL CUTTING FORCES ON THE FORMATION OF SURFACE TEXTURE IN FINISH TURNING

by

Ajit Kumar Rakhit

A THESIS

IN THE

FACULTY OF ENGINEERING

Presented in Partial Fulfillment of the Requirements

for the

Degree of DOCTOR OF ENGINEERING

at

Sir George Williams University

Montreal, Canada

January, 1974

ABSTRACT

A new approach for the assessment of a machined surface is presented on the reasoning that the surface is formed by the superposition of i) a theoretical or basic profile which results due to the operation kinematics of the machine tool system and ii) a random or fundamental roughness caused by the relative vibrations between the cutting edge and the workpiece.

To determine the response of the machine tool system, the equations of motion are formulated by considering the machine tool as a two degree-of-freedom system, being excited by the randomly varying metal cutting forces. The excitation is accounted for in the form of an equivalent white noise spectral density of the cutting forces experienced by the machine tool under specific cutting conditions. An analytical expression for the response of the tool is obtained from the stationary solution of the probabilistic equations which describe the mean square response of the system. Using the root mean square value, RMS, as a measure of surface roughness amplitudes, an expression is derived to estimate the CLA-value of the surface roughness of the machined component.

A series of tests was performed for a finish turning operation in which the random cutting forces and the corresponding surface roughness of the workpiece were measured, recorded

and analyzed. Results indicate close agreement between the CLA-values of the measured and computed surface roughnesses.

To establish direct relationships between the stochastic characteristics of the cutting forces and surface texture produced, the recorded signals were processed through a sequence of computer programs and various excursion parameters such as mean crest excursion, root mean square crest excursion, etc., about pre-selected levels from the CLA-value were computed. For the values of the probabilistic parameters of the forces and surfaces which are of significance in finish turning, the results indicate that the inter-relationships could be approximated to linear relationships. From these relationships, it may be possible to estimate the quality of the surface finish from the cutting conditions employed.

Finally, it is proposed that a library of information be established on the cutting force fluctuation characteristics with the corresponding surface roughness parameters for all cutting conditions and workpiece materials through exhaustive tests similar to the one presented in this investigation. A quantitative analysis of this information will lead to a set of graphs from which it could be possible to estimate the quality of the surface from the cutting conditions for different workpiece materials.

ACKNOWLEDGEMENTS

The author wishes to express his gratitude and deep appreciation to his thesis supervisors, Dr. T.S. Sankar and Dr. M.O.M. Osman, for initiating the project and providing continued guidance throughout the investigation.

The author gratefully acknowledges the National Research Council of Canada for the Post-Industrial Experience Research Fellowship, held during the tenure of this investigation. The financial support of the National Research Council, grants numbers A7104 and A5181, and La Formation de Chercheurs et d'Action Concertée of the Government of Quebec, grant number 242-110, is also acknowledged.

TABLE OF CONTENTS

LIST OF FIGURES

LIST OF TABLES

NOMENCLATURE

a	length of the workpiece
a_n, b_n	coefficients
AMS or η'	absolute mean slope of surface texture
AWL	average wave length
B	gain setting on the charge amplifier
C_i, C_e	internal and external viscous damping coefficients
CLA	center line average
D_{ij}	algebraic co-factor of determinant D
E [ ]	ensemble average
EI	equivalent rigidity of the spindle-workpiece unit
E-system	envelope reference profile
h	chip thickness
$H_1(j\omega)$	complex frequency response function of the workpiece
$H_2(j\omega)$	complex frequency response function of the spindle
$H_1^*(j\omega)$	complex conjugate of $H_1(j\omega)$
$H_2^*(j\omega)$	complex conjugate of $H_2(j\omega)$
k	constant that depends on the elasto-plastic deformation properties of the workpiece material
K_{ij}	correlation coefficient for the random function Y(X) at x_i and x_j
k_s	static stiffness of the machine tool system

l	length of the spindle
L	sampling length
m_1, m_2	lumped masses of the workpiece and spindle respectively
M-system	mean-line reference profile
MCE	mean crest excursion
MVE	mean valley excursion
n	number of data-points
n	numeral
N_c	number of crossings per unit length
$p_c(\lambda)$	probability density of crest excursions
$p_v(\Lambda)$	probability density of valley excursions
$p_1(t)$	random cutting force
$p_1(j\omega)$	complex random cutting force in the frequency domain
P_o	steady state cutting force
P(t)	cutting force
Q	the charge in pico-Coulomb
r	tool nose radius
RMS or σ	root mean square value
RMSCE	root mean square value of crest excursions
RMSS or σ'	root mean square value of the slope Y'(X)
RMSVE	root mean square value of valley excursions
s	depth of cut
s	Laplace Transform variable
S	cutting feed

S_o	constant power spectral density of the exciting force under white noise idealization
$S_x(\omega)$	power spectral density of the response of the workpiece
$S_y(\omega)$	power spectral density of the response of the spindle
$S_z(\omega)$	power spectral density of the exciting force $p_1(t)$
U_1	theoretical surface profile
U_2	the fundamental surface profile
v	cutting speed
V	the voltage reading on oscilloscope
W	total surface profile
X	lengthwise directional coordinate
$x, \dot{x}, \ddot{x}$	amplitude, velocity and acceleration of the workpiece in the principal mode
$x(j\omega)$	response of the workpiece in the frequency domain
$\bar{Y}$	average of Y_i, $i = 1...n$
$y, \dot{y}, \ddot{y}$	amplitude, velocity and acceleration of the spindle in the principal mode
$y(j\omega)$	response of the spindle in frequency domain
$Y(X)$	function of the signal reproduced by a measurement of a surface
$Y'(X)$	slope of the function $Y(X)$
Y_1	pre-selected crossing level measured from the mean line equal to (CLA)
α	clearance angle
$\alpha_{11}, \alpha_{12}, \alpha_{21}$	influence coefficients
β	wedge angle
ϕ	shear angle
χ	approach angle

γ	rake angle
$\Delta\lambda$	increment of λ
ϵ	uncut minimum depth of cut or tool nose angle
ϵ_e	uncut depth of cut due to elastic deformation of workpiece material
ϵ_p	uncut depth of cut due to plastic deformation of workpiece material
ζ	damping factor
λ	duration of excursion
λ_f	CLA-value of the random profile
λ_{mes}	CLA-value of the surface profile measured after cutting tests
λ_{Th}	CLA-value of the theoretical surface profile
λ_{Tot}	CLA-value of the total surface profile
Λ	interval between excursions
ν	multiplication factor to determine crest calculation level in terms of CLA value
ρ	cutting edge radius
σ_l	variance of the slope of random profile
σ_f	RMS-value of the random profile
σ_{Th}	RMS-value of the theoretical profile
σ_{Tot}	RMS-value of the total surface profile
σ^2	variance
ω_l	critical frequency of the machine tool system
$(\ )_F$	parameter corresponding to cutting force
$(\ )_S$	parameter corresponding to surface

CHAPTER 1

INTRODUCTION

CHAPTER 1

INTRODUCTION

Vibrations arise in all metal cutting operations and are undesirable especially from the viewpoints of surface finish and dimensional accuracy of the manufactured component. The formation of surface texture depends on the vibratory response of the tool which in turn depends on the nature of the metal cutting forces.

1.1 Review of Previous Work

A considerable amount of research has been published on the analysis of the effect of vibrations on the machine tool system as well as on the quality of the finished product. Most of the researchers developed mathematical models of the machine tool system under self-excited and forced vibrations, and established stability criteria in terms of the rotational frequency. These models [1-6] consider deterministic equations of motion of the system with a harmonic cutting force excitation. With such deterministic models it is only possible to investigate phenomena like chatter instability during a rough machining operation, where maximum metal removal rate is of prime importance. On the other hand, the quality of surface finish and dimensional accuracy are the major objectives in a finish machining operation, which is characterized by low feed rates and high cutting speeds. Therefore it is essential to

analyze the vibrations of the system during finish machining, which in turn depend on the stability of the spindle-workpiece system.

Although very little research has been carried out on the stability of machine tool spindle systems under finish machining conditions, there has been a good deal of work done on the stability of symmetrical and unsymmetrical rotating shafts by a number of authors [7, 8, 9]. The information available from these research works can be effectively utilized in determining the stability and response of a machine tool spindle system under finishing operations. Presentation of a complete survey of all such research papers would be a major undertaking and hence, only those papers which are considered extremely relevant to the present investigation are mentioned. Most of the authors are of the opinion that the instability of transverse motion of symmetrical shafts can occur, in the absence of internal damping, only at certain speeds of rotation, whereas instability can occur in the case of unsymmetrical shafts for a whole range of speeds. It was suggested by Kimball and Newkirk [10] that the internal friction might be caused by elastic hysteresis which would act as a damping force rotating with the shaft. Later, Robertson [11] summarized the causes of vibrations in rotating shafts in a series of theoretical and experimental investigations. In particular, he challenged the concept of the viscous law of internal friction, discarding it in favour

of a law by which damping forces were a function of the change of strain. It may be noted that such a treatment of hysteretic forces gives a better explanation of known experimental results. But neither Robertson's nor those involving rotating viscous damping is exact and such refinement of the mathematical model is not always essential. It may be worthwhile to consider the rotating viscous damping of the spindle under certain conditions and is utilized in the present investigation.

In all the above mentioned papers, self-induced vibrations of the rotating shafts were studied and the stability boundary is defined in terms of the ratio of external damping of the system to the internal damping of the rotating shaft. Over and above the causes of vibrations in a rotating shaft, the dynamic analysis of the machine tool spindle system should include the effect of external excitation due to the fluctuation of the metal cutting forces during the finishing operation. C. Bagci [12] used matrix method to solve torsional, coupled torsional and lateral vibrations of shafts. In this approach, lumped mass parameter system is employed and a digital computer technique is developed to determine the natural frequencies of the system.

The probabilistic approach for analyzing the machine tool vibrations is very recent. In fact, it is only after Bickel [13] and Field [14] had recognized the stochastic nature of

the metal cutting forces that attention is now focussed on such approaches. A better understanding of the vibratory response of the machine tool system could be obtained only if the cutting force variations are represented stochastically in the equations of motion of the system. However, the justification for such an improved model will depend upon the degree of randomness of the cutting forces which, in turn, depend on the type of machining operation such as rough turning, finish turning, milling, grinding, etc. The results obtained by Bickel [13] show that the degree of randomness could be as high as 30% of the steady state cutting force. For finish turning and grinding operation a degree of randomness as low as 10% could produce a detrimental effect on the surface texture of the manufactured component. Peklenik and Kwiatkowski [15] attributed the following reasons for such random fluctuations of the cutting forces:

1) Non-homogenous properties of the workpiece material,
2) Randomness of workpiece input dimensions, and
3) Irregular machine structural properties.

Although techniques exist for determining the response of a generalized system under random exciting forces, there has been no significant attempt to utilize these theories in the field of machine tool dynamics. Caughey and Stumpf [16] introduced techniques for obtaining the transient solution of a

single degree-of-freedom system when excited by random forcing functions. A similar paper had been published by Hu [17]. The approach of these investigators may be adopted to solve the differential equation of motion of a machine tool system provided it can be modeled as a single degree-of-freedom system.

Bhandari and Sherer [18] solved both single and two degree-of-freedom systems for random excitation using the Fokker-Planck approach. In their two degree-of-freedom system model, the forcing functions are arranged in such a way that there was no coupling in the equations of motion whereas in most physical phenomena it is usually found that the forcing functions are coupled. For example, a force applied to the mass of a system may not produce pure translatory motion. A small eccentricity might result in a torque in addition. Such is the nature of the cutting forces on a machine tool system and the investigation of the dynamics of the system is more complicated than the method shown by these authors.

Very recently, Sankar and Osman [19] published a qualitative paper on the flexural stability of a machine tool spindle under randomly fluctuating cutting forces. In their analysis, they assumed that the torsional forces acting on the spindle were constant and the components of the cutting force affected only the flexural stability of the spindle. Thus, they were able to reduce the system to an equivalent single degree-of-

-freedom and then analyzed the stability using the Fokker-Planck technique.

To find the response of a machine tool during finishing operation it is necessary to consider the spindle and workpiece as an integral unit. The cutting forces acting on a workpiece will have an influence on the machine spindle, thereby introducing at least two degree -of-freedom system in the mathematical model. Such an approach is presented in this investigation. Roberts [20] reported a method of obtaining the response of linear vibratory system to random impulses. In his opinion such a method can be successfully utilized to find the response of a linear system for continuous excitation provided the time interval between two impulses is sufficiently small.

Kwiatkowski and Bennett [21] used the correlation technique to determine the machine tool receptance. This technique as described fulfills the requirement of a quick test but it is no better in achieving realistic test results than the frequency response method, due to noise neutralization by time averaging. Osman and Sankar [22] developed a short-time acceptance test for machine tools where the dynamic response of the machine-tool-workpiece system under random cutting forces was utilized to determine the dynamic stiffness of the machine tool.

1.2 Limitations of Analytical Approach

To establish a valid stochastic model for a machining

process like finish turning and grinding, it is necessary that complete statistical characteristics of the cutting forces, that cause the random vibrations of the components of the machine tool, are available. Such stochastic representation of the cutting forces can be obtained only through a number of exhaustive tests under all possible cutting conditions. From the analysis of the experimental records of the cutting force signals, idealization could then be attempted to represent the random cutting forces in the mathematical model as stationary or non-stationary, Gaussian or non-Gaussian, broad or narrow band process.

Even if the machine tool system with its cutting forces was represented by an acceptable mathematical model in terms of a probabilistic differential equation, the determination of the solutions for the response process will depend upon the degrees of freedom, degree of linearity and modes of vibration of the system. Further, the exact representation of the stiffness, internal and external damping of the system in the mathematical model are difficult because such characteristics are influenced by the principal modes of vibrations and would require elaborate experimental investigations. Hence, a comprehensive solution for such a model to give all necessary responses will be difficult.

The vibratory response of a machine tool system is of interest for two reasons. First, it determines the functional

constraints of the machine tool such as stability and secondly, it contains information on the quality of surface texture of the machined component. The investigation reported here deals only with the latter aspect of the problem. The relation between the vibratory response of the tool tip and the amplitude fluctuations of the surface produced is not exactly known because of the various unknown quantities such as elasto-plastic flow of the chip, interface temperature distribution, the relevant thermodynamic process involved, etc. Therefore, to establish, purely through analytical reasoning, the characteristics of the surface texture from the knowledge of the response of the machine tool system, which in turn is dictated by the random fluctuations of the cutting forces, is an extremely complex problem. But, if through detailed experimentation probabilistic data on the cutting force fluctuations were obtained for a wide range of cutting conditions and the statistical characteristics of the corresponding surface texture were evaluated, then it might be possible to establish at least some empirical relations between the cutting conditions and the expected surface texture. Such empirical relationships are presented in this thesis for a finish turning operation.

1.3 Scope of the Research Work

The purpose of this investigation is to present a limited analytical investigation and supplementary experimental evidence

on the stochastic characteristics of the cutting forces in finish turning and the parameters describing the resulting surface roughness. With this information, it would be possible to relate directly the major probabilistic parameters of the surface to the corresponding cutting force descriptions or the cutting conditions that would produce such cutting forces. The aim of such a procedure will be to make available, eventually, a library of information on cutting forces under all cutting conditions for different machining processes with parametric description of the surfaces produced from which empirical relations could result for estimating the surface texture directly from the given cutting conditions during a particular machining operation. In other words, it would be possible to specify the controllable variables of the machine tool such as feed rates, speed for a particular material and the machining process (turning, milling, grinding, etc.) to obtain the required quality of the surface finish.

In Chapter 2, the mechanism of the formation of the surface texture is described. Then a critical review of the existing surface description methods is presented and an improved method of surface texture description is proposed.

The mathematical model of the machine-tool-workpiece system is formulated in Chapter 3, by taking into account the following features:

a) randomness of the cutting forces,

b) axial symmetry of the bearings,

c) absence of any unbalance in the spindle,

d) bearings exhibiting viscous damping properties, and

e) viscous damping properties at the cutting zone.

The analytical expressions for the random response of the tool-workpiece-system and spindle are obtained from the stationary solution of the probabilistic equations and are outlinde in Chapter 3. Using internationally accepted parameter RMS (root mean square of surface irregularities) as a measure of surface texture, an expression is formulated to describe the random or fundamental roughness of the surface using the response characteristics of the system.

In Chapter 4, a procedure is described to assess a surface texture from the cutting conditions and the RMS-value of the tool-workpiece response.

Experimental investigations are presented in Chapter 5 for turning operation with specific cutting conditions. The cutting forces and surface roughness profiles were measured and recorded using commercially available laboratory equipment. The viscous damping coefficient of the machine tool system is then determined from the frequency response test.

The recorded signals were then processed and analyzed to determine the frequency spectrum, spectral density and

probability density of the cutting forces and surface roughnesses as described in Chapter 6. A computational procedure for the CLA-value of the surface is also presented in this chapter.

Experimental investigations are presented in Chapter 7 for estimation of surface roughness parameters from the cutting force fluctuation characteristics. From the results of the investigations, correlations are then established between the cutting force fluctuation characteristics and the corresponding surface roughness parameters. For a lengthwise correlation, the analog signals of the cutting forces and surface roughnesses were converted to a set of discrete data points by a sequence of computer programs. These data points are analyzed to calculate the various statistical parameters such as mean crest excursion, RMS-value of crest excursions, average wave length of the profiles, etc. With the help of these parameters, relationships between the cutting force and the surface roughness characteristics are established through a set of plots.

Investigations reported also contain the effect of cutting speed and tool wear on the cutting force and surface roughness characteristics. Results show that the cutting speed and tool wear do not have any appreciable effect on these characteristics as indicated in Chapter 8.

Finally, discussion of the results, conclusion and recommendations for future work are presented in Chapter 9.

CHAPTER 2

SURFACE TEXTURE IN METAL MACHINING

CHAPTER 2

SURFACE TEXTURE IN METAL MACHINING

2.1 Formation of a Surface Texture in Metal Cutting

In any metal removal process, a surface profile is produced on the workpiece after each cut. The texture that remains on the workpiece surface at the end of the final cut is known as the surface texture of the manufactured component The cutting conditions that are employed during this final cut are of special nature for a finishing operation and are usually characterized by low feed rate, high cutting speed and small depth of cut.

In the present investigation, the surface texture that is formed during a finishing operation is of interest. Surface texture obtained by finish machining consists of two distinct components —

a) a theoretical or basic roughness and

b) a random or fundamental roughness superimposed over the theoretical roughness.

The theoretical roughness is formed due to the operation kinematics of the machine, such as feed, tool geometry, etc. and is shown in Figure 2.1. The random roughness is primarily caused by the relative vibration between the tool and the workpiece which in turn depends on the randomly fluctuating metal cutting forces. The formation of the random roughness

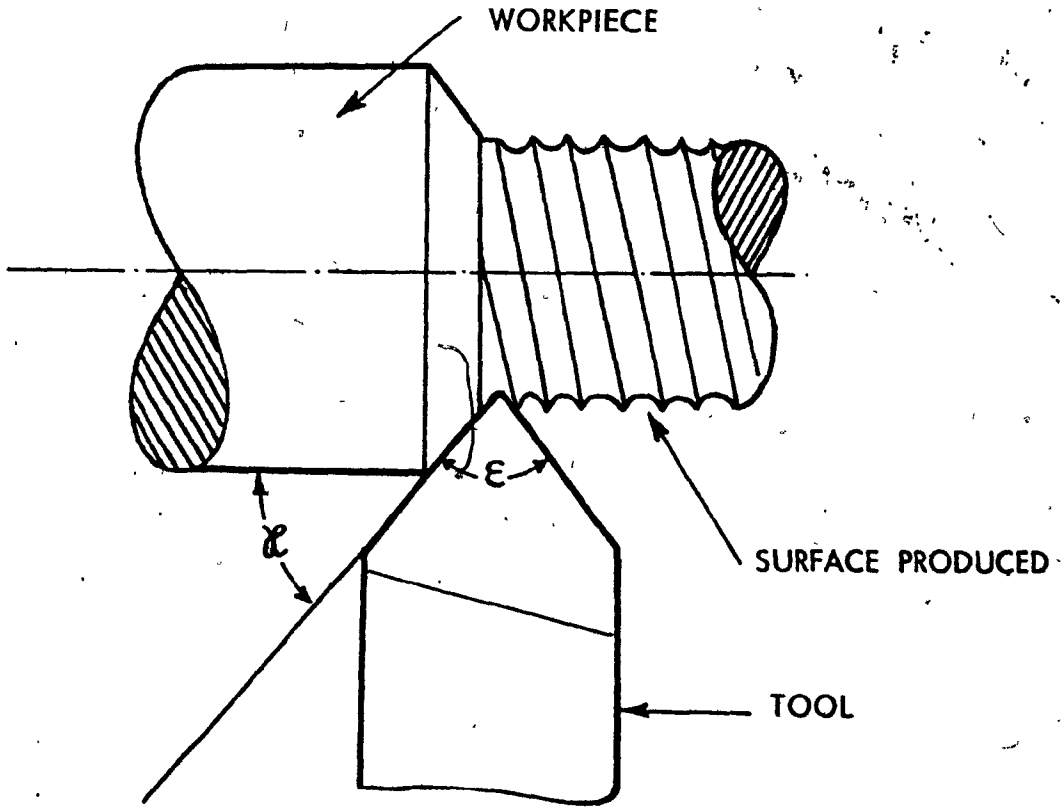

Figure 2.1 THE MECHANICS OF THE FORMATION OF A BASIC SURFACE PROFILE IN A TURNING OPERATION

can be explained in the following manner.

In any metal cutting operation, the metal near the cutting edge is deformed plastically until the chip is sheared at a plane of maximum strain defined by the shear angle ϕ, as shown in Figure 2.2. Due to the high value of the combined shear and compressive stresses at the cutting edge, a micro-crack develops and propogates in front of the cutting edge at a level given approximately by the expression $(s - \epsilon)$ where ϵ is the uncut minimum depth of cut and s is the depth of cut. This is also illustrated in Figure 2.2. According to Sokolowski [23] and Lambert [24] the value of ϵ depends on general conditions of machining, primarily on the radius ρ of the cutting edge. This uncut depth ϵ is squeezed by the cutting edge undergoing elastic and plastic deformations. Thus it can be written

$$\epsilon = \epsilon_p + \epsilon_e \tag{2.1}$$

where ϵ_p is the part due to plastic deformation and ϵ_e is due to elastic deformation.

As the tool moves forward, the elastic deformation ϵ_e of the uncut depth tries to spring back to its original shape. In the absence of any vibrations of the tool, there will be no texture formation on the surface of the workpiece. However, if the tool is vibrating, which is the case in all machining operations, due to the regenerative cutting forces acting on the machine tool system, the elastic deformation ϵ_e will not

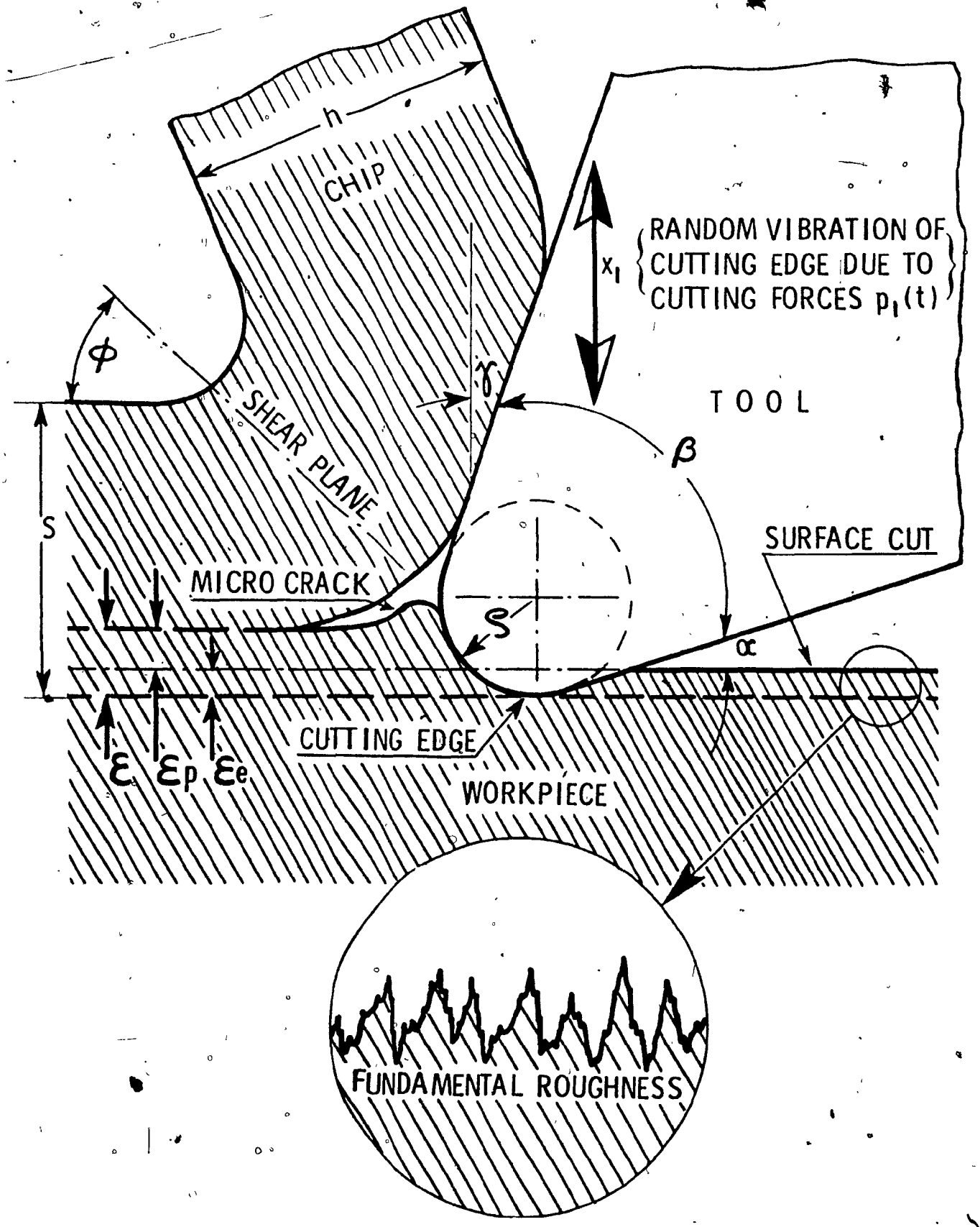

Figure 2.2 THE MECHANICS OF THE FORMATION OF A RANDOM SURFACE PROFILE

be allowed to regain fully its original shape because of the oscillation of the tool. The vibratory response of the tool, which is basically random in character during finish machining, will be reproduced on the workpiece surface, along the direction of cutting, forming a random roughness profile. In the case of turning operation, such random roughness formation is produced along the circumference of the workpiece thereby giving rise to a transverse or circumferential roughness. Successive sets of transverse roughnesses along the feed direction of the tool give rise to the longitudinal roughness of the surface, which is of interest in this investigation.

Now, to describe these roughnesses, as any other random signal, certain statistical parameters are necessary. The more commonly used parameters are the centre line average or CLA value, the RMS-value, etc. In the following section a review of literature that used various stochastic parameters to describe a surface profile is presented.

2.2 Surface Texture as a Random Process

The micro-geometrical characteristics of machined surfaces are so complex that their precise description with a single index like centre line average or CLA value is almost impossible. For this reason, the roughness standards that are presently available and the definitions which are associated with them are not completely satisfactory. From the point of view of industrial applications, advances in surface

texture assessment should lead to some universal method of predicting the performances of all types of manufactured surfaces.

Fatigue strength, surface bearing capacity, wear resistance, friction characteristics and surface lubricability are examples of the many requirements that are directly affected by the surface roughness of the manufactured component. The need for a meaningful method of describing a machined surface and establishment of relationship between manufacturing processes and the necessary functional properties of a surface, therefore, seems evident.

Deterministic methods of describing surface roughness fail because of the fact that surface fluctuations are essentially random in nature. This is why statistical methods are being developed to define the complex character of a surface. Pesante [25] suggested the amplitude density curve for the determination of the surface roughness typology, while Peklenik [26], considering a surface profile as a stationary random process, introduced the correlation functions as the most comprehensive method for surface description. Nakamura [27] and Onishy [28] utilized the autocorrelation function and dispersion spectra or the root-mean-square value for defining surface texture. Spragg and Whitehouse [29] emphasized the use of average wave length of profile as a measure of surface texture. Later, Peklenik [30] introduced the mean thickness of the profile and autocorrelation of the slope.

These two parameters were computed in terms of the average number of crossings of the sample record per unit length. The average profile thickness was defined as the ratio between the length of the surface texture record above a preselected amplitude level "a_m" and the number of crossings at this level. The second parameter, the standard deviation of the slope, was computed by considering the second derivative of the auto-correlation corresponding to a zero lag value.

While the auto-correlation function discriminates between periodic and random components of the profile, suggesting a means of typological surface classification, it appears to be too complex an undertaking for practical application. It is also possible to have two distinctly different surfaces possessing almost the same autocorrelation values and average wavelengths. Furthermore, these methods do not provide a means for the lengthwise description of the extent of crests and valleys present in the surface profile. Description along the length of the surface is important because the mechanical properties such as bearing strength and lubricability depend to a great extent on the lengthwise characteristics of the surface typology. Sankar and Osman [31] employed the theory of stochastic excursions to obtain probabilistic parameters describing crest widths and valley spacings about different levels measured in terms of the basic CLA-value. It was proposed that such an approach would give a sufficient

number of key surface roughness parameters for both height and lengthwise characterizations, namely, the CLA- and RMS-values for amplitude descriptions and the mean and variance for the intercept excursion descriptions. The method was also computerized for practical applications.

In this thesis, the CLA- and RMS-values are employed to describe the surface roughness amplitudes. These characteristics of the roughness amplitudes are analytically obtained from the vibratory response of the tool. In order to determine the vibratory response of the tool the equations of motion of the machine-tool-workpiece system are solved to give the response of the tool-workpiece system which is then utilized to derive an expression for the fundamental surface roughness of the workpiece. Although the vibratory response is also responsible for the lengthwise formation of the surface it is difficult to derive the excursion parameters from this response, because of the difficulty in measuring the actual response of the tool close to the tool-workpiece interface. On the other hand, the cutting forces that are responsible for this tool response can easily be measured with a force measuring dynamometer. The method of Sankar and Osman [31] is utilized to compute the cutting force excursion parameters as well as the surface roughness excursion parameters. The purpose of this investigation would be to establish some direct relationships, if any exist, between the excursion parameters of the cutting forces and the corresponding surface

roughnesses. From such relationships it might then be possible to estimate the surface roughness quality directly from the cutting force characteristics for any given cutting condition.

CHAPTER 3

DYNAMICAL ANALYSIS OF A MACHINE-TOOL-WORKPIECE SYSTEM

CHAPTER 3

DYNAMICAL ANALYSIS OF A MACHINE-TOOL-WORKPIECE SYSTEM

3.1 Description of the System

A machine-tool-workpiece system consists of a machine, a tool with a cutting edge and a workpiece from which metal is removed. For any metal removal process, a relative motion between the cutting tool and the workpiece is essential. The workpiece material being softer than the cutting tool, metal is removed from the workpiece in the form of chips. In general, there are two groups of machine-tool-workpiece systems that are classified on the basis of the type of relative motion between the tool and the workpiece.

a) In the first group, the workpiece is attached to the machine spindle and has a rotary motion, whereas the tool is fixed on the machine bed and has a translatory motion, for example: lathes, boring machines, etc.

b) In the second group, the tool is attached to the machine spindle and has a rotary motion, whereas the workpiece is fixed on the machine bed and has a translatory motion, examples being milling machines, drilling machines, etc.

As far as metal removal is concerned, these two groups of machine-tool-workpiece systems are the same since both involve relative motion between tool and workpiece. In this

thesis, machine-tool-workpiece systems belonging to the first group are investigated. Figure 3.1 describes the major components of a lathe system.

3.2 Assumptions

Several assumptions are made regarding the mathematical model of the machine-tool-workpiece system. The workpiece is considered to be rigidly attached to the machine spindle and forms an integral part of the spindle. The bearings in which the spindle-workpiece unit rotates are taken to be rigidly mounted in the housing. The inner races of these bearings are considered to exhibit some viscous damping and stiffness properties, and could be represented by a viscous damper and a linear spring in the mathematical model. In reality, during any metal cutting process, the contact friction between the tool face and the chip gives rise to Coulomb type of friction damping. The dissipative forces of such friction damping have non-linear variation with the relative velocity of the tool and workpiece. Because of the complexity involved in evaluating this type of non-linear damping force, previous investigators [32] defined an equivalent viscous damping and obtained responses that compared reasonably well with the actual responses measured. Similarly, in the present analysis, the friction damping between the tool faces and the chip is approximated by an equivalent viscous damping and is represented by a dashpot between the tool and the workpiece,

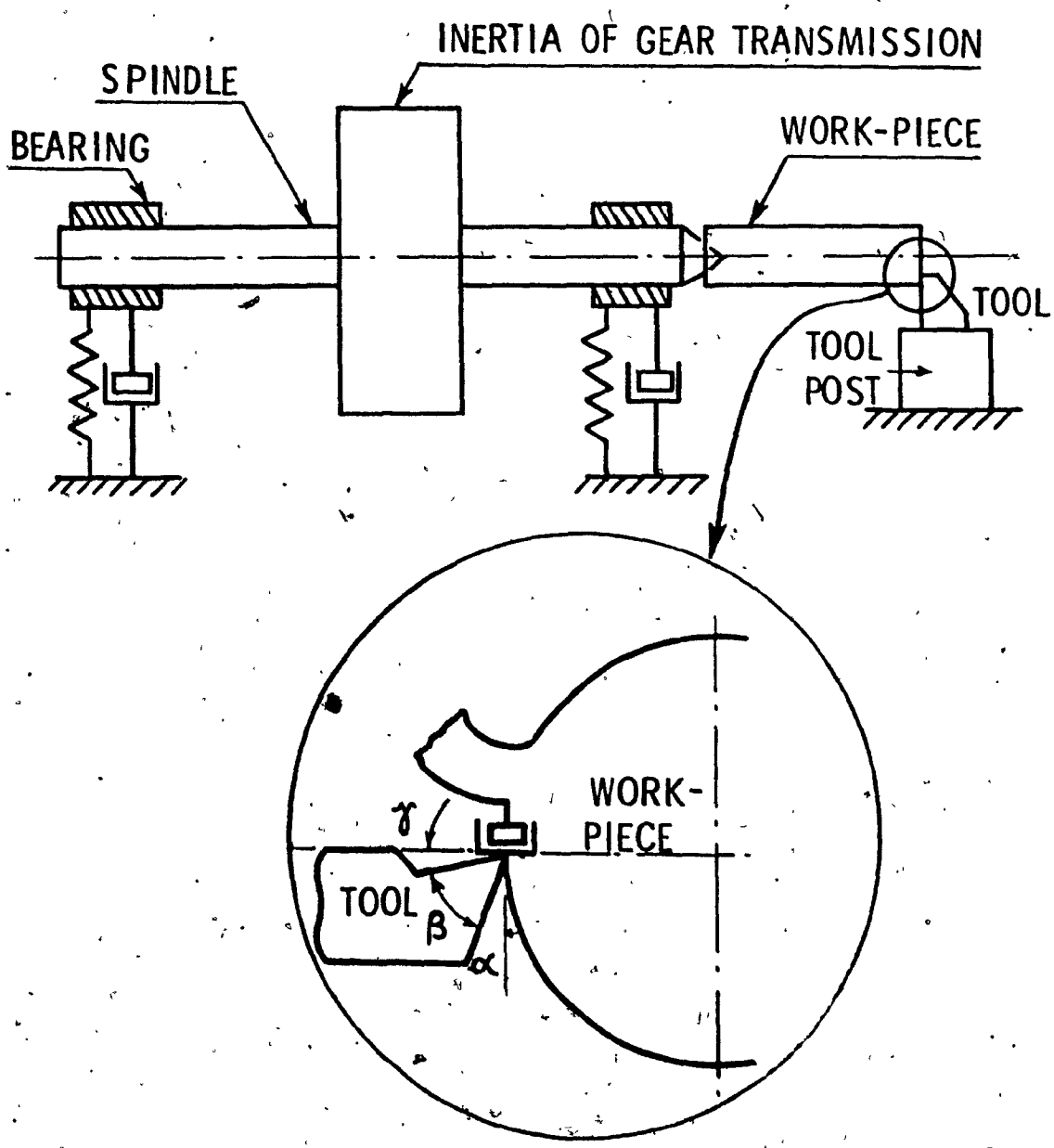

Figure 3.1 A PHYSICAL MODEL OF A LATHE

as shown in Figure 3.1. Further, the tool is assumed to be rigidly mounted on the toolpost.

In addition to the above assumptions, the spindle is taken to be of constant cross-section in the analysis even though in an actual machine, the spindle has varying cross-sections as shown in Figure 3.2. Further, it must be recognized that the cross-section of the workpiece changes after every cut. In order to simplify the model, it is decided to perform the dynamical analysis using an equivalent uniform cross-section for the spindle-workpiece unit. The complete spindle-workpiece unit is then replaced by a set of lumped masses connected by massless shafts as illustrated in Figure 3.3.

During a turning operation, in addition to the flexural motion of the spindle-workpiece unit, there exists a torsional motion due to the flexure-torsional action of the cutting forces as described in Figure 3.4. The effect of the torsional action depends on the relative magnitude of the components of the cutting forces and the workpiece dimension. In a roughing operation where maximum metal removal rate is of primary concern, the cutting forces are relatively large and hence, the torsional action of the cutting forces might be expected to influence the stability such as chatter during machining. On the other hand, surface roughness and workpiece accuracy are of major importance in a finishing operation. The cutting conditions employed for finishing induce cutting

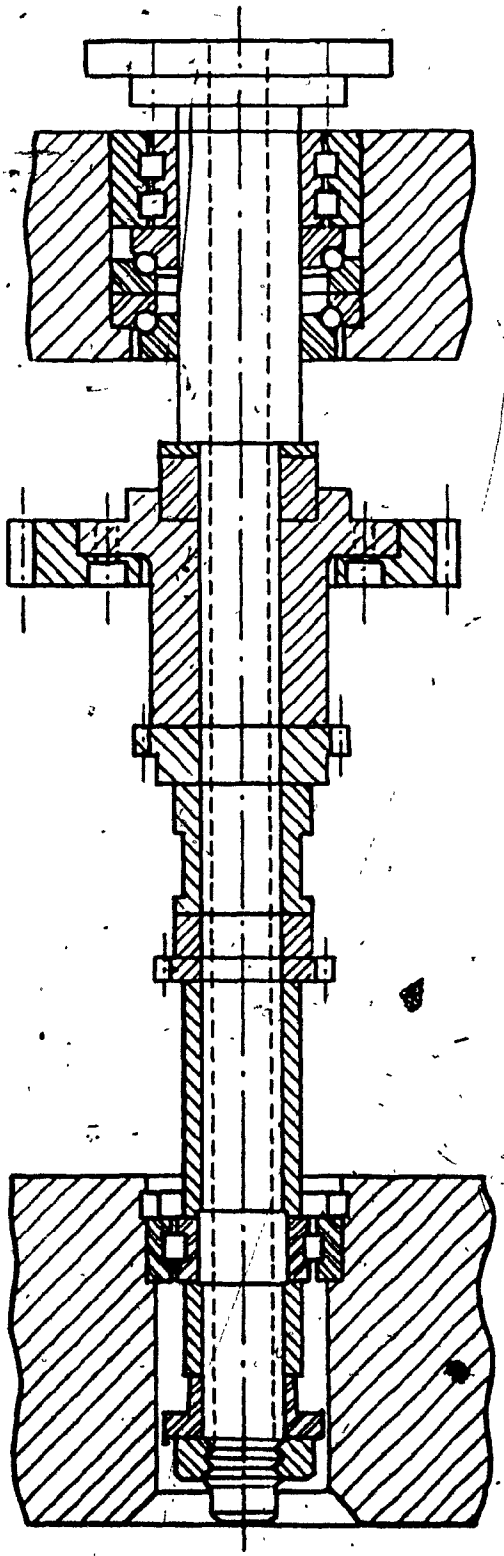

Figure 3.2 A CROSS-S[illegible]N OF THE MACHINE TOOL SPINDLE

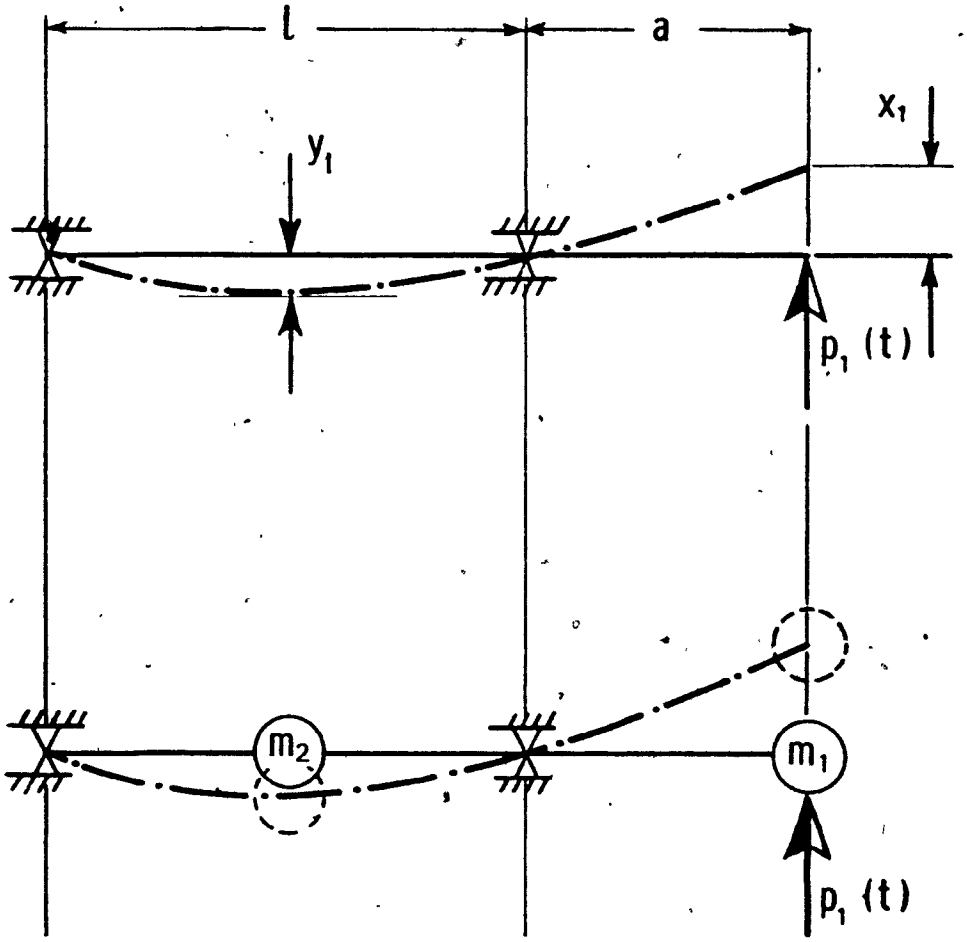

Figure 3.3 LOCATION OF LUMPED MASSES IN THE MODELING OF THE SPINDLE-WORKPIECE-TOOL SYSTEM

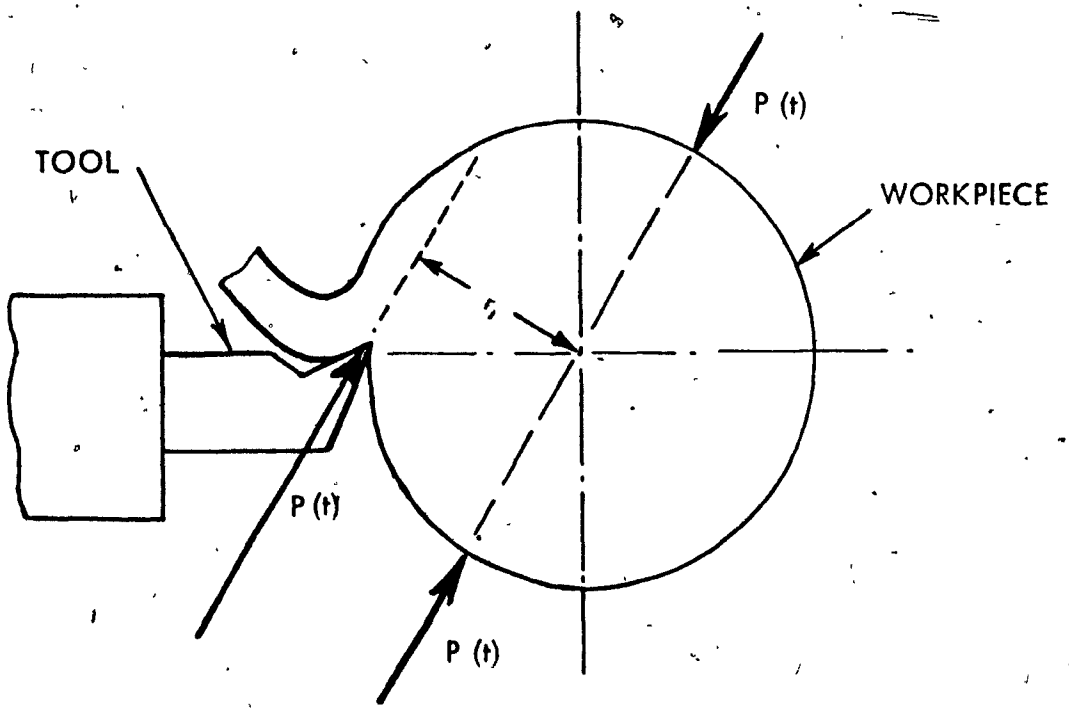

Figure 3.4 FLEXURAL-TORSIONAL ACTION OF THE CUTTING FORCE

forces that are comparatively small in magnitude and have little influence on the stability of the machine system. Also, the external torque produced by the cutting forces is negligible compared to the magnitude of the flexural forces. It may then be reasonable to neglect the torsional action of the cutting forces in the dynamic analysis of the machine-tool-workpiece system under finish machining conditions.

3.3 The Mathematical Model

Exciting Forces: The vibratory behaviour of a machine tool system depends on its dynamic characteristics and on the type of external excitations which originate from the drive and the machining process employed. For the finishing operation, high precision machine tools are normally employed and hence disturbances arising from machine drive are negligible compared to those contributed by the external cutting process.

Stiffness of the System: The mathematical model presented in this investigation considered the cutting forces to be random and introduces the effect of the spindle stiffness on the response of the tool-workpiece system. The spindle-workpiece unit is taken to be statically and dynamically balanced and is considered to be running at a constant speed. The system is assumed to exhibit some viscous damping properties along with linear stiffness properties under the action of the cutting forces.

Damping: When the machine system is subjected to dynamic

cutting forces, it exhibits two types of dissipating forces — external and internal damping. The external damping is caused by the environment of the spindle at the bearings and the workpiece at the cutting zone, while the internal damping is accounted for by the material of the spindle-workpiece system due to elastic hysteresis. These damping effects can effectively be treated by introducing the concept of equivalent viscous damping. The external damping can represent the effects of a stationary viscous environment, while the internal one can be thought of as being caused by a viscous medium which rotates with the spindle, the two dissipating media co-existing but independent.

3.4 Equations of Motion of the System

On the basis of the approximations employed for the stiffness, damping and exciting forces in the machine-tool-workpiece system, the equations of motion of the system can be derived and expressed in terms of either a set of stationary or rotating axes. In the present case, the equations are written in terms of a set of stationary axes. Since the internal damping depends on the absolute velocity of the system, it is necessary to transform the damping term with respect to a stationary coordinate system.

As shown in Figure 3.3, the system consists of a spindle of length "l" supported between two bearings and a workpiece of length "a". The cutting forces acting between the tool

and the workpiece, produces a deflection "x" of the workpiece and "y" of the spindle.

Let OXZ be the plane in which the flexural motion of the workpiece takes place due to the cutting force and $x(z,t)$ be the displacement of an arbitrary point on the workpiece. To refer this displacement relative to the rotational movement of the spindle-workpiece unit, let $u(z,t)$ designate the displacement of the same point on the workpiece with respect to the rotating plane OUZ as shown in Figure 3.5. The displacement "u" is then related to the displacement "x" by the transformation

$$u = x \cos\theta \tag{3.1}$$

where θ is the angular displacement of the point considered on the workpiece surface. Similarly, if $y(z,t)$ is the displacement of a point on the spindle with reference to the stationary plane and $v(z,t)$ is the corresponding displacement in terms of the rotating axes, one can write

$$v = y \cos\theta \tag{3.2}$$

Let α_{ij} be the influence coefficient of the system, which defines a deflection at a location "i" due to a unit load at "j". Then the deflection "x" of the workpiece under dynamic conditions will be the summation of the deflections due to inertial, damping and stiffness forces and the external exciting forces. For the case of the workpiece, deflection

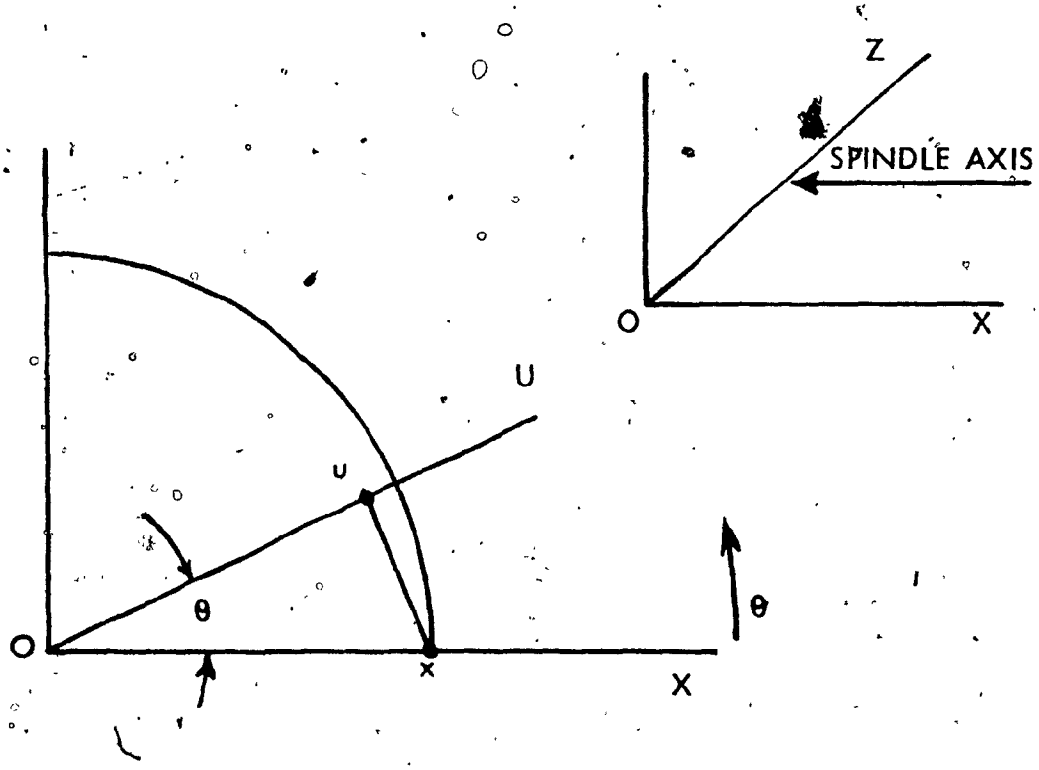

Figure 3.5. THE STATIONARY AND ROTATING COORDINATE SYSTEM

due to the inertia forces is given by the expression

$$-[m_1\ddot{x}\alpha_{11} + m_2\ddot{y}\alpha_{12}],$$

where m_1 and m_2 are the masses of the workpiece and spindle respectively,

x is the deflection of the workpiece,

y is the deflection of the spindle, and

α_{11}, α_{12} are the influence coefficients.

As indicated previously, there are two types of damping forces — internal and external. Since both of these dissipative forces are considered to be viscous, they are proportional to the velocity of the mass of the system and can be written as

$$C_i \frac{d}{dt}(x\cos\theta),\quad C_e \frac{d}{dt}(x),\quad C_i \frac{d}{dt}(y\cos\theta) \text{ and } C_e \frac{d}{dt}(y).$$

Here,

C_i represents the internal viscous damping coefficient, and

C_e represents the external viscous damping coefficient.

Hence, the deflection of the workpiece due to these damping forces may be expressed as

$$-[C_i \frac{d}{dt}(x\cos\theta)\alpha_{11} + C_e \frac{d}{dt}(x)\alpha_{11} +$$

$$C_i \frac{d}{dt}(y\cos\theta)\alpha_{12} + C_e \frac{d}{dt}(y)\alpha_{12}].$$

Using the beam theory the spring forces experienced by the workpiece and the spindle under the action of cutting forces can be written as

$$EI\frac{d^4x}{dz^4} \text{ and } EI\frac{d^4y}{dz^4}$$

respectively. Thus the deflection of the workpiece due to these spring forces can be expressed as

$$-\left[EI\frac{d^4x}{dz^4}\alpha_{11} + EI\frac{d^4y}{dz^4}\alpha_{12}\right]$$

where EI represents the rigidity of the equivalent spindle-workpiece unit.

The deflection of the workpiece due to the external cutting force P(t) is

$$P(t)\,\alpha_{11}.$$

Hence the total deflection "x" of the workpiece can be written as

$$\begin{aligned} x = &-m_1\ddot{x}\alpha_{11} - m_2\ddot{y}\alpha_{12} - C_i\frac{d}{dt}(x\cos\theta)\alpha_{11} \\ &- C_e\frac{d}{dt}(x)\alpha_{11} - C_i\frac{d}{dt}(y\cos\theta)\alpha_{12} - \\ &C_e\frac{d}{dt}(y)\alpha_{12} - EI\frac{d^4x}{dz^4}\alpha_{11} - EI\frac{d^4y}{dz^4}\alpha_{12} + P(t)\alpha_{11} \end{aligned} \qquad (3.3)$$

Similarly the deflection of the spindle "y" can be expressed as

$$y = -m_1\ddot{x}\alpha_{21} - m_2\ddot{y}\alpha_{22} - C_i\frac{d}{dt}(x\cos\theta)\alpha_{21} -$$

$$C_e\frac{d}{dt}(x)\alpha_{21} - C_i\frac{d}{dt}(y\cos\theta)\alpha_{22} - C_e\frac{d}{dt}(y)\alpha_{22} \quad (3.4)$$

$$- EI\frac{d^4x}{dz^4}\alpha_{21} - EI\frac{d^4y}{dz^4}\alpha_{22} + P(t)\alpha_{21}$$

For small values of the angular displacement θ,

$$\cos\theta \simeq 1$$

Hence, the equations (3.3) and (3.4) are rewritten as

$$x = -[m_1\ddot{x}\alpha_{11} + m_2\ddot{y}\alpha_{12} + C_i\dot{x}\alpha_{11} + C_e\dot{x}\alpha_{11} + C_i\dot{y}\alpha_{12}$$

$$+ C_e\dot{y}\alpha_{12} + EI\frac{d^4x}{dz^4}\alpha_{11} + EI\frac{d^4y}{dz^4}\alpha_{12} + P(t)\alpha_{11}] \quad (3.5)$$

$$y = -[m_1\ddot{x}\alpha_{21} + m_2\ddot{y}\alpha_{22} + C_i\dot{x}\alpha_{21} + C_e\dot{x}\alpha_{21} + C_i\dot{y}\alpha_{22}$$

$$+ C_e\dot{y}\alpha_{22} + EI\frac{d^4x}{dz^4}\alpha_{21} + EI\frac{d^4y}{dz^4}\alpha_{22} - P(t)\alpha_{21}] \quad (3.6)$$

Further,

$$C = C_i + C_e \quad (3.7)$$

where C is the coefficient of the total viscous damping in the system. The value of C is experimentally determined by measuring the response of the machine tool system under trial tests and is explained in Chapter 5.

Substituting equation (3.7) into equations (3.5) and (3.6) one can write

$$x = -[m_1\ddot{x}\alpha_{11} + m_2\ddot{y}\alpha_{12} + C\dot{x}\alpha_{11} + C\dot{y}\alpha_{12} + EI\frac{d^4x}{dz^4}\alpha_{11} + EI\frac{d^4y}{dz^4}\alpha_{12} - P(t)\alpha_{11}] \quad (3.8)$$

$$y = -[m_1\ddot{x}\alpha_{21} + m_2\ddot{y}\alpha_{22} + C\dot{x}\alpha_{21} + C\dot{y}\alpha_{22} + EI\frac{d^4x}{dz^4}\alpha_{21} + EI\frac{d^4y}{dz^4}\alpha_{22} - P(t)\alpha_{21}] \quad (3.9)$$

The values of the influence coefficients α_{ij} depend on the relative lengths of the spindle and the workpiece. In the present investigation the ratio of the length of the spindle to the length of the workpiece is taken as 2 and the values of α_{ij} are computed using simple beam analysis as indicated below

$$\alpha_{11} = \frac{l^3}{8EI}, \quad \alpha_{22} = \frac{l^3}{48EI}, \quad \text{and} \quad \alpha_{12} = \frac{l^3}{32EI}$$

and by Maxwell's reciprocal theorem

$$\alpha_{12} = \alpha_{21}.$$

Now, for harmonic vibrations of the spindle-workpiece unit, one can write for the principal mode of vibration

$$x(z,t) = x(t)\sin\frac{\pi z}{l} \quad (3.10)$$

$$y(z,t) = y(t)\sin\frac{\pi z}{l} \quad (3.11)$$

Substituting the values of the influence coefficients and the responses (3.10) and (3.11) into equations (3.8) and (3.9) the equations of motion of the spindle-workpiece unit may be expressed in the form

$$m_1\ddot{x} + C\dot{x} + \frac{113EI}{l^3}x - \frac{19EI}{l^3}y = P(t) \qquad (3.12)$$

$$m_2\ddot{y} + C\dot{y} + \frac{174EI}{l^3}y - \frac{19EI}{l^3}x = 0 \qquad (3.13)$$

Since a stationary random signal may be represented by a steady state value with a randomly fluctuating component superimposed on it, the random cutting force P(t) is written in the form

$$P(t) = P_o + p(t) \qquad (3.14)$$

where P_o is the steady state value of P(t) and p(t) is the random component and is considered to be stationary and Gaussian in distribution. Since the spindle-workpiece system is linear the total response can be taken as the response due to the random component of the cutting forces superimposed on the response due to the steady state value of the cutting force.

The steady state response x_o of the workpiece is evaluated from elementary machanics, as

$$x_o = \frac{P_o}{k_s}$$

$$= \frac{P_o}{m_1 \omega_1^2}$$

where m_1, k_s and ω_1 are the mass, static stiffness and fundamental frequency of the tool-workpiece system respectively.

The dynamic response of the tool-workpiece under the action of the random part of the cutting forces is to be determined from the solution of the following equations of motion

$$m_1\ddot{x} + C\dot{x} + \frac{113EI}{l^3} x - \frac{19EI}{l^3} y = p(t) \qquad (3.15)$$

$$m_2\ddot{y} + C\dot{y} + \frac{174EI}{l^3} y - \frac{19EI}{l^3} x = 0 \qquad (3.16)$$

3.5 Response of the System

To find the stochastic responses of the workpiece and the spindle unit, it is necessary to solve the two probabilistic equations (3.15) and (3.16). Since the cutting forces are considered to be stationary and Gaussian, which is justified in the results of the tests carried out and reported in Chapter 5, the mean square responses of x and y are found out, employing the frequency response method as described below.

Equations (3.15) and (3.16) are rewritten in the form

$$\ddot{x} + \frac{C}{m_1}\dot{x} + \frac{113EI}{m_1 \ell^3} x - \frac{19EI}{m_1 \ell^3} y = z(t) \qquad (3.17)$$

$$\ddot{y} + \frac{C}{m_2}\dot{y} + \frac{174EI}{m_2 \ell^3} y - \frac{19EI}{m_2 \ell^3} x = 0 \qquad (3.18)$$

where $z(t) = \frac{p(t)}{m_1}$.

Taking the Laplace transform of the equations (3.17) and (3.18), and using the initial conditions

$$x(0) = 0 = \dot{x}(0)$$
$$y(0) = 0 = \dot{y}(0) \qquad (3.19)$$

one can write

$$s^2 x + s\left(\frac{C}{m_1}\right) x + \frac{113EI}{m_1 \ell^3} x - \frac{19EI}{m_1 \ell^3} y = z(s) \qquad (3.20)$$

$$s^2 y + s\left(\frac{C}{m_2}\right) y + \frac{174EI}{m_2 \ell^3} y - \frac{19EI}{m_2 \ell^3} x = 0 \qquad (3.21)$$

where s is the Laplace transform variable. Equations (3.20) and (3.21) are rearranged as

$$\left[s^2 + s\left(\frac{C}{m_1}\right) + \frac{113EI}{m_1 \ell^3}\right] x - \left[\frac{19EI}{m_1 \ell^3}\right] y = z(s) \qquad (3.22)$$

$$\left[-\frac{19EI}{m_2 \ell^3}\right] x + \left[s^2 + s\left(\frac{C}{m_2}\right) + \frac{174EI}{m_2 \ell^3}\right] y = 0 \qquad (3.23)$$

The solution of the above simultaneous equations, using

Cramer's rule, yields

$$x(s) = \frac{1}{D} \begin{vmatrix} z(s) & -\frac{19EI}{m_1 l^3} \\ 0 & [s^2 + \frac{C}{m_2}s + \frac{174EI}{m_2 l^3}] \end{vmatrix} \qquad (3.24)$$

and

$$y(s) = \frac{1}{D} \begin{vmatrix} [s^2 + \frac{C}{m_1}s + \frac{113EI}{m_1 l^3}] & z(s) \\ [-19\frac{EI}{m_2 l^3}] & 0 \end{vmatrix} \qquad (3.25)$$

where D, the determinant of the coefficients, is given by

$$D = \begin{vmatrix} [s^2 + \frac{C}{m_1}s + \frac{113EI}{m_1 l^3}] & [-19\frac{EI}{m_1 l^3}] \\ [-19\frac{EI}{m_2 l^3}] & [s^2 + \frac{C}{m_2}s + \frac{174EI}{m_2 l^3}] \end{vmatrix} \qquad (3.26)$$

From equations (3.24) and (3.25), one can write

$$x(s) = \frac{1}{D}[s^2 + \frac{C}{m_2}s + \frac{174EI}{m_2 l^3}]\, z(s) \qquad (3.27)$$

$$y(s) = \frac{1}{D}[\frac{19EI}{m_2 l^3}]\, z(s) \qquad (3.28)$$

Equations (3.27) and (3.28) can now be written in the form

$$x(j\omega) = H_1(j\omega)\ z(j\omega) \tag{3.29}$$

$$y(j\omega) = H_2(j\omega)\ z(j\omega) \tag{3.30}$$

where,

$$H_1(j\omega) = \frac{1}{D}\left(-\omega^2 + j\omega\frac{C}{m_2} + \frac{174EI}{m_2 l^3}\right) \tag{3.31}$$

$$H_2(j\omega) = \frac{1}{D}\left(\frac{19EI}{m_2 l^3}\right) \tag{3.32}$$

$H_1(j\omega)$ and $H_2(j\omega)$ are known as the complex frequency response functions of the workpiece and spindle system respectively. Suppose the spectral density $S_z(\omega)$ of the random cutting forces is known. Then, the spectral densities $S_x(\omega)$ and $S_y(\omega)$ of the responses of the tool-workpiece and spindle systems are given through the relations

$$S_x(\omega) = H_1(j\omega)\quad H_1^*(j\omega)\quad S_z(\omega) \tag{3.33}$$

$$S_y(\omega) = H_2(j\omega)\quad H_2^*(j\omega)\quad S_z(\omega) \tag{3.34}$$

where $H_1^*(j\omega)$ and $H_2^*(j\omega)$ are the complex conjugates of the frequency response functions $H_1(j\omega)$ and $H_2(j\omega)$ respectively.

To calculate the mean square responses $E[x^2]$ and $E[y^2]$ it is necessary to know the autocorrelation functions $R_x(\tau)$ and $R_y(\tau)$ of the responses. $R_x(\tau)$ and $R_y(\tau)$ are given by the

transform relationships

$$R_x(\tau) = \frac{1}{2\pi} \int_{-\infty}^{+\infty} S_x(\omega) \; e^{-j\omega\tau} \; d\omega \qquad (3.35)$$

$$R_y(\tau) = \frac{1}{2\pi} \int_{-\infty}^{+\infty} S_y(\omega) \; e^{-j\omega\tau} \; d\omega \qquad (3.36)$$

For $\tau = 0$

$$R_x(0) = \frac{1}{2\pi} \int_{-\infty}^{+\infty} S_x(\omega) \; d\omega \qquad (3.37)$$

$$= E[x^2]$$

$$R_y(0) = \frac{1}{2\pi} \int_{-\infty}^{+\infty} S_y(\omega) \; d\omega \qquad (3.38)$$

$$= E[y^2]$$

Substituting the values of $S_x(\omega)$ and $S_y(\omega)$ from equations (3.33) and (3.34), equations (3.37) and (3.38) become

$$E[x^2] = \frac{1}{2\pi} \int_{-\infty}^{+\infty} |H_1(\omega)|^2 \; S_z(\omega) \; d\omega \qquad (3.39)$$

$$E[y^2] = \frac{1}{2\pi} \int_{-\infty}^{+\infty} |H_2(\omega)|^2 \; S_z(\omega) \; d\omega \qquad (3.40)$$

Since the present investigation is carried out to find the effect of stochastic response of tool-workpiece system on the formation of surface texture of the workpiece, the mean square

response $E[x^2]$ is of importance because it relates to the RMS value of the surface roughness.

The evaluation of the integral $\int_{-\infty}^{+\infty} |H_1(\omega)|^2 S_z(\omega)\, d\omega$ is complex and depends mainly upon the nature of the power spectral density $S_z(\omega)$ of the cutting forces. The problem can be simplified if, for the purpose of analysis, an equivalent white noise density S_o is considered. Such equivalent white noise density may be approximately obtained by averaging the actual measured spectral density over the entire frequency range of interest.

Replacing $S_z(\omega)$ by S_o, a constant value for the frequency range that is of concern, equation (3.39) simplified to

$$E[x^2] = S_o \int_{-\infty}^{+\infty} |H_1(\omega)|^2\, d\omega \qquad (3.41)$$

Evaluation of $\int_{-\infty}^{+\infty} |H_1(\omega)|^2\, d\omega$

From equation (3.31)

$$H_1(j\omega) = \frac{1}{D}\left[s^2 + \frac{C}{m_2}s + \frac{174EI}{m_2 l^3}\right] -$$

Expanding the determinant given in equation (3.26), it yields

$$D = s^4 + \left(\frac{C}{m_1} + \frac{C}{m_2}\right)s^3 + \left[\frac{C^2}{m_1 m_2} + \frac{174EI}{m_2 l^3} + \frac{113EI}{m_1 l^3}\right]s^2 + \left[C\left(\frac{174EI}{m_1 m_2 l^3}\right) + C\left(\frac{113EI}{m_1 m_2 l^3}\right)\right]s + \frac{19260(EI)^2}{m_1 m_2 l^6} \qquad (3.42)$$

Substituting the values of the determinant D and s, equation (3.31) is expressed in the form

$$H_1(j\omega) = \frac{-j\omega^3 B_3 - \omega^2 B_2 + j\omega B_1 + B_0}{\omega^4 A_4 - j\omega^3 A_3 - \omega^2 A_2 + j\omega A_1 + A_0} \qquad (3.43)$$

where A_0, A_1, A_2, A_3, A_4, B_0, B_1, B_2 and B_3 are all constants and their values are

$$A_0 = \frac{19260(EI)^2}{m_1 m_2 l^6}$$

$$A_1 = C\left(\frac{174EI}{m_1 m_2 l^3} + \frac{113EI}{m_1 m_2 l^3}\right)$$

$$A_2 = \frac{174EI}{m_2 l^3} + \frac{4C}{m_1 m_2} + \frac{113EI}{m_1 l^3}$$

$$A_3 = \frac{C}{m_1} + \frac{C}{m_2}$$

$$A_4 = 1$$

$$B_0 = \frac{174EI}{m_2 l^3}$$

$$B_1 = \frac{C}{m_2}$$

$$B_2 = 1$$

$$B_3 = 0$$

Applying the method of residues given by James, Nichols and

Phillips[33], integration of equation (3.41) is evaluated as

$$\int_{-\infty}^{+\infty} |H_1(\omega)|^2 d\omega = \frac{\pi}{\eta_5} \left[\eta_1 \left(\frac{B_0^2}{A_0}\right) + \eta_2 A_3 + \eta_3 A_1 + \eta_4 \left(\frac{B_3^2}{A_4}\right)\right] \quad (3.44)$$

where

$$\eta_1 = A_2A_3 - A_1A_4$$

$$\eta_2 = B_1^2 - 2B_0B_2$$

$$\eta_3 = B_2^2 - 2B_1B_3$$

$$\eta_4 = A_1A_2 - A_0A_3$$

$$\eta_5 = A_1(A_2A_3 - A_1A_4) - A_0A_3^2$$

Substituting the value of $\int_{-\infty}^{+\infty} |H_1(\omega)|^2 d\omega$ in equation (3.41) one can write

$$E[x^2] = \frac{S_o \pi}{\eta_5} \left[\eta_1 \left(\frac{B_0^2}{A_0}\right) + \eta_2 A_3 + \eta_3 A_1 + \eta_4 \left(\frac{B_3^2}{A_4}\right)\right] \quad (3.45)$$

The RMS-value, σ_f, of the surface profile depends on the RMS-value of the tool-workpiece response. The RMS-value of the tool-workpiece response can be computed from the mean square response $E[x^2]$ of the system.

To compute $E[x^2]$ from equation (3.45), the constant spectral density, S_o, of the cutting forces is to be known. Experiments were carried out under different cutting conditions to measure spectral densities of the cutting forces from which S_o is calculated and they are described in Chapter 5.

CHAPTER 4

ASSESSMENT OF SURFACE TEXTURE FROM THE CUTTING CONDITIONS AND FROM THE RESPONSE OF THE TOOL-WORKPIECE SYSTEM

CHAPTER 4

ASSESSMENT OF SURFACE TEXTURE FROM THE CUTTING CONDITIONS AND FROM THE RESPONSE OF THE TOOL-WORKPIECE SYSTEM

4.1 Objective

It was already established that the surface roughness of a machined component consists of a theoretical (basic) profile with random fluctuations superimposed on it. Figure 4.1 describes the diagramatic representation of the theoretical profile, random roughness profile and the resulting total surface profile for a turning operation.

The theoretical profile depends on the kinematic conditions such as the feed and the tool nose radius. The CLA-value of this profile can be computed using the method shown by Osman and Sankar [34]. The random or the fundamental roughness profile is caused by the relative vibratory response of the tool with respect to the workpiece. This dynamic response may be determined directly if a complete knowledge of the dynamic cutting forces and the system parameters as expressed in equation (3.45) are known.

From the system response, the random profile may be evaluated using physical arguments.

Expressions are derived in the following section to obtain the total surface roughness from the knowledge of theoretical and random profiles.

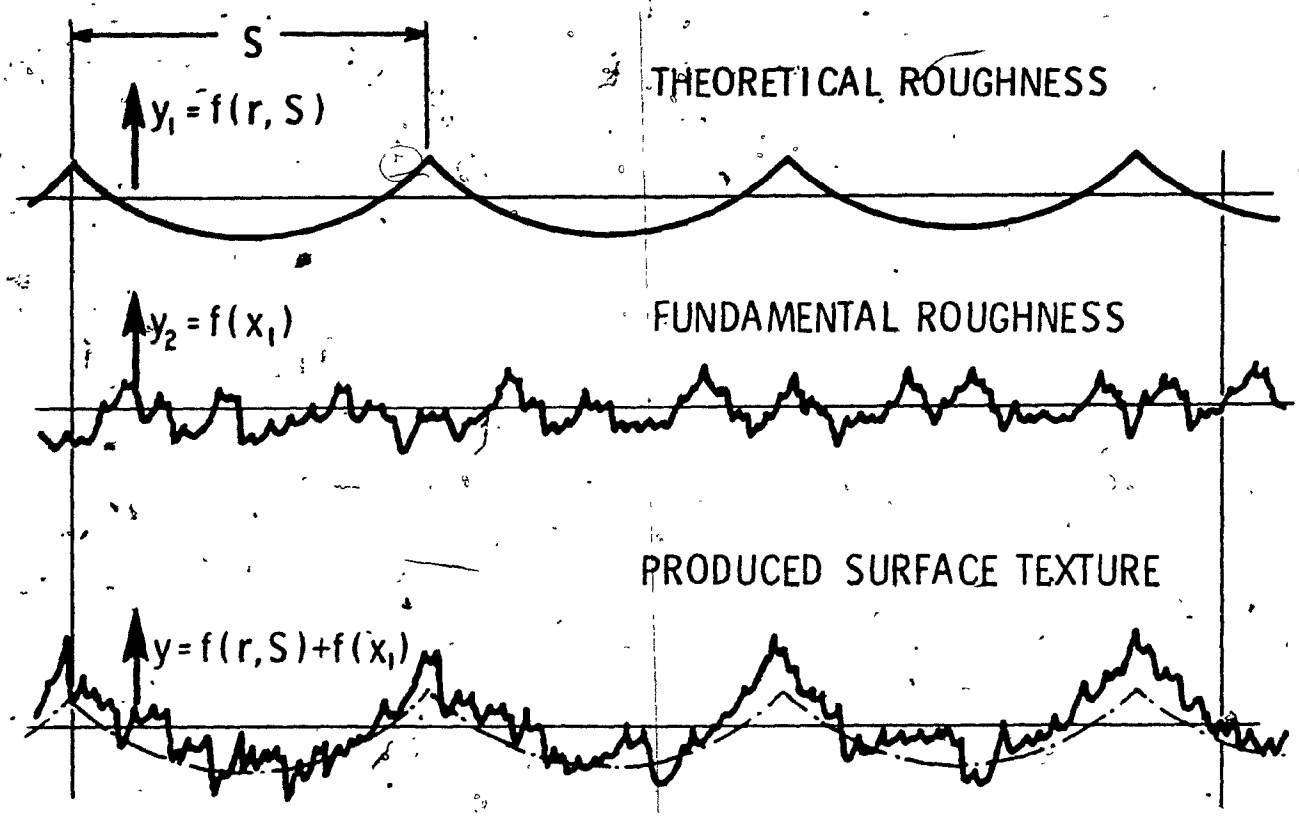

Figure 4.1 THE TOTAL SURFACE ROUGHNESS PROFILE

4.2 Total Surface Profile

The theoretical profile U_1 of a manufactured surface can be expressed in the form

$$U_1 = f(r,S) \tag{4.1}$$

where r is the tool nose radius and S is the feed/revolution of the workpiece.

Also, the fundamental random profile U_2 can be written in a functional form as

$$U_2 = f(x) \tag{4.2}$$

where x is the response of the tool-workpiece system due to the dynamic action of metal cutting forces.

Thus, the total surface profile W becomes, by superimposition

$$\begin{aligned} W &= U_1 + U_2 \\ &= f(r,S) + f(x) \end{aligned} \tag{4.3}$$

For two uncorrelated processes, U_1 and U_2, one can write

$$E[U_1U_2] = E[U_2U_1] \neq 0$$

This relationship yields

$$E[(U_1+U_2)(U_1+U_2)] = E[U_1^2] + E[U_2^2] + E[U_1U_2] + E[U_2U_1] \tag{4.4}$$

from which

$$E[W^2] = E[U_1^2] + E[U_2^2] \tag{4.5}$$

It is explained in Chapter 2 that the theoretical profile on a surface is produced due to operation kinematics of the machine tool and the random profile is due to the tool-work-piece response. Since operation kinematics of the machine tool is independent of the reasons that cause vibrations between the tool and workpiece, the theoretical and the random profiles are considered as two completely uncorrelated processes.

Hence, this means that

$$\sigma_{Tot}^2 = \sigma_{Th}^2 + \sigma_f^2 \tag{4.6}$$

where σ_{Tot}, σ_{Th} and σ_f are the RMS-values of the total, theoretical and fundamental profiles respectively.

If the tool nose curvature is considered as a part of a parabola it may be shown [34]

$$\sigma_{Th} = S^2 / (12\sqrt{5})r \tag{4.7}$$

and

$$\lambda_{Th} = S^2 / (18\sqrt{3})r \tag{4.8}$$

where λ_{Th} is the CLA-value of the theorical surface profile. By combining the abobe two equations one can write

$$\sigma_{Th} / \lambda_{Th} \neq 1.16 \qquad (4.9)$$

For a random profile with a Gaussian distribution, the ratio between the RMS- and the CLA- values is given by the standard form

$$\sigma_f / \lambda_f = 1.25 \qquad (4.10)$$

It has been experimentally observed that, for any finishing operation, the surface roughness has stationary property with a Gaussian probability distribution and hence, is the validity of the relationship (4.10) between the RMS- and CLA-values of the total surface roughness in a finish turning operation.

It was already explained that in any metal cutting process the material at the cutting zone is elastically and plastically deformed and because of the elastic and plastic deformation, the relative vibratory response of the tool with respect to the workpiece is not fully reproduced on the workpiece surface. Thus, it may then be possible to write the RMS-value of roughness from the RMS-value of the response x as,

$$\sigma_f = k\{E[x^2]\}^{\frac{1}{2}} \qquad (4.11)$$

where $E[x^2] = \sigma_x^2$ = variance of x, and k is a factor that depends on this elasto-plastic deformation property of the workpiece material. In effect, this factor represents a reduction in the linear transfer of the tool oscillations onto the

workpiece as surface roughness formation. For material like steel, the value of k varies between 0.8 to 0.9. In the present investigation it is taken to be 0.85.

Now, substituting equations (4.9) and (4.10) in equation (4.6) and rearranging, one can write

$$\lambda_{Tot} = [0.865\lambda^2_{Th} + \lambda^2_f]^{\frac{1}{2}} \qquad (4.12)$$

or

$$\lambda_{Tot} = [0.865\lambda^2_{Th} + 0.640\sigma^2_f]^{\frac{1}{2}} \qquad (4.13)$$

It may be noted that the total and the theoretical surface roughnesses in equation (4.13) are expressed in terms of the CLA-values and the random profile in terms of the RMS-value. The advantage of expressing the total roughness in terms of the CLA-value lies in the fact that the majority of commercially available surface roughness measuring equipments read the CLA-value directly. Further, no conversion from σ to λ is needed because equation (4.11) gives the RMS-value of the random profile explicitly, and can be used directly in equation (4.13). By this method, the total roughness of a manufactured surface can be computed in terms of its CLA-value and then may be compared with the corresponding CLA-values obtained by actual

measurement in order to establish the reliability of the analytical procedure proposed. For instruments that read directly the RMS-value, equation (4.6) may be rearranged in the form

$$\sigma_{Tot} = [\sigma_{Th}^2 + \sigma_f^2]^{\frac{1}{2}} \qquad (4.14)$$

The relationship expressed by the equation (4.12) shows that it is possible to estimate the CLA-value of a surface to be produced if the CLA-values of the theoretical and random profiles are known. The CLA-value of the theoretical profile can be calculated from the equation (4.8) for any given cutting conditions. On the other hand, to obtain the CLA-value of the random or fundamental profile it is necessary that the tool-workpiece response which in turn depends on the random cutting forces, be known. The relationship between the tool-workpiece response and the random cutting forces is illustrated by the equation (3.45) which indicates that the spectral density of the cutting forces is required to compute the tool-workpiece response.

Machining tests were carried out on a lathe with different cutting conditions to measure the spectral density of the cutting forces. Such measurement procedure is described in the following chapter. To verify the computed surface roughness with the actual, surface profiles obtained after each test were also measured.

CHAPTER 5

MEASUREMENT OF CUTTING FORCES AND SUPFACE ROUGHNESS, AND DETERMINATION OF THE MACHINE TOOL DAMPING COEFFICIENT

CHAPTER 5

MEASUREMENT OF CUTTING FORCES AND SURFACE ROUGHNESS, AND DETERMINATION OF THE MACHINE TOOL DAMPING COEFFICIENT

5.1 Objective

An analytical procedure for evaluating the surface roughness quality may be based on the mean square response of the tool-workpiece system and has already been described in Chapters 3 and 4. To compute the mean square response it is necessary that the spectral densities of the cutting forces be completely known. For this purpose experiments were carried out on a lathe for measuring the dynamic characteristics of the cutting forces and were then analyzed to give the power spectral density. Further, the actual surface roughnesses produced in the cutting tests were measured after each test for comparison with the roughness values computed using the technique described in Chapter 4.

In order to investigate the effect of the variation of the cutting speed on the quality of surface roughness, experiments were carried out at two distinct cutting speeds. A frequency response test of the machine tool system was then performed to obtain the equivalent viscous damping coefficient that is necessary for computing the response of the tool-workpiece system given in Chapter 3. For measuring the dynamic cutting forces accurately, a special dynamometer [35] was

developed. The essential features of this dynamometer are described in the following section.

5.2 Dynamic Cutting Force Measurements

5.2.1 Dynamometer : To measure the cutting forces accurately, a dynamometer which uses piezo-electric crystals was developed. These crystals have the property of converting mechanical stresses into electrical field. In the dynamometer used, the crystals are so arranged that all the components of cutting forces can be measured independent of the point of application of the forces. This arrangment allows the cutting forces to be measured accurately although their point of action is located at the interface between the tool and chip. Figure 5.1 describes the cross-section of the dynamometer illustrating the essential features such as base plate, tool holder, bolts for preloading, piezo-electric cells and the main frame. These parts are designed in such a way that the dynamometer possesses a response over a wide frequency range and also, has a high resolution making the dynamometer capable of measuring even the smallest variation in the cutting forces. The loading capacities are calculated to be 500 pounds in both radial and feed directions, and 1000 pounds in the direction of the main cutting force. Further, the natural frequencies in both feed and main cutting force directions are found to be 10 KHz whereas along the radial direction, the natural frequency of the dynamometer was 13 KHz.

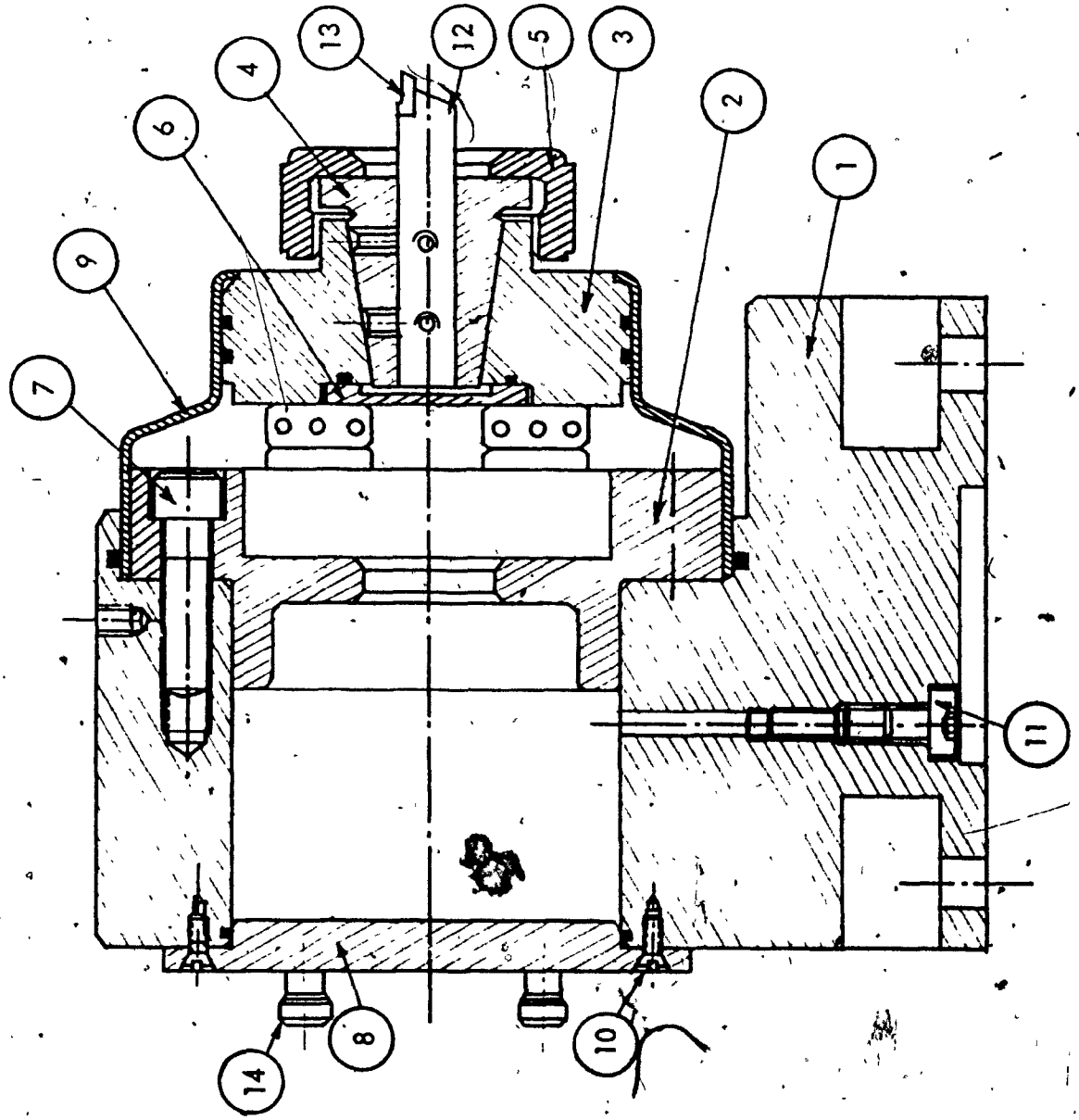

Figure 5.1 A CROSS-SECTION OF THE DYNAMOMETER

Calibration of the Dynamometer: The dynamometer must be calibrated both under static and dynamic loads before installing it for measuring any metal cutting forces. The static calibration chart may be used over the frequency range that is of interest in a system such as a machine tool, if such a dynamometer is mounted on a rigid base. However, when mounted on the machine tool table and when the machine tool is dynamically excited, the dynamic response of the dynamometer will reflect the dynamic characteristics of the machine and it may behave as an accelerometer monitoring the motion of the machine tool structure. This action of the dynamometer will give a distorted signal at those values of frequencies in the vicinity of the machine's natural frequencies, and consequently, the static calibration charts will not be valid.

To improve the accuracy of measurement over the entire frequency range that is of interest, the dynamometer must be calibrated under dynamic loads. This will yield a dynamic calibration chart from which a corrected dynamometer reading may be obtained at each frequency.

5.2.2 Static Calibration of the Dynamometer: The static calibration was performed with the dynamometer mounted on the lathe bed. A schematic of the set up is shown in Figure5.2. For a proper calibration of the dynamometer, it is essential that the calibration loads that are applied on the dynamometer

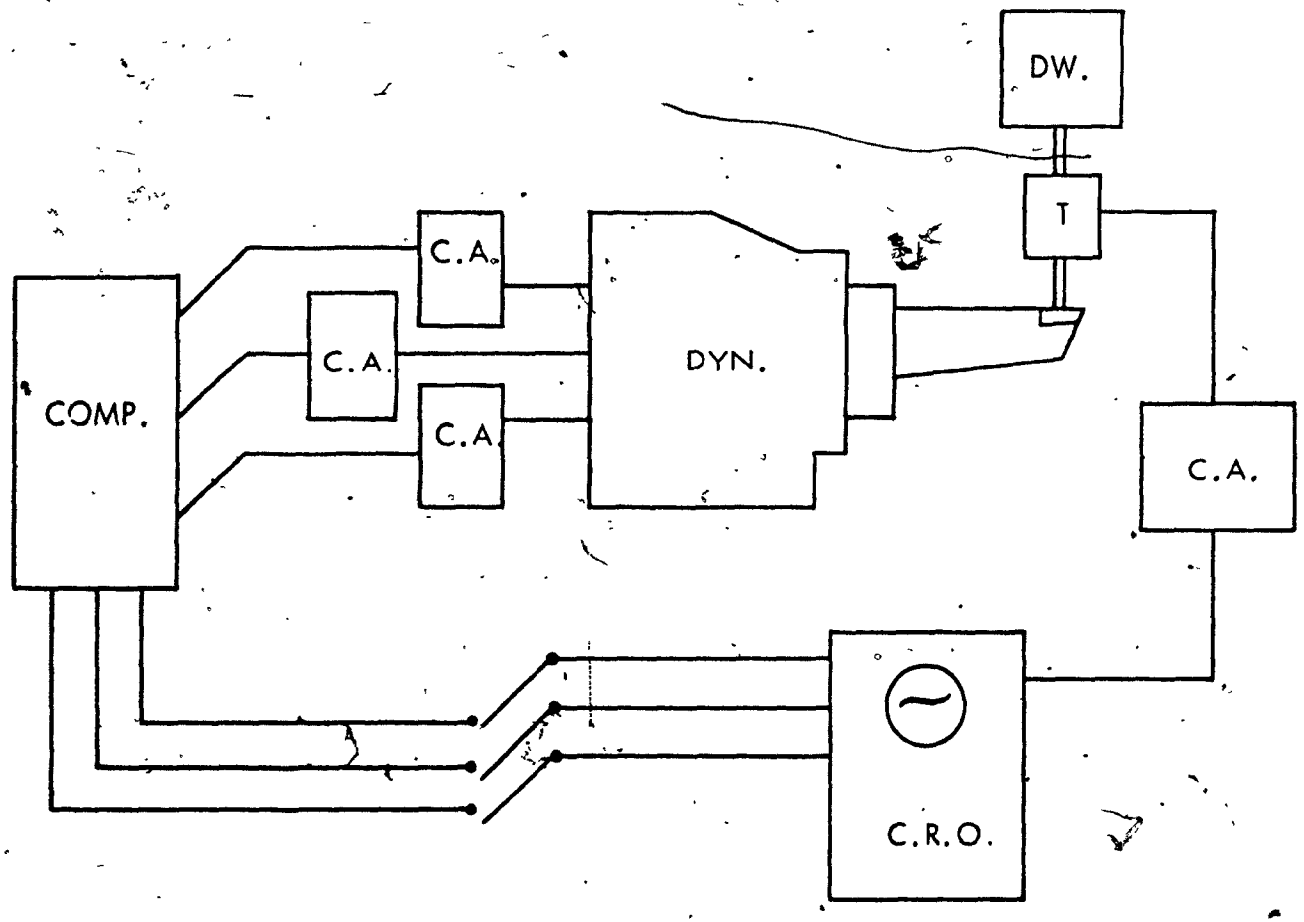

T. : CALIBRATED FORCE TRANSDUCER

DYN.: DYNAMOMETER

C.A. : CHARGE AMPLIFIER

CRO : CATHODE RAY OSCILLOSCOPE

COMP.: COMPENSATOR

D W. : DEAD WEIGHT

Figure 5.2 SCHEMATIC DIAGRAM OF THE SET UP FOR STATIC CALIBRATION OF THE DYNAMOMETER

be uniaxial so that the cross interference between the three axial directions is minimized. This was achieved by employing a special tool holder as illustrated in Figure 5.3. Charge amplifiers were used for converting electrical charges produced, during calibration loading, by the piezo electric quartz, of the dynamometer into a corresponding analog voltage. A x-y-z compensator was included for minimizing any cross-sensitivity that might occur between the three directions of the force components.

By slowly increasing the applied load on the tool holder, the voltage produced was read on an oscilloscope for specific settings on the charge amplifier. The electrical charge produced by the dynamometer is calculated from the following relationship:

$$Q = B \cdot V \tag{5.1}$$

where Q is the charge in pico-Coulomb

V is the voltage reading on the oscilloscope,

and B is the gain setting on the charge amplifier.

Figure 5.4 presents the calibration curves obtained, where the ordinate represents the actual electrical charge produced, and the abscissa represents the magnitude of loads applied. The magnitude of the applied unidirectional loads was measured using a Kistler force transducer that was inserted between the load and the tool holder. To ensure that any form of

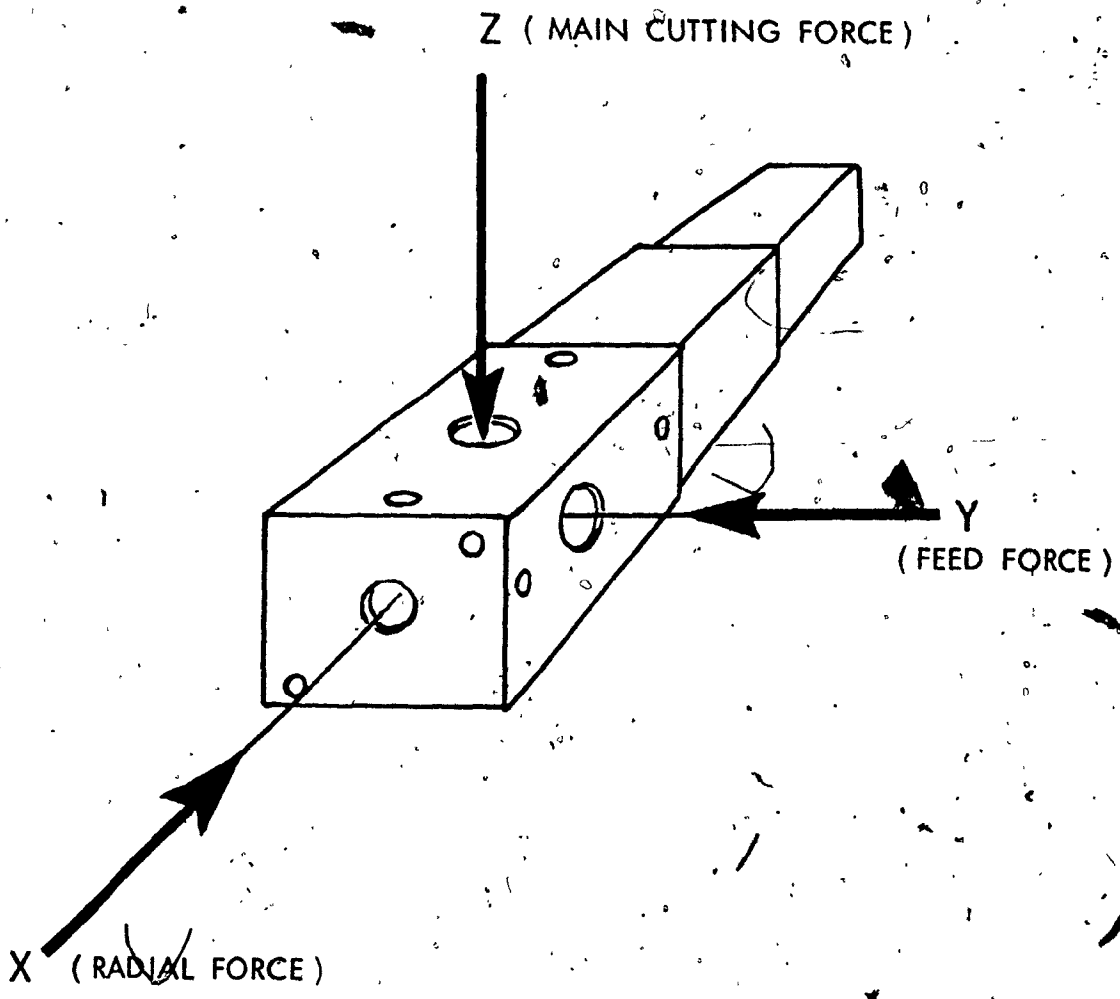

Figure 5.3 SPECIAL TOOL HOLDER FOR APPLYING UNIAXIAL LOAD

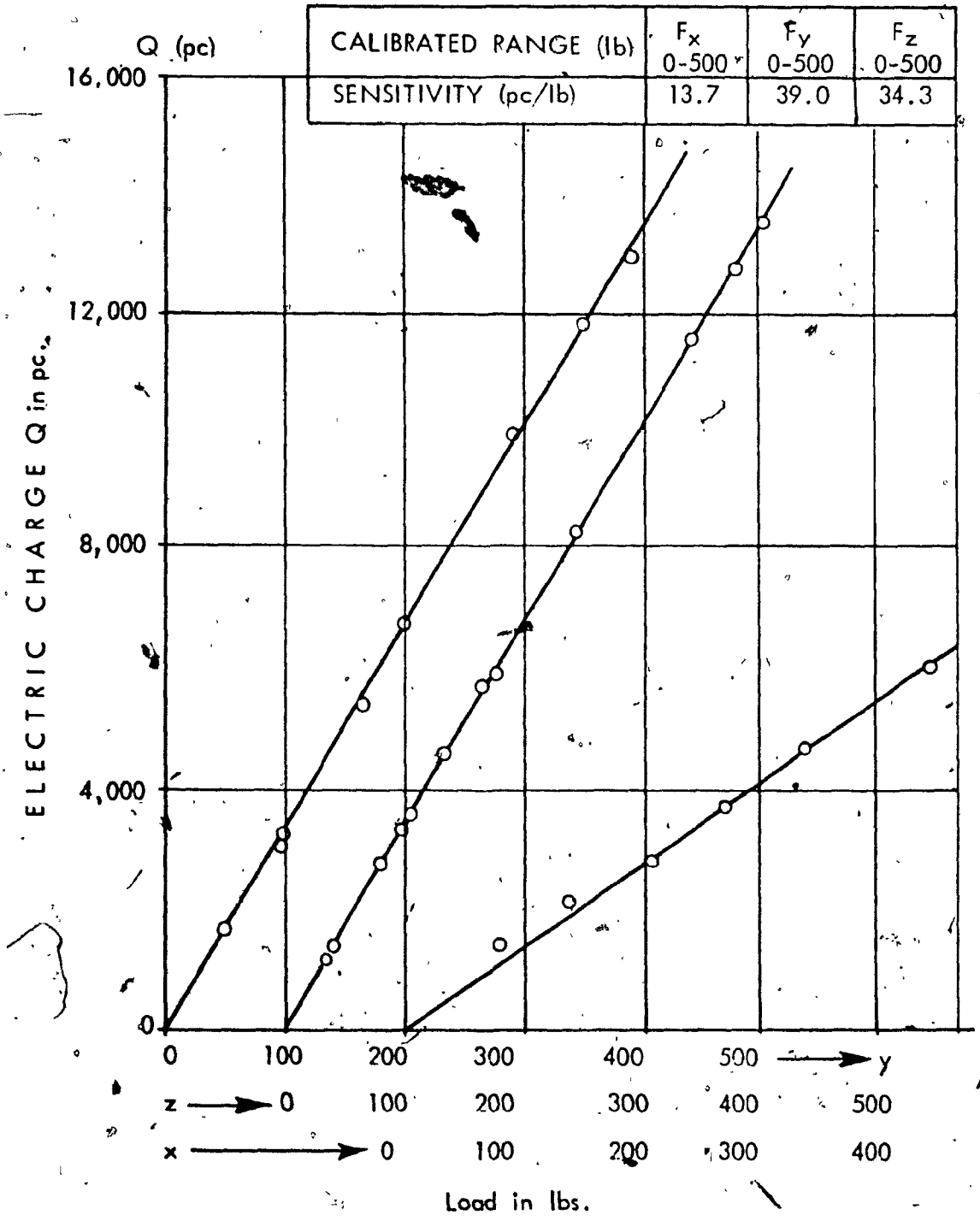

Figure 5.4 STATIC CALIBRATION CHART OF THE DYNAMOMETER

hysteresis loss is avoided, the loading was increased in short steps up to a maximum and decreased similarly down to zero. The loading and unloading curves were linear and were coincident for the range of loads applied. This shows that there was negligible hysteresis loss involved during the performance of calibration.

5.2.3 Dynamic Calibration : The purpose of dynamic calibration is to plot a chart from which a corrected dynamometer reading may be obtained at each frequency value over the entire frequency range that is of interest during the measurement of cutting forces. This can be achieved by determining the natural frequencies of the tool-dynamometer system along the three perpendicular directions of the components of the resultant cutting force and by finding the characteristics of the dynamometer in the frequency range of the cutting forces.

The natural frequencies of the dynamometer were determined using the impulse loading method. In this method a steel ball of 0.625 inch diameter was dropped from a certain height on each of the three faces of the tool. The frequency response curves for the system were observed on an oscilloscope and the natural frequencies were determined to be approximately 13 KHz along the radial direction and approximately 9 - 10 KHz in the other two directions.

To find the characteristics of the dynamometer in the

frequency range of the cutting forces measured, a dynamic load was then applied at the tool tip and kept constant by a feed back loop controlling the Brüel and Kjaer exciter. The schematic of the set up is shown in Figure 5.5. The frequency of the input dynamic load was varied from 20 Hz to 8 KHz and the magnitude of the output force was observed on the oscilloscope. A plot of the ratio of the input to output forces at different frequencies is shown in Figure 5.6. The plot shows that the ratio of input to output forces is almost unity up to a frequency of 8 KHz. This indicates that the static calibration of the dynamometer is not distorted upto a frequency of 8 KHz.

For finish turning operation, it is expected that the frequency of the cutting forces will not exceed 8 KHz. Experimental investigation carried out and described in chapter 6 justifies the validity of this statement. Hence, only the static calibration chart of the dynamometer is needed for the measurement of the cutting forces during all the cutting tests.

5.2.4 Cutting Force Measurements: The equipment used for conducting the cutting tests is divided into two groups. The first group consists of the dynamometer, the tool, the workpiece and the Lathe on which tests were carried out. The second group consists essentially of the electronic instrumentation for measuring and recording the dynamic characteristics of the cutting forces. The general layout of the set up is shown in

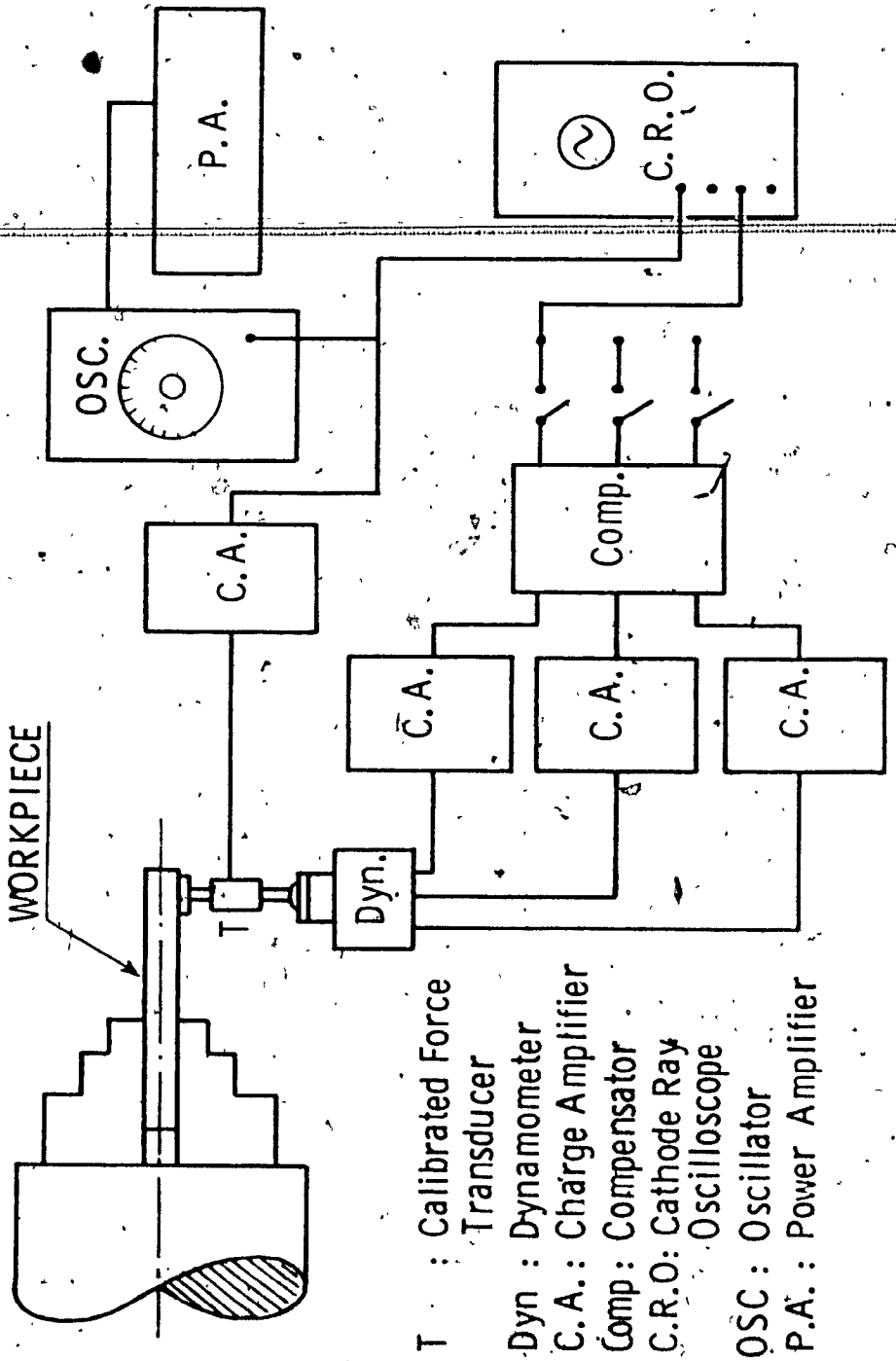

Figure 5.5 SCHEMATIC SET UP USED FOR DYNAMIC CALIBRATION

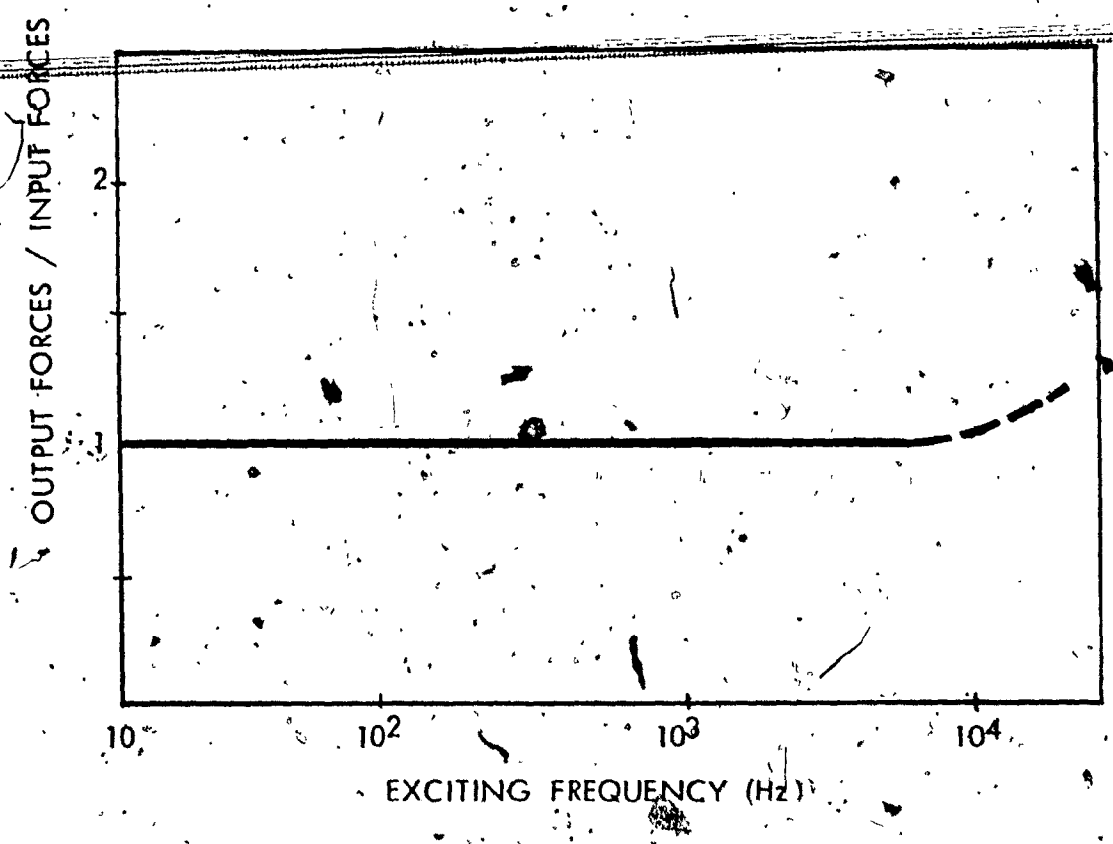

Figure 5.6 DYNAMIC CALIBRATION CHART OF THE DYNAMOMETER

Figure 5.7(a). A pictorial view of the test equipment is also presented in Figure 5.7(b).

A series of finish machining tests was performed on a 10 H.P. Demoor lathe with different cutting conditions obtained by varying the feed between 0.0017 and 0.008 in/rev and a depth of cut of .010 inches for different tool nose radii. The cutting forces were measured and recorded for each different feed on a magnetic tape. Recording of the dynamic cutting force signals was done with a "Sanborn" magnetic Tape Recorder. To minimize the loss of any higher frequencies of the cutting forces, recording must be carried out at the highest available speed. The maximum speed available on the recorder is 60 inches per second and this speed was used for recording the cutting force signals.

The procedure was repeated with tools of three different radii, namely, 1/64 in., 1/32 in. and 3/64 in. The material used in the tests was AISI 1015 steel. Figure 5.8 illustrates typical records of dynamic cutting forces obtained during the tests. This indicated that the cutting forces are essentially random in nature and are present over a wide frequency range.

5.2.5 Accuracy of the Cutting Force Measurements: In order to obtain an accurate reading of the dynamic variation of the cutting forces, the static force or the mean steady state component was measured separately from the superimposed ran-

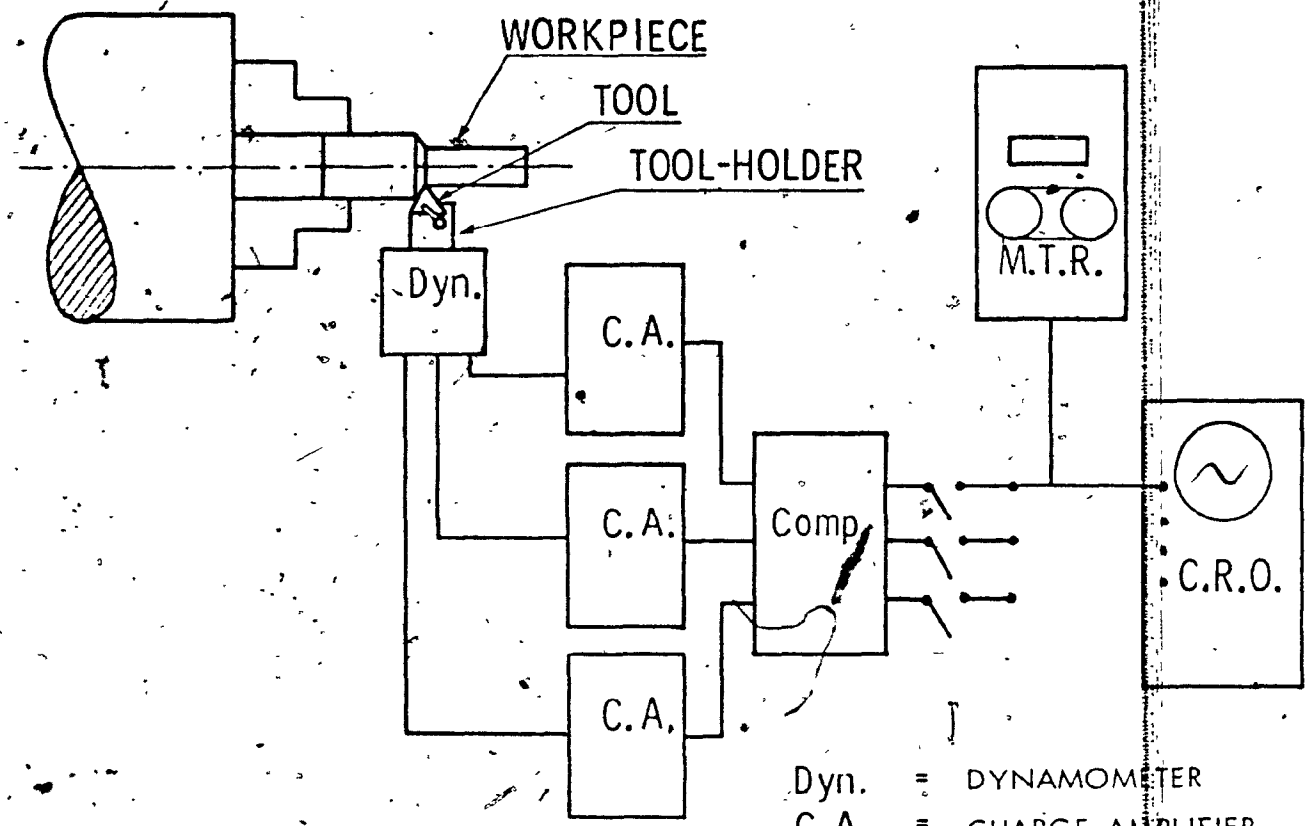

Dyn. = DYNAMOMETER
C.A. = CHARGE AMPLIFIER
Comp. = COMPENSATOR
C.R.O. = CATHODE-RAY OSCILLOSCOPE
M.T.R. = MAGNETIC TAPE RECORDER

Figure 5.7(a) DIAGRAMMATIC REPRESENTATION OF THE SET UP USED FOR THE MEASUREMENT OF THE CUTTING FORCES

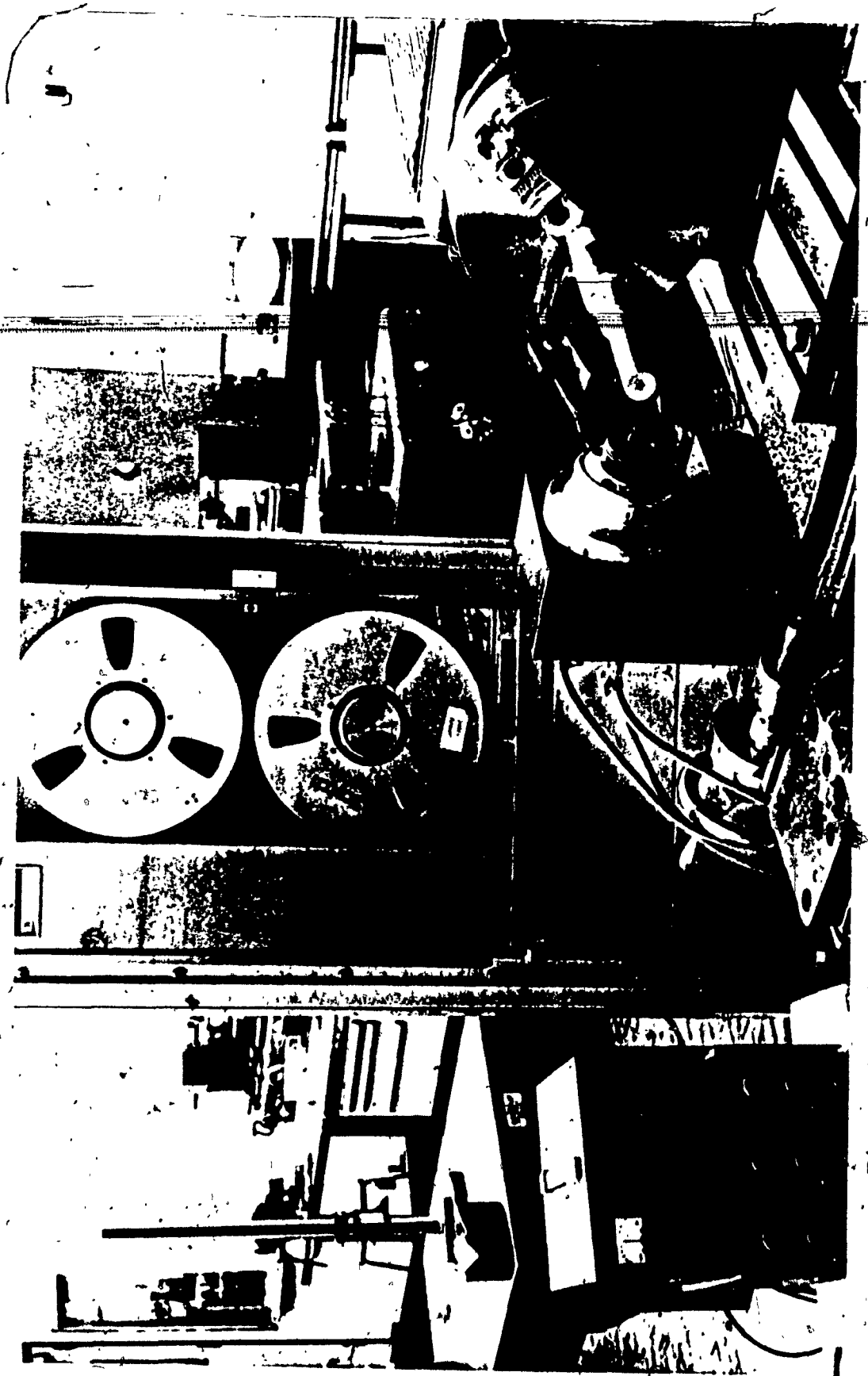

Figure 5.7(b) PICTORIAL VIEW OF THE EQUIPMENT USED IN THE SET UP FOR CUTTING FORCE MEASUREMENTS

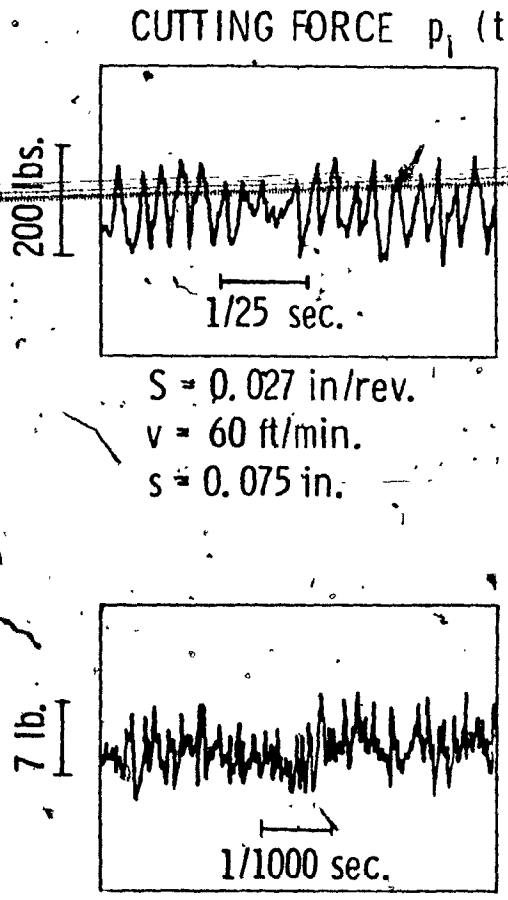

Figure 5.8. TYPICAL RECORDS OF THE CUTTING FORCE FLUCTUATIONS

-domly fluctuating component. The steady state component of the force was measured by setting the time constant of the charge amplifiers to "long", which in effect changes the time constant of the measuring system to a high value. To measure the random fluctuations of the cutting forces that act over the steady, static component, the charge amplifiers were switched to the "reset" position and then to the "operate" mode. This has the effect of shifting the output signals with respect to the static force as the datum to a zero level. Then the time constant switch on the charge amplifiers was changed from "long" to "short" position and thereby increasing the sensitivity of the amplifier. A line diagram showing the effect of resetting the charge amplifier to a more sensitive range is presented in Figure 5.9.

5.3. Surface Roughness Measurements

5.3.1 M- and E- Systems: Several measuring methods have been developed to characterize the profile of a machined surface. All these methods are based on the assessment of surface texture by measuring the deviation of the measured surface profile from a defined reference profile. The most commonly used methods are the M-system or the mean line system and the E-system, or the envelope system. The principal concepts of these measuring techniques are illustrated in Figure 5.10.

In the M-system, a reference line is so positioned that the sum of the squares of the departures of the signals from

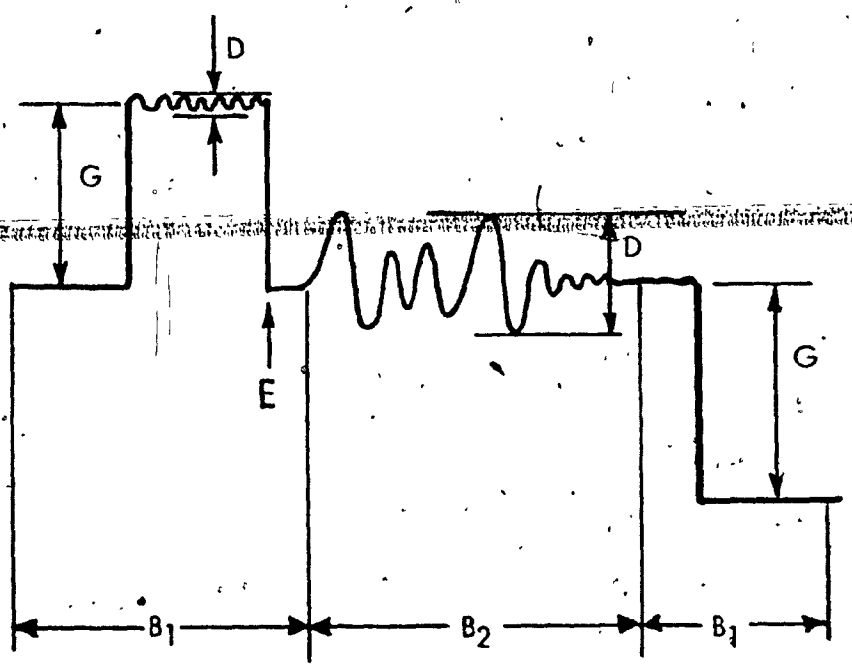

B_1 = RANGE 1 (eg. 100 lb/v)

B_2 = RANGE 2 (eg. 5 lb/v)

G = STATIC FORCES

D = SUPERIMPOSED DYNAMIC FORCES

E = AMPLIFIER RESET

Figure 5.9 LINE DIAGRAM SHOWING THE EFFECT OF RESETTING THE CHARGE AMPLIFIER TO HIGHER SENSITIVITY

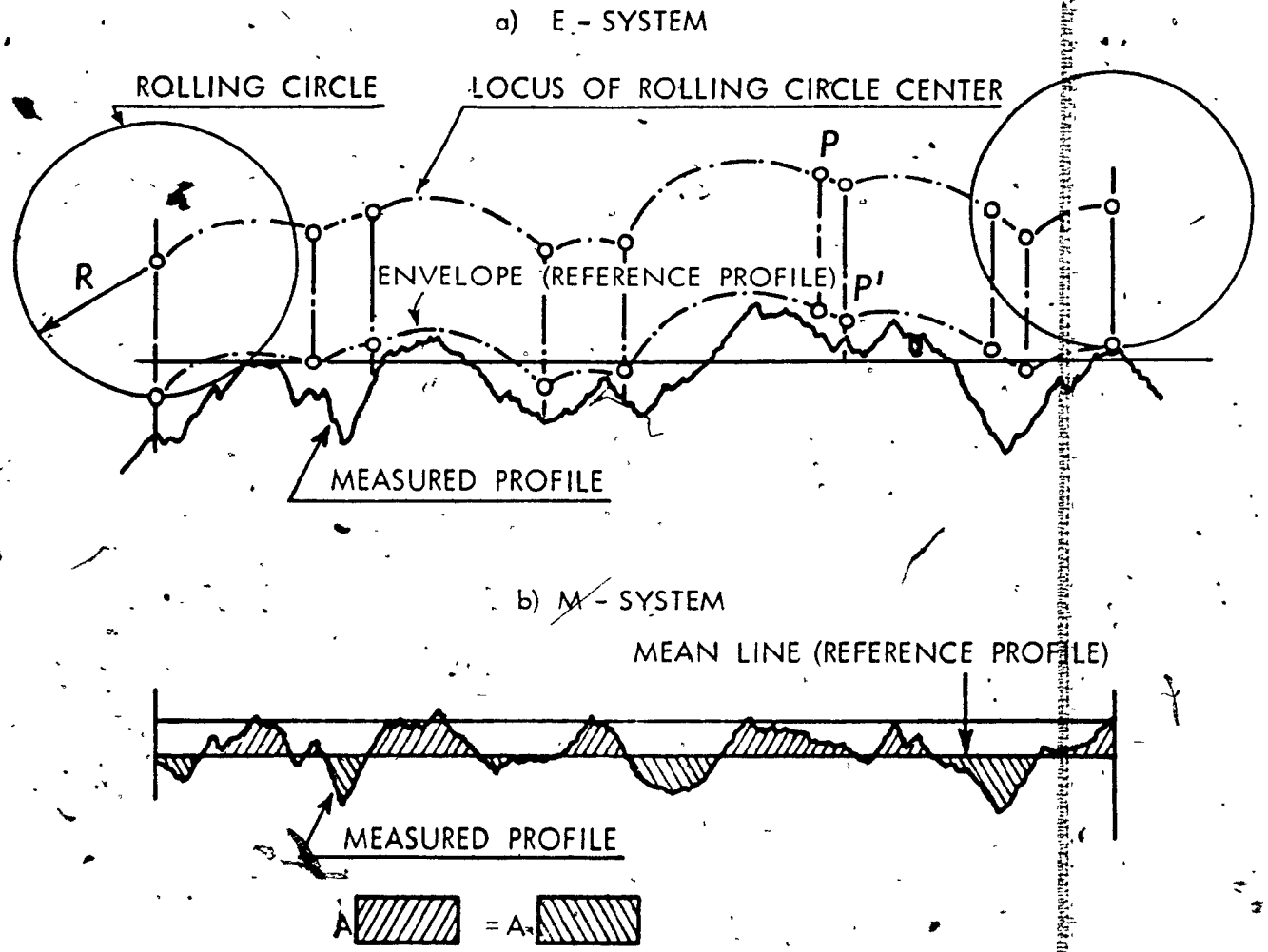

Figure 5.10 DEFINITION OF MICRO-GEOMETRICAL ERROR OF A MANUFACTURED SURFACE IN E - AND M - SYSTEM.

the reference line has a minimum value. The indices measured are expressed either in terms of root-mean square value or centre line average (CLA) value. In the E-system the reference line is defined by the envelope produced by a rolling circle on the surface. The radius of the rolling circle determines uniquely the area enclosed between the actual surface profile and the envelope reference profile and serves as an exactly defined high-pass filter. Unfortunately, until now there is no commercial measuring device based on the principle of the E-system because of the difficulty in separating the surface roughness from the waviness and error of form. On the other hand, the reference profile in the M-system is created solely by the function of the electronic high-pass filter incorporated in the measuring device.

The measuring equipment used in the present investigation are Taylor Hobson Talysurf 4 and Talyrond 51. Both Talysurf 4 and Talyrond 51 use the principle of the M-system in their design.

5.3.2 Surface Roughness in a Turning Operation: In a turning operation the surface textures that determine the finish are: a) transverse or circumferential roughness along the cutting direction and b) longitudinal roughness along the feed direction. These two surface textures are closely inter-related because the longitudinal surface finish is formed by successive sets of circumferential roughnesses. It has also been shown by

Osman and Sankar [34] that the CLA-value in the longitudinal direction is approximately 97% of the CLA-value in the transverse direction. This means that either of the two surface finishes can be considered to represent the texture of the machined component. Normally, the longitudinal roughness is easier to measure and may, in general, be taken to represent the surface quality of the product.

Even though the longitudinal surface finish could represent reasonably the effect of the cutting forces in turning, the accuracy of the results can be improved by evaluating the surface profiles along the circumferential or along the cutting direction. With the circumferential characteristics of a surface profile, more reliable relationships between the cutting forces and the surface texture may be obtained.

Measurement of Longitudinal Roughness: The longitudinal surface roughness of the workpiece was measured and recorded after each cutting test using Taylor-Hobson Talysurf 4 instrument. The set up used is illustrated in Figure 5.11. The Talysurf 4 makes use of a sharply pointed stylus to trace the profile of the surface irregularities. A flat shoe on a rounded skid is used for providing a datum from which deviations of surface profiles are measured. The pick-up carrying the stylus and skid is traversed across the surface by means of a motorized unit. Using an inductive transducer the up and down movements of the stylus, relative to the skid or the shoe, are converted

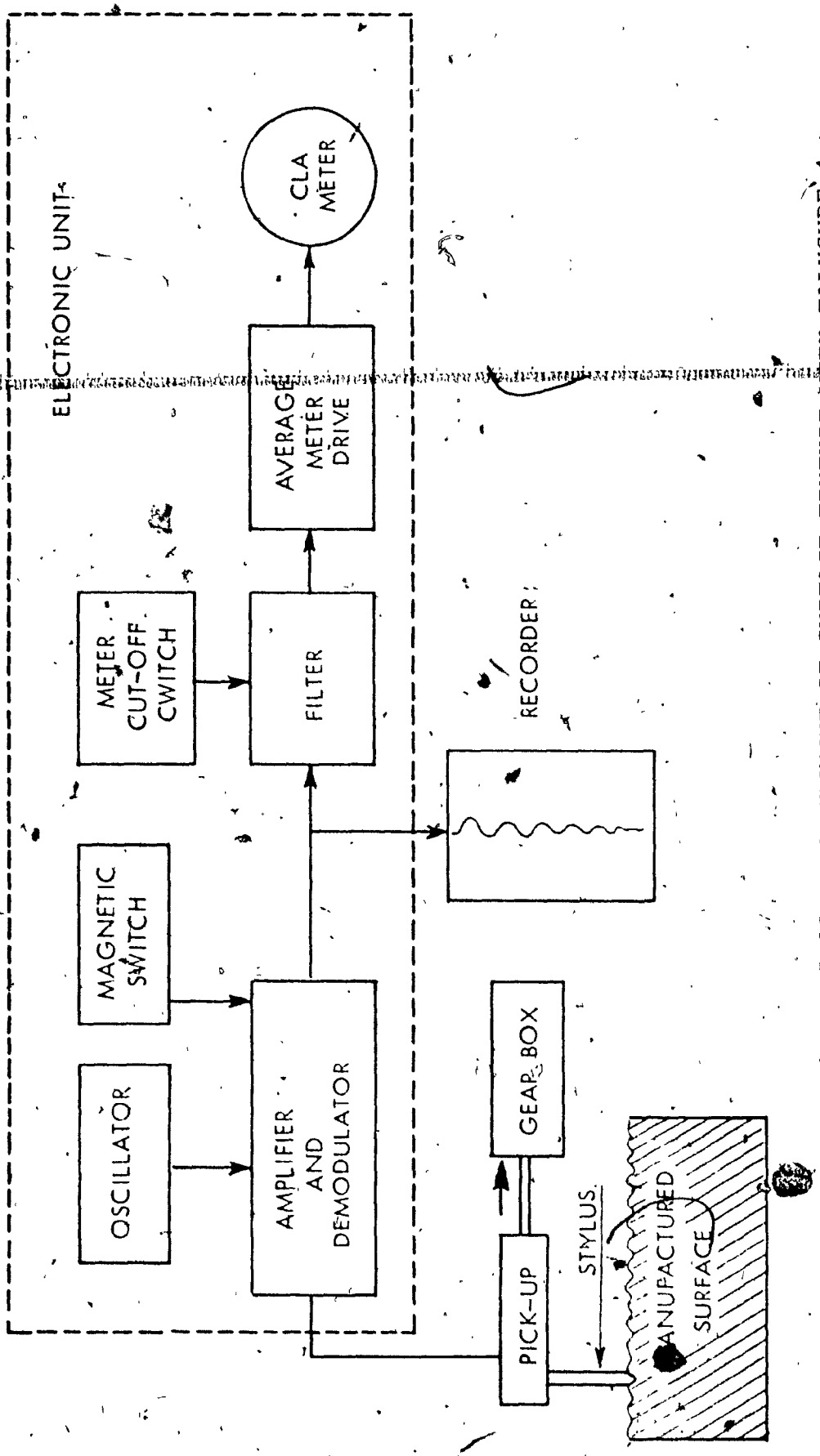

Figure 5.11 MEASUREMENT OF SURFACE TEXTURE WITH TALYSURF 4

into corresponding changes in electric current. These changes are amplified to control an "averaging" meter from which the CLA-values of all irregularities coming within a standardized length of surface such as 10 mm., 2.5 mm., or 0.8 mm. can be read. The electric current generated drives a graph recorder to trace a record of the surface profile measured. Typical records obtained during the tests and their CLA-values are presented in Figure 5.12.

Measurement of Transverse Roughness: Taylor Hobson Talyrond 51 was used for measuring the surface roughness in the transverse or circumferential direction of the workpiece. The diagrammatic representation of the set up is indicated in Figure 5.13. Talyrond 51 measuring device works on the principle that an electrically operated displacement indicator carried on an optically aligned precision spindle of extreme accuracy is rotated outside the surface to be measured. The workpiece itself remains stationary on the worktable. The signal from the indicator is amplified and then applied to a polar coordinate recorder giving radial ordinates of the profile. The rotation of the chart on the recorder is synchronized with that of the indicator spindle. Talyrond 51 is normally employed for measuring the out-of-roundness or the circumferential waviness of the profile of a turned component. With the help of a special filter, this device can also be used for the measurement of circumferential roughness which is formed

MATERIAL : AISI 1015 STEEL

S = 0.01 in.

v = 375 ft/min.

r = 1/64 in.

SURFACE ROUGHNESS PROFILE

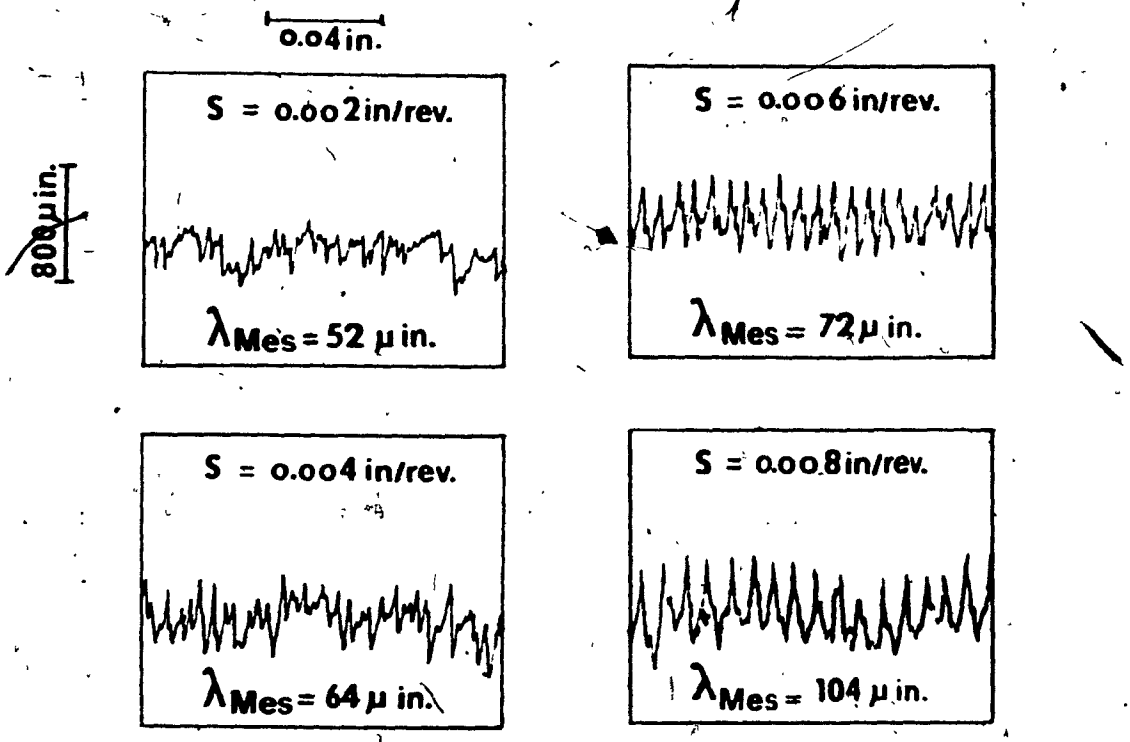

Figure 5.12 TYPICAL RECORDS OF SURFACE ROUGHNESS AND THEIR CLA-VALUES AS MEASURED BY TALYSURF 4

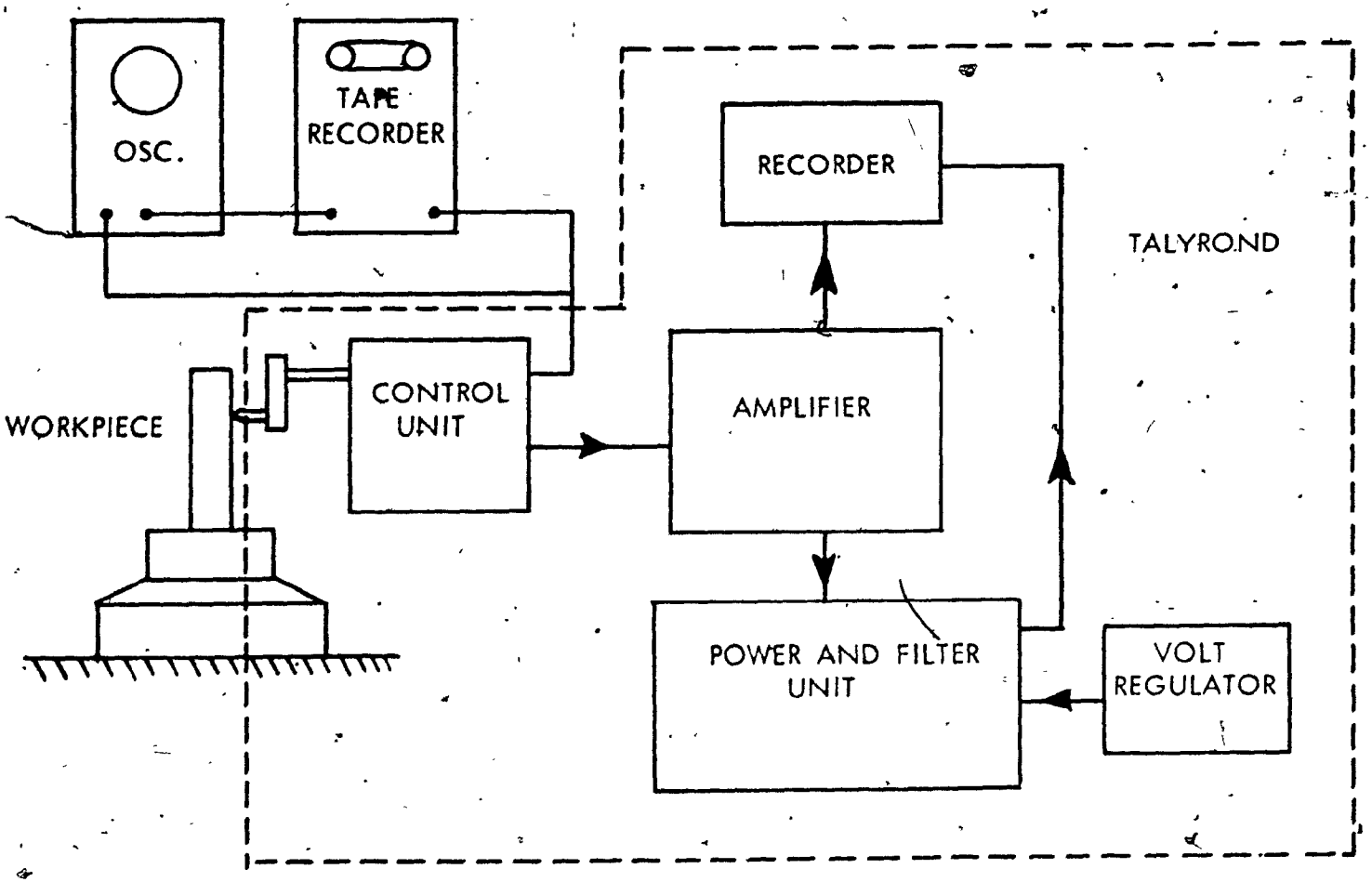

Figure 5.13 DIAGRAMMATIC REPRESENTATION OF THE SET UP FOR MEASURING SURFACE PROFILE WITH TALYROND 51

over the waviness of the part.

In the present investigation, the amplitude fluctuations in the transverse direction are of interest and all the measurements taken with the Talyrond were filtered to eliminate the frequency of out-of-roundness of the component. A typical record showing the amplitude fluctuations of the circumferential roughness is presented in Figure 5.14.

The longitudinal and transverse surface roughness signals recorded during the experimentation were then analyzed to obtain various stochastic parameters of the surface roughnesses and are described in Chapter 6. The measured CLA-values of the surfaces obtained from longitudinal roughness measurements with the Talysurf 4 instrument compared favourably with those given by the computer analysis of the roughness profile obtained using the Talyrand 51 instrument.

Further, the CLA-value of the surfaces computed analytically from the tool-workpiece response given by the equation (3.45) are compared with the measured CLA-values of the surface and found to agree within ±10% of each other as is elaborated in Chapter 6.

5.4 Experimental Determination of the Damping Coefficient of the Machine-Tool-Workpiece System

5.4.1 General: The frequency response of a linear system may be employed for the determination of the damping coefficient of the system. In the case of vibration of a machine-tool-

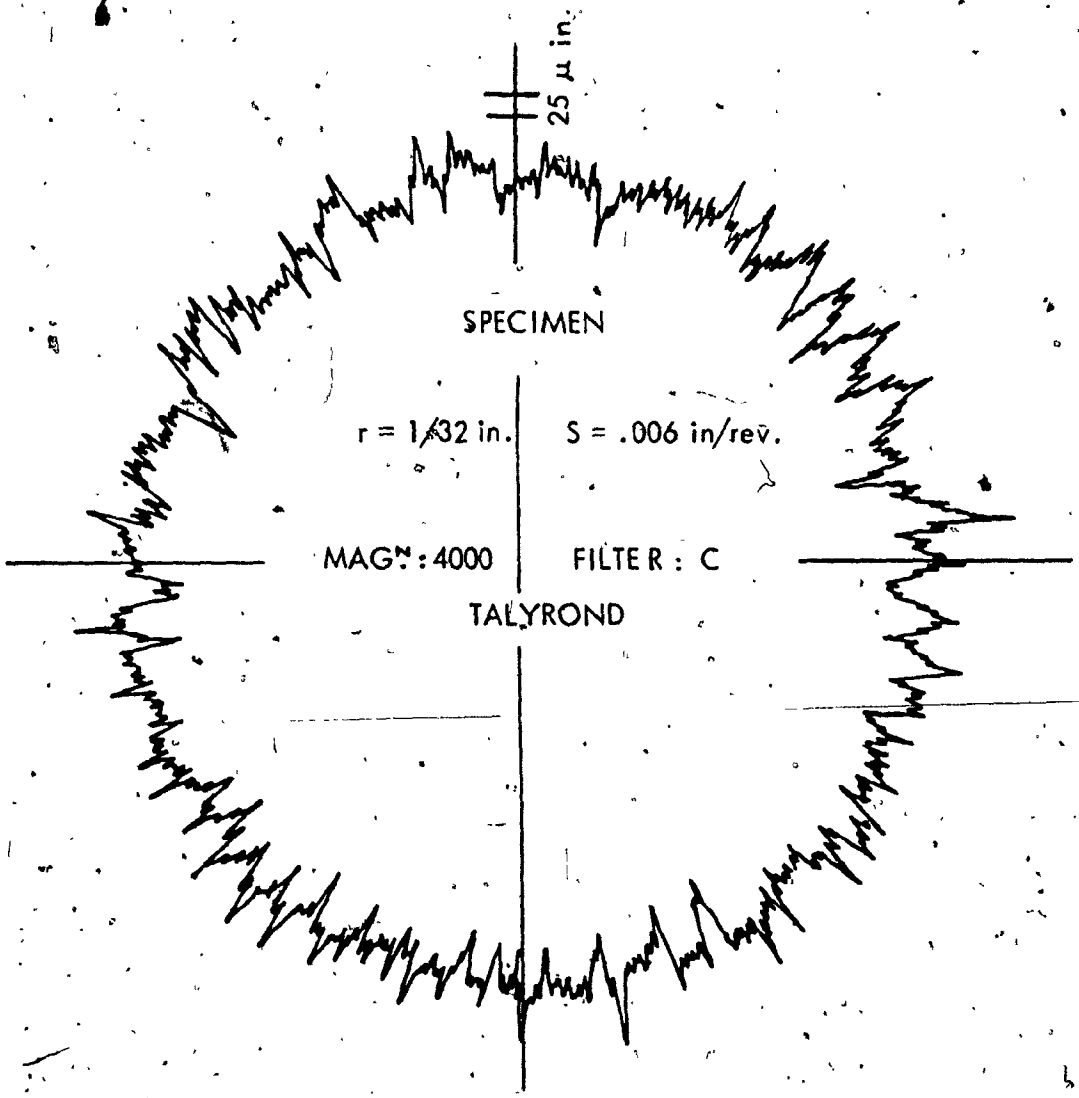

Figure 5.14 TYPICAL RECORD OF SURFACE ROUGHNESS MEASURED WITH TALYROND 51

workpiece system, the frequency response can be obtained by introducing a harmonic exciting force between the tool and workpiece thus simulating the dynamic cutting conditions. In the particular case of turning, the response in the direction of the main cutting force is of importance and therefore it is essential to excite the machine tool system in this particular direction to obtain the total vibrational characteristics of the machine-tool-workpiece system.

Even though, in Chapter 3, the mathematical model of the machine-tool-workpiece is a two degrees-of-freedom system for computing the dynamic response of the tool-workpiece unit, the machine tool is assumed to be a single degree-of-freedom system in order to evaluate the equivalent viscous damping coefficient through an experimental investigation of the problem. It is then assumed in the present investigation that the viscous damping factor obtained under the assumption of a single degree-of-freedom for the machine tool system can represent approximately the uncoupled damping coefficient to be used in evaluating the response using equation (3.45)

Then, for a single degree-of-freedom machine tool system the differential equation of motion may be written as

$$\ddot{q} + 2\zeta\omega_1\dot{q} + \omega_1^2 q = P_o + p(t) \qquad (5.2)$$

where q is the principal mode response amplitude of the machine tool due to the dynamic forces

ζ is the equivalent viscous damping factor, and

ω_1 is the first critical frequency.

The exciting function in equation (5.2) has been written in terms of a steady state static component P_o and a dynamical component p(t). Under purely dynamic consideration, equation (5.2) may be considered in the form

$$\ddot{q} + 2\zeta\omega_1\dot{q} + \omega_1^2 q = p(t) \qquad (5.3)$$

The static stiffness K_s of the machine tool determines the resistance of the system against the static component of the cutting force P_o. The damping factor ζ and the first undamped critical frequency ω_1 should be known if the dynamic response of the machine-tool-workpiece is to be investigated. The damping factor ζ includes the internal damping due to hysteretic friction and the external damping due to fluid couplings in the bearings, joints, guideways of the machine and in the cutting zone.

The actual values of K_s, ω_1, and ζ may be experimentally obtained if the frequency response curve for the machine tool system is available. In this test procedure, the machine tool system is subjected to excitation of known amplitude F_0 and variable frequencyω in the direction of the primary cutting force component and the response amplitudes X are measured over the frequency range. By noting the amplitude X_o at $\omega/\omega_1 \simeq 0$ and the amplitude X corresponding to any arbitrary

frequency ratio ω/ω_1, the values of K_s, ω_1 and ζ can be obtained from the following equations that are derived from basic forced vibration analysis of one degree-of-freedom linear mechanical systems.

$$K_s = \frac{F_o}{X_o}$$

$$\omega_1 = \left(\frac{K_s}{m}\right)^{\frac{1}{2}} \qquad (5.4)$$

and

$$\zeta^2 = \frac{1}{4\left(\frac{\omega}{\omega_1}\right)^2}\left[\left(\frac{X_o}{X}\right)^2 - \left\{1 - \left(\frac{\omega}{\omega_1}\right)^2\right\}^2\right] \qquad (5.5)$$

where m is the equivalent mass of the vibratory elements of the machine tool system, for example, spindle, chuck, work-piece, etc.

Equation (5.5) shows that the value of the damping factor ζ can be calculated for any value of the exciting frequency ω if the fundamental frequency of vibration ω_1, the response amplitude X at the frequency of interest and the response amplitude X_o at $\omega = 0$ are known. To determine the response amplitudes at different exciting frequencies a frequency response test is carried out on the machine tool as described in the following section.

From the knowledge of ζ, the damping coefficient C can be directly computed. The value of C is then used in equation (3.45) to determine the tool-workpiece response under random cutting forces.

5.4.2 Experimental Evaluation of ζ: To evaluate the value of the damping factor ζ a frequency response test was carried out on the machine-tool-workpiece system. Figure 5.15(a) illustrates the schematic diagram of the set up used and a pictorial view is presented in Figure 5.15(b). A certain preload was applied to the workpiece by controlling the d.c. level of the excitor. The frequency of excitation was then gradually varied from values well below and above the first natural frequency until the response curve of the system was obtained. To obtain a reasonably accurate response curve it is essential that the magnitude of the exciting force remains at constant value throughout the test. Normally, the magnitude of the exciting force tends to decrease as the frequency of excitation is increased. The excitor control is provided with a feed back loop at the compressor mode and tests were carried out with the excitor control switched to this mode in order to ensure that the exciting force remained constant throughout the experiment.

The frequency response curve plotted by the level Recorder is presented in Figure 5.16. This figure shows the response amplitudes obtained at different exciting frequencies and

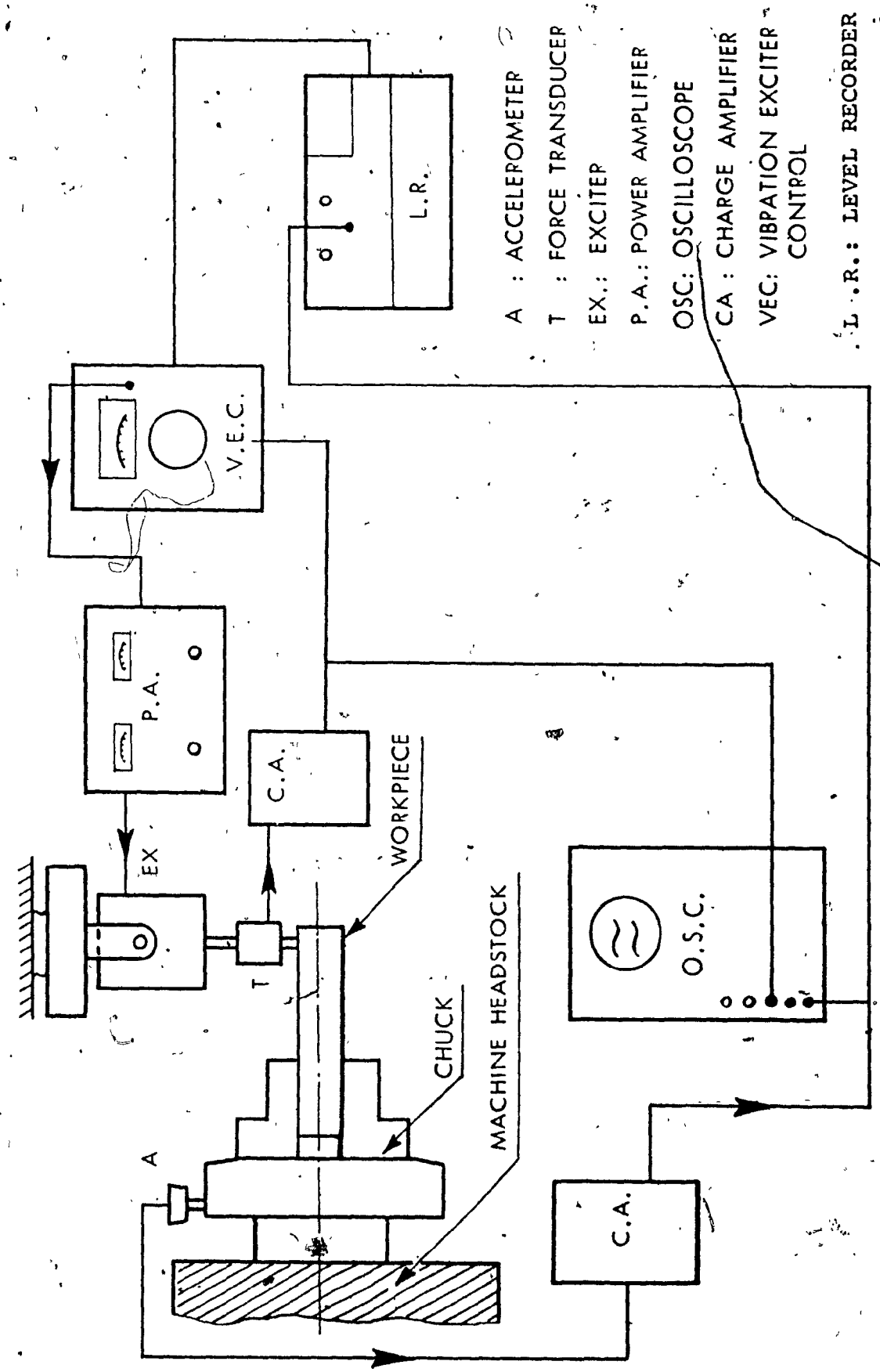

Figure 5.15(a) SCHEMATIC OF THE SET UP FOR A FREQUENCY RESPONSE TEST

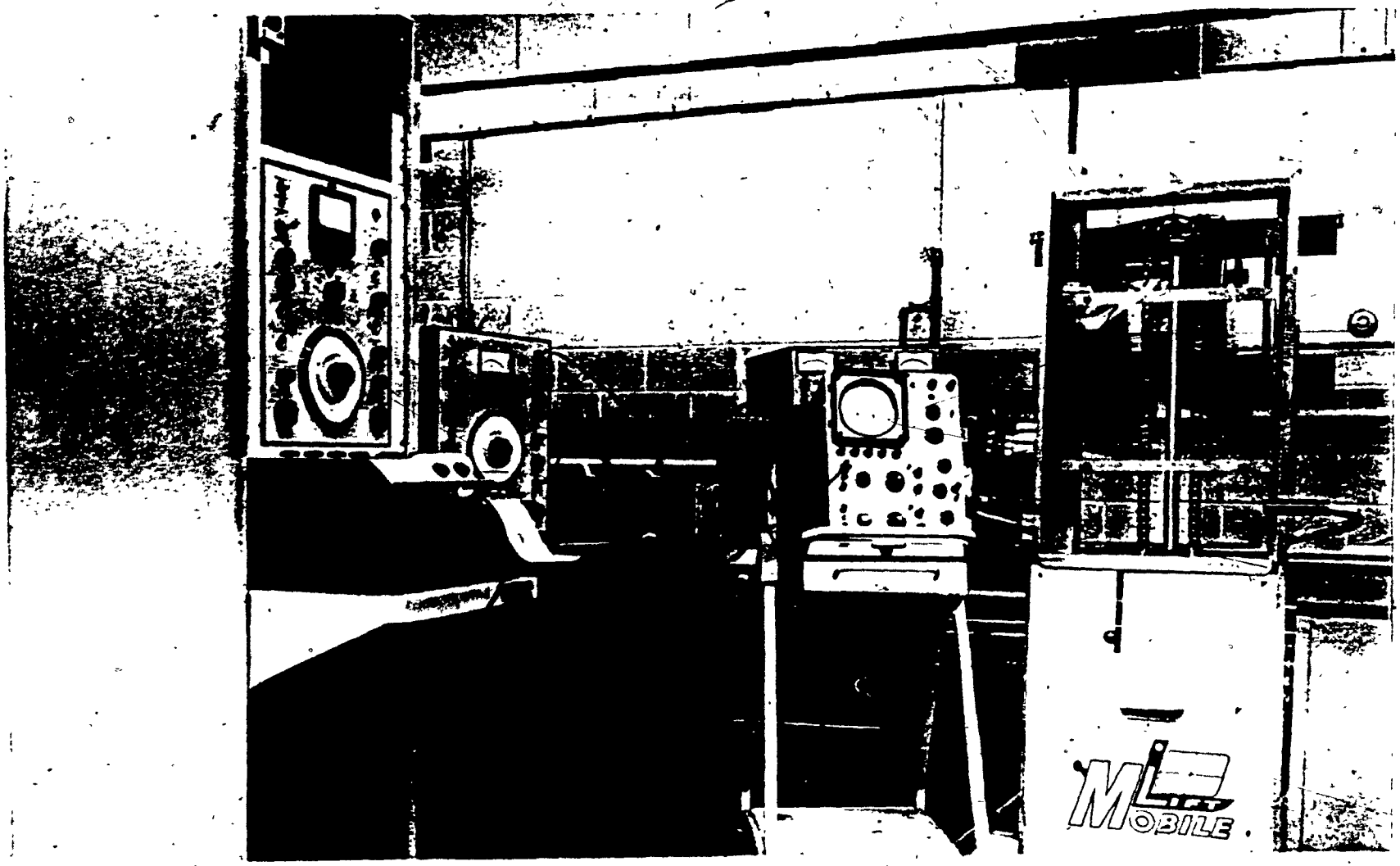

Figure 5.15(b) PICTORIAL VIEW OF THE EQUIPMENT USED FOR FREQUENCY RESPONSE TEST

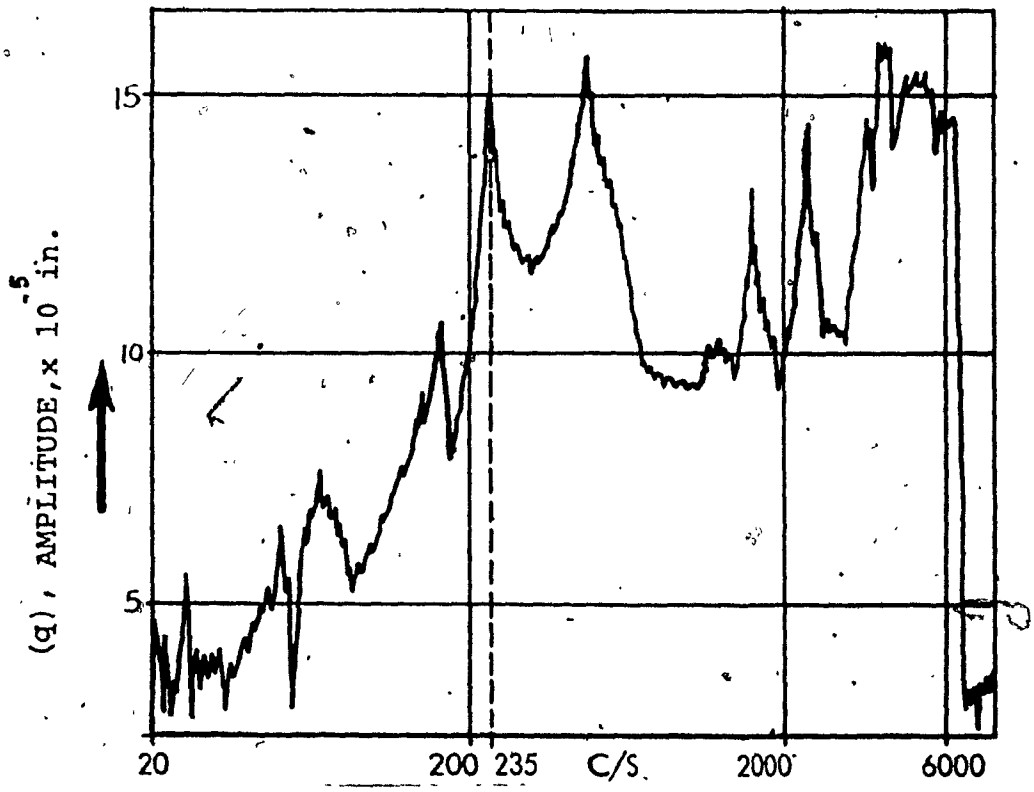

Figure 5.16 FREQUENCY RESPONSE CURVE OF THE MACHINE-TOOL-WORKPIECE SYSTEM

indicates that damped natural frequency of the system is at 235 Hz.

Calculation of the damping factor ζ and the damping coefficient C

The value of ζ evaluated near the damped natural frequency is taken to be the damping factor of the machine tool system. The values of X and X_o are read from the frequency response curve illustrated in Figure 5.16. Substituting these values in equation (5.5), the value of ζ is calculated as 0.14. The detailed calculation procedure is presented in Appendix I. Now, from the relationship

$$\zeta = \frac{C}{C_C}$$

$$= \frac{C}{2m\omega_{n1}}$$

the value of the damping coefficient C can be determined. It is calculated as

$$C = 275 \text{ lb.sec/in}$$

Discussion of Results: In a system like machine tool there is normally a large damping present because of the various bearings, joints and guideways and the value of ζ may be expected to be higher than 0.14 as obtained in this investigation. The reason that the damping factor ζ obtained is of low value is the difficulty of obtaining an accurate response

curve of the system. An accurate frequency response curve can be obtained only by exciting the machine spindle directly. Since the machine spindle was not accessible for applying external forces in the present investigation, the frequency response was obtained by exciting the workpiece. Hence the frequency response curve thus obtained represents only that of the tool-workpiece system.

Further, even if the value of the damping coefficient C is accurate it does not change the tool workpiece response as shown by the equation (3.45) to any great extent. In the present investigation the tool-workpiece response is of importance since it primarily affects the formation of surface texture. Thus, a lower value of C will not affect the evaluation of the surface texture. The value of C becomes particularly important while determining the stability criteria for the machine tool system as a unit.

CHAPTER 6

ANALYSIS OF THE CUTTING FORCE AND SURFACE TEXTURE SIGNALS

CHAPTER 6

ANALYSIS OF THE CUTTING FORCE AND SURFACE TEXTURE SIGNALS

Experimental investigations carried out to measure the random cutting forces and surface roughness signals have already been described in the previous chapter. These signals were recorded to analyse their stochastic properties. For this purpose the frequency analysis, spectral density analysis and probability density analysis of the signals were performed as described in this Chapter.

To establish the relationships that may exist between stochastic parameters of the cutting force and surface roughness, it is necessary to analyse these signals obtained on a specific length (equal to the circumference) of the workpiece. In the present investigation, an analysis of both force and surface signals corresponding to one revolution of the workpiece is performed.

6.1 Frequency Analysis

The purpose of frequency analysis is to find the dominant frequencies of a signal that are identified by relatively large amplitude values. In the present investigation, the cutting force and the corresponding surface profile signals were analyzed to determine the frequency zones at which the signals have significant amplitudes. A Brüel and Kjaer

Frequency Analyzer Type 2107 possessing a frequency range of 20 Hz to 20 KHz was used for this purpose. The set up used is described in Figure 6.1(a), with a photograph shown in Figure 6.1(b). The recorded signals from the cutting tests and surface texture measurements reported in Chapter 5 were fed from the tape recorder to the frequency analyzer and the results of the analysis are plotted with a level recorder.

Typical frequency spectrum for the cutting force and the surface texture signals obtained are presented in Figures 6.2 and 6.3. Results indicate that the dominant cutting force frequencies are present in the range 1 KHz to 3 KHz. The occurrence of some large amplitudes at frequencies below 50 Hz in the spectrum are due to interaction of the cutting force signals with the rotational frequency of the machine tool. Further, the frequency components of the cutting force are spread over a wide range. Hence by neglecting the frequency components below 50 Hz no appreciable error is introduced in the analysis of the cutting force. The surface roughness frequency spectrum, on the other hand, does not show any significant frequency components above 1 KHz. The presence of lower frequency components in the surface signal indicates that the tool-workpiece response induced by the random cutting forces, is not fully reproduced on the workpiece surface, due to the transfer characteristics between the tool and workpiece. The complex thermodynamic process involved in

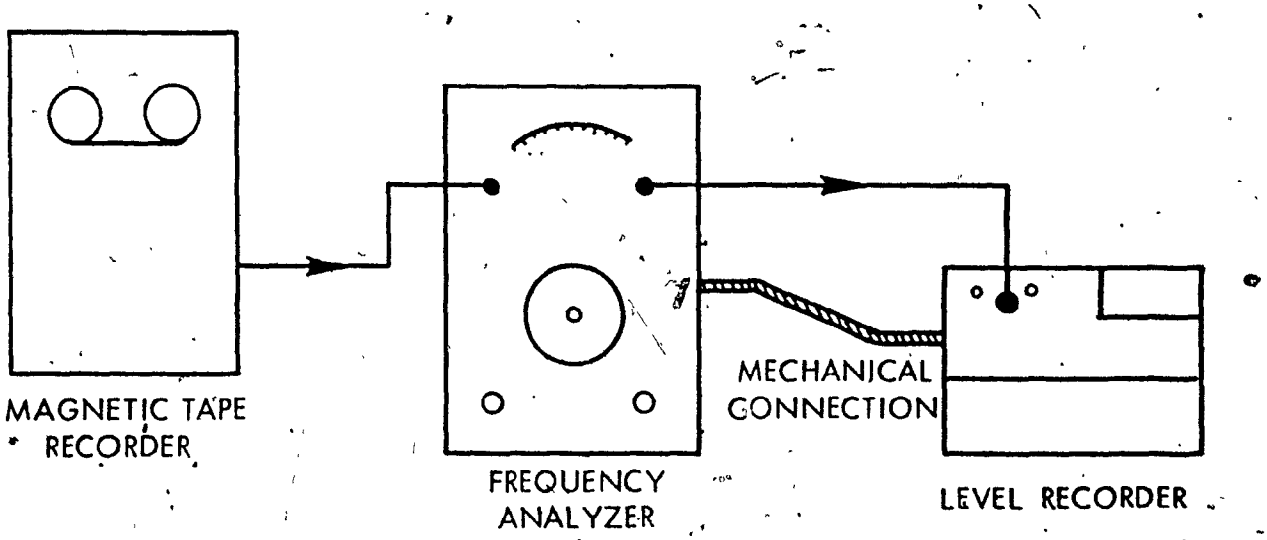

Figure 6.1(a) SCHEMATIC OF THE SET UP USED FOR FREQUENCY ANALYSIS OF THE RANDOM SIGNALS

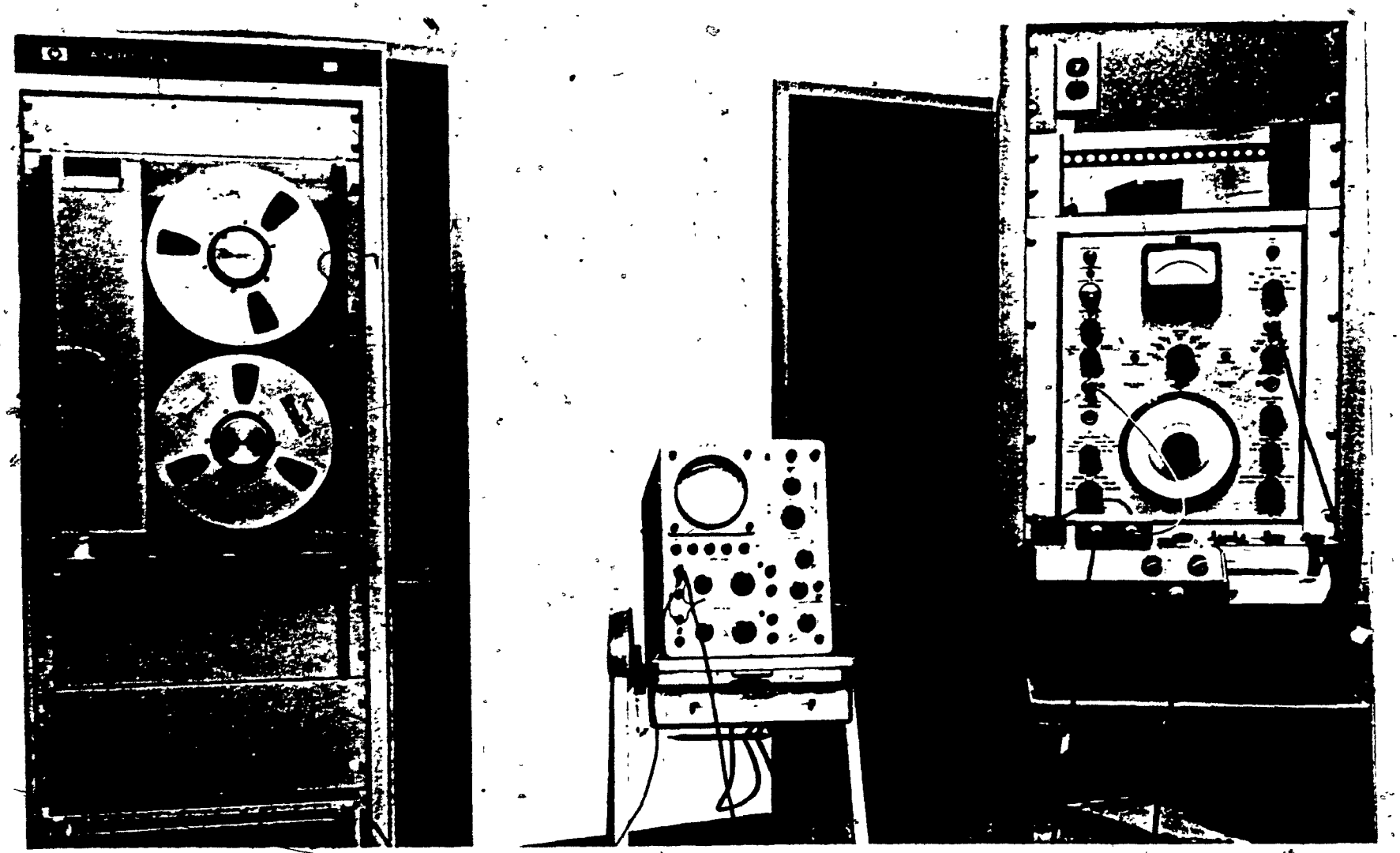

Figure 6.1(b) PICTORIAL VIEW OF THE EQUIPMENT USED FOR FREQUENCY ANALYSIS OF RANDOM SIGNALS

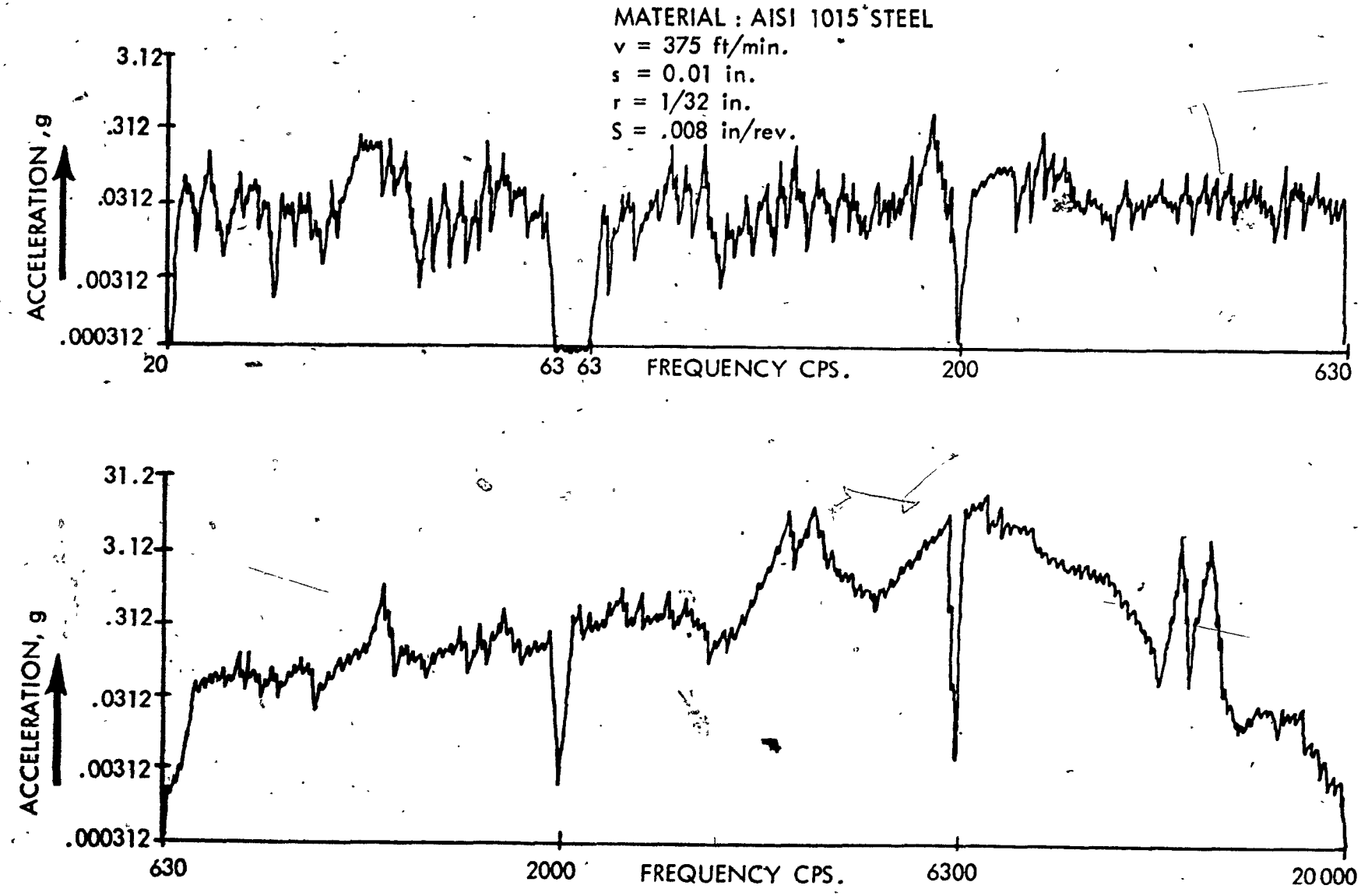

Figure 6.2 FREQUENCY SPECTRUM OF THE CUTTING FORCES

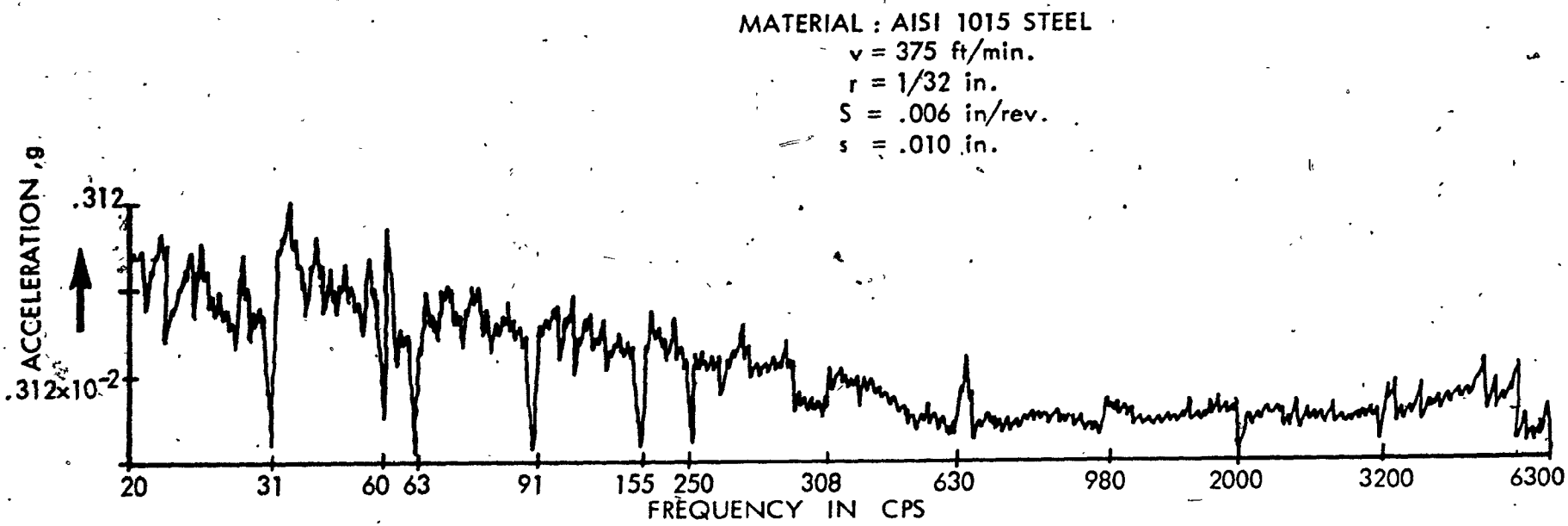

Figure 6.3 FREQUENCY SPECTRUM OF THE SURFACE ROUGHNESS

the cutting zone, damping in the machine tool system, etc. act as a low pass filter between the tool and workpiece, thus absorbing high frequency components.

6.2 Spectral Density Analysis

A spectral analysis of a signal provides information on the power content of the signal at various frequencies. Such an analysis is particularly important when the signal processed is random in nature and consists of a wide range of frequencies. Spectral analysis, like frequency analysis, also shows the dominant frequency bands of a signal. In other words, this analysis might serve as a check for the results obtained from frequency analysis. Further, to obtain the tool-workpiece response from the knowledge of the cutting forces as described in equation (3.45), it is essential that the spectral densities of the cutting forces be known.

To measure the spectral density of the cutting force fluctuations and the surface roughness, the recorded signals were fed through an automatic shock-random equalizer-analyzer (Brüel and Kjaer type number 3379B). The set up employed is illustrated in Figure 6.4(a) along with a photograph of the layout of all the instruments shown in Figure 6.4(b). The automatic equalizer-analyzer system used has a maximum frequency coverage from 20 Hz to 2 KHz, and features a very flexible arrangement of a number of filter channels. The bandwidths of these filters vary from 10 Hz to 50 Hz with

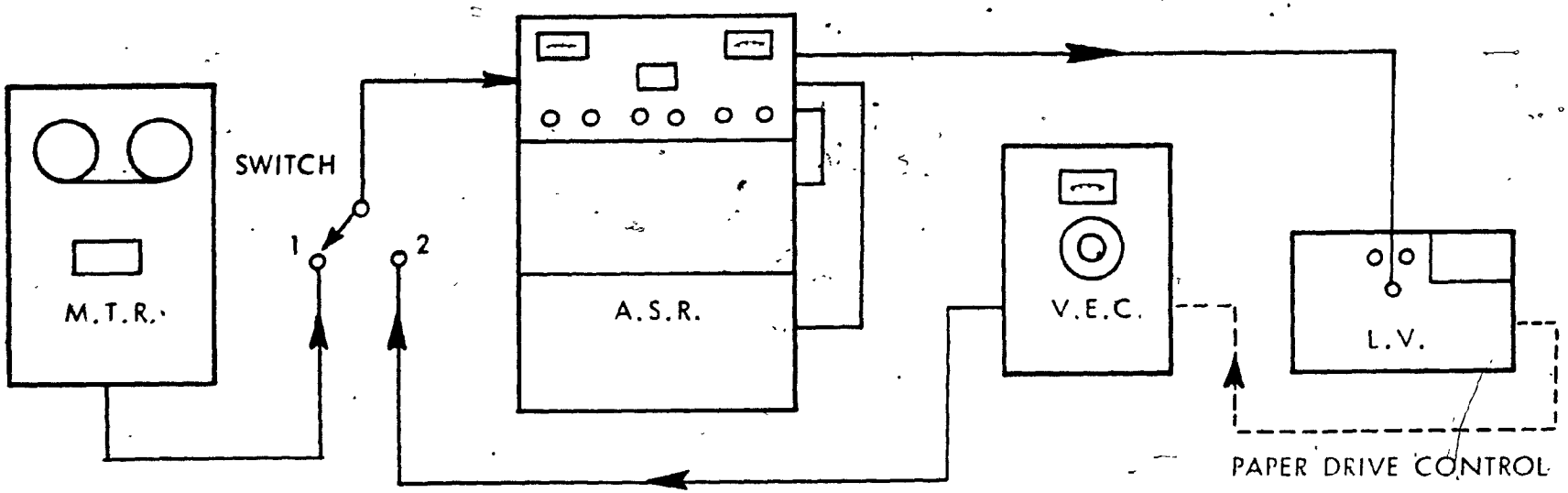

A.S.R. : AUTOMATIC SHOCK-RANDOM EQUALIZER ANALYZER

V.E.C. : VIBRATION EXCITER CONTROL

L.V. : LEVEL RECORDER

M.T.R : MAGNETIC TAPE RECORDER

Figure 6.4(a) DIAGRAMMATIC REPRESENTATION OF THE SET UP USED FOR MEASURING THE POWER SPECTRAL DENSITY OF THE CUTTING FORCES AND SURFACE ROUGHNESS

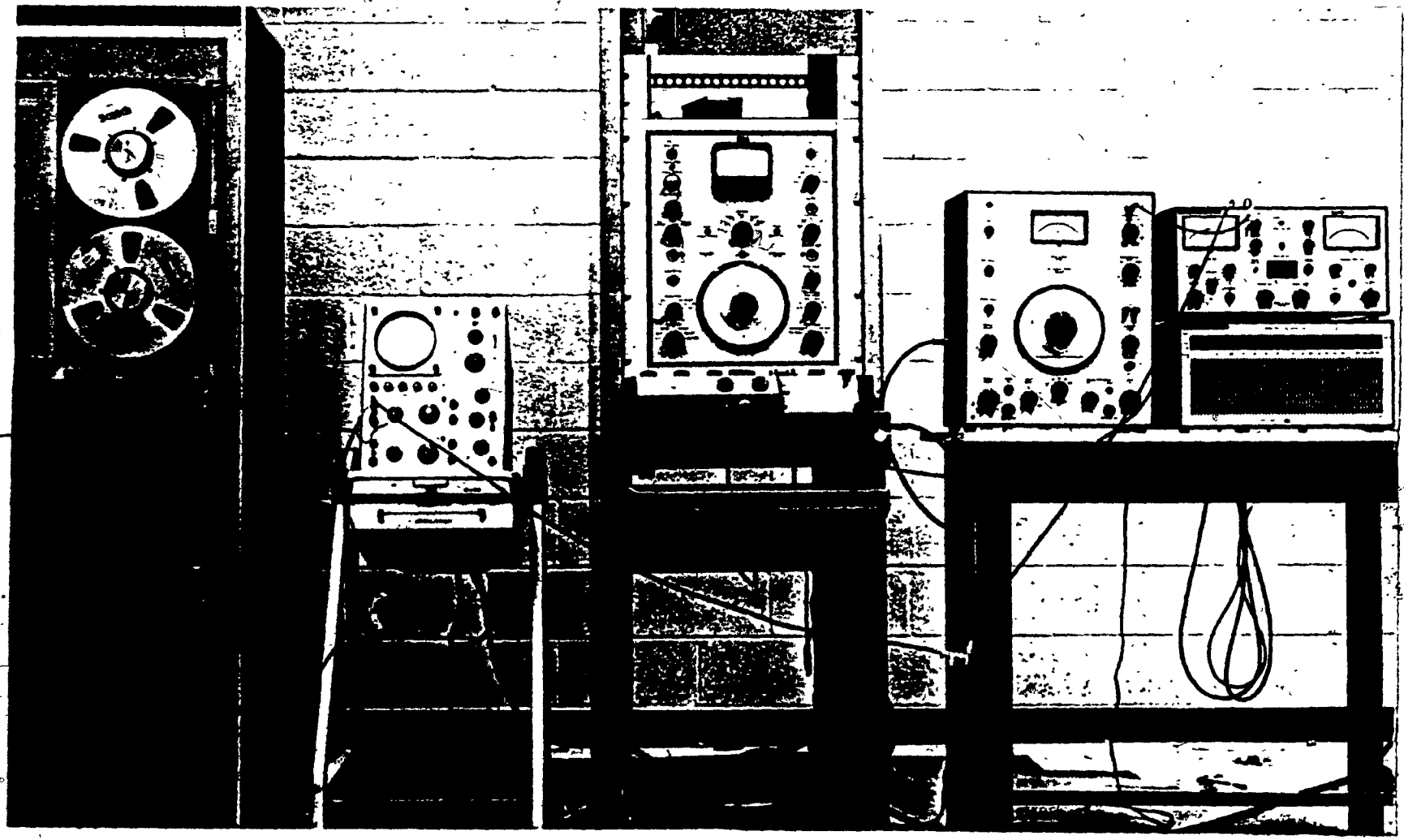

Figure 6.4(b) PICTORIAL VIEW OF THE EQUIPMENT USED FOR MEASURING THE POWER SPECTRAL DENSITY

increasing centre frequencies. The Brüel and Kjaer equalizer-analyzer instrument employed in the tests is calibrated in terms of g^2/Hz. Before starting the measurement, the level recorder, Brüel and Kjaer 2305 was calibrated with a Beat Frequency Oscillator, Brüel and Kjaer 1022, in terms of g^2/Hz.

The recorded signals were then fed through the equalizer-analyzer and plots of spectral density curves were obtained. The power spectral density values were computed from these plots using the following relationship.

$$dB - dBr = 10 \log_{10} \frac{D}{D_r}$$

where D is the spectral density of the signal,

D_r is the spectral density reference level, and

$(dB - dB_r)$ is the distance in decibels of the frequency response from the reference level.

To measure spectral density of the cutting forces above 2 KHz frequency levels, a -3dB octave filter was employed in conjunction with a frequency analyzer and the set up used is illustrated in Figure 6.5.

Spectral density plots obtained for the cutting force and surface signals for different cutting tests performed are presented in Figures 6.6, 6.7, 6.8 and 6.9. The cutting force spectral plots indicate the presence of high power

a)

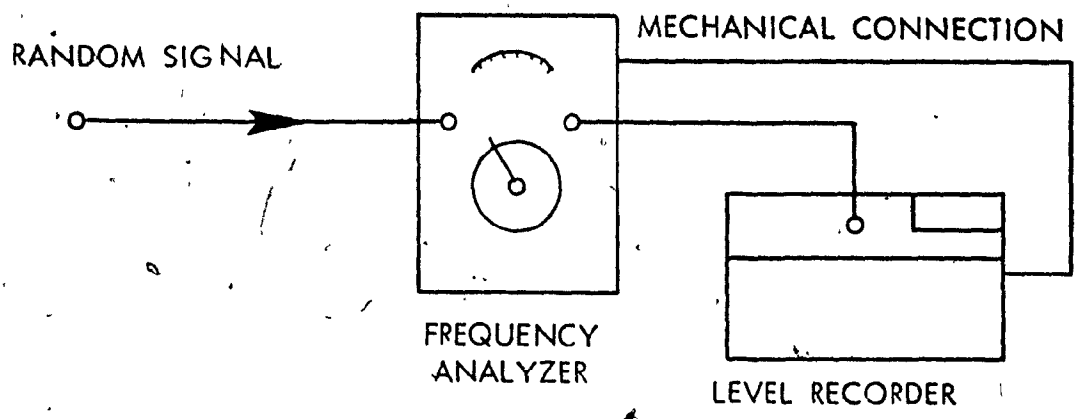

CALIBRATION OF FREQUENCY ANALYZER FOR SPECTRAL DENSITY MEASUREMENT WITH-3dB OCTAVE FILTER

b)

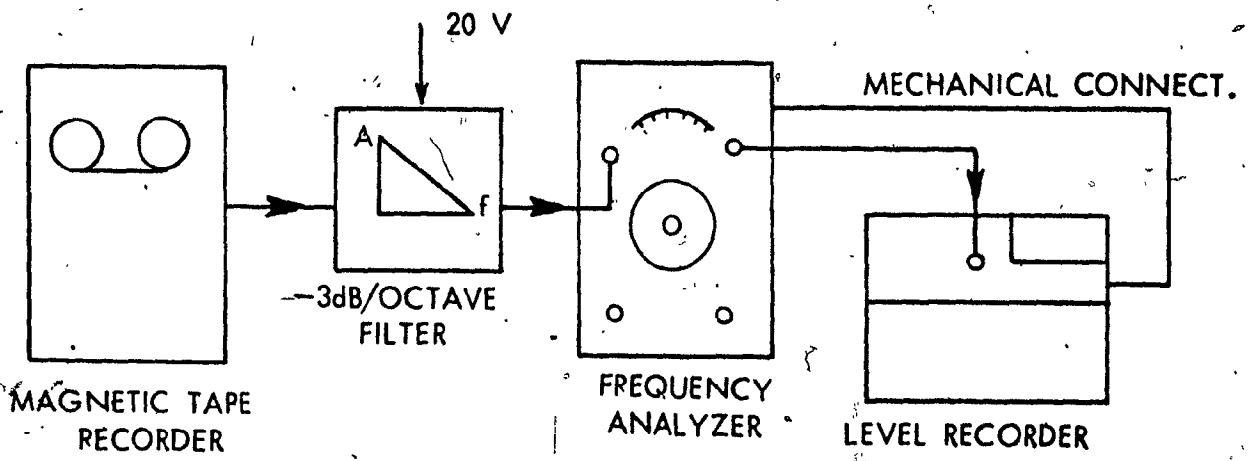

Figure 6.5 SCHEMATIC OF THE SET UP USED FOR MEASURING SPECTRAL DENSITY WITH -3dB OCTAVE FILTER

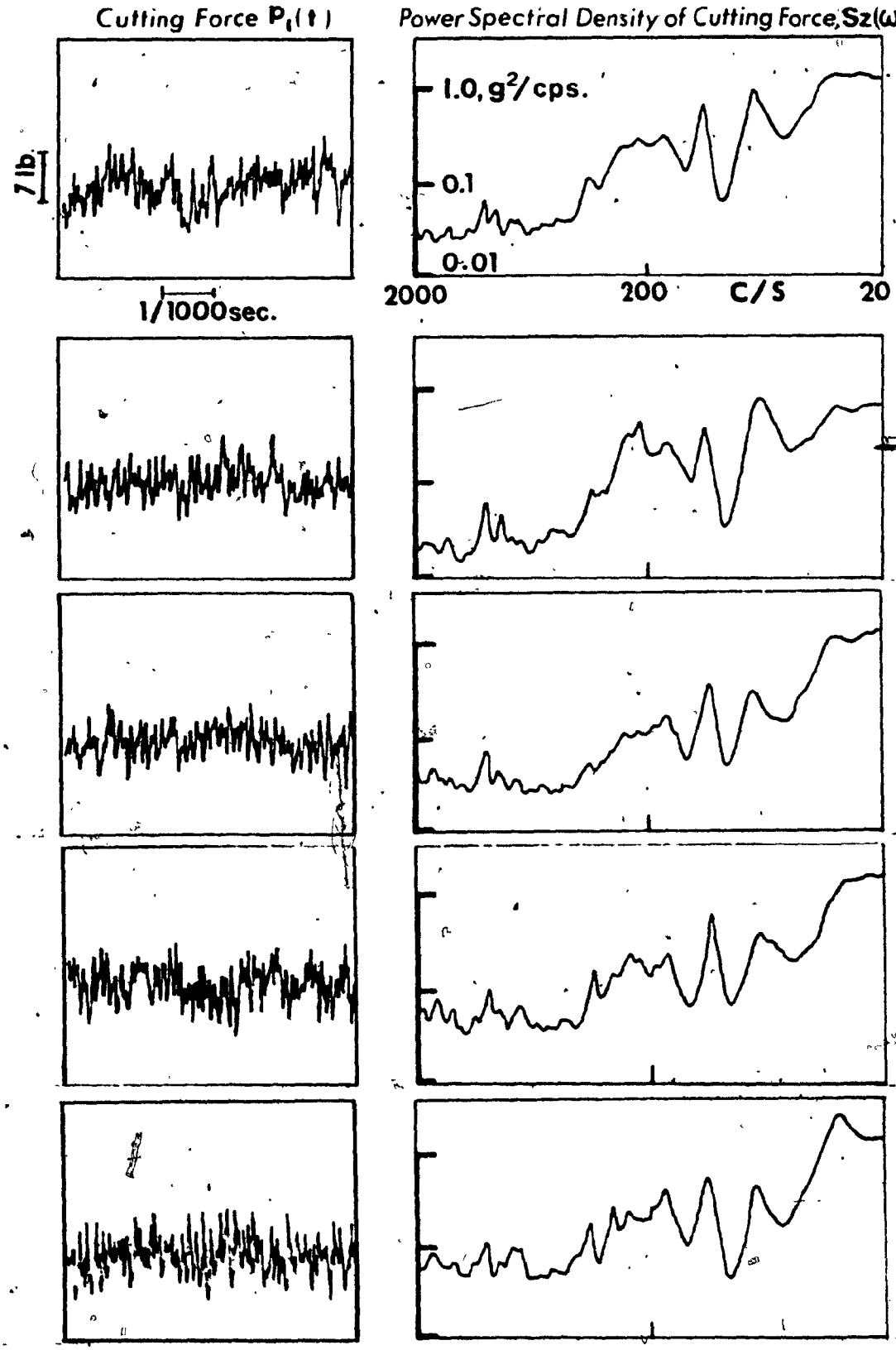

Figure 6.6 TYPICAL SPECTRAL DENSITY PLOTS OF THE CUTTING FORCES

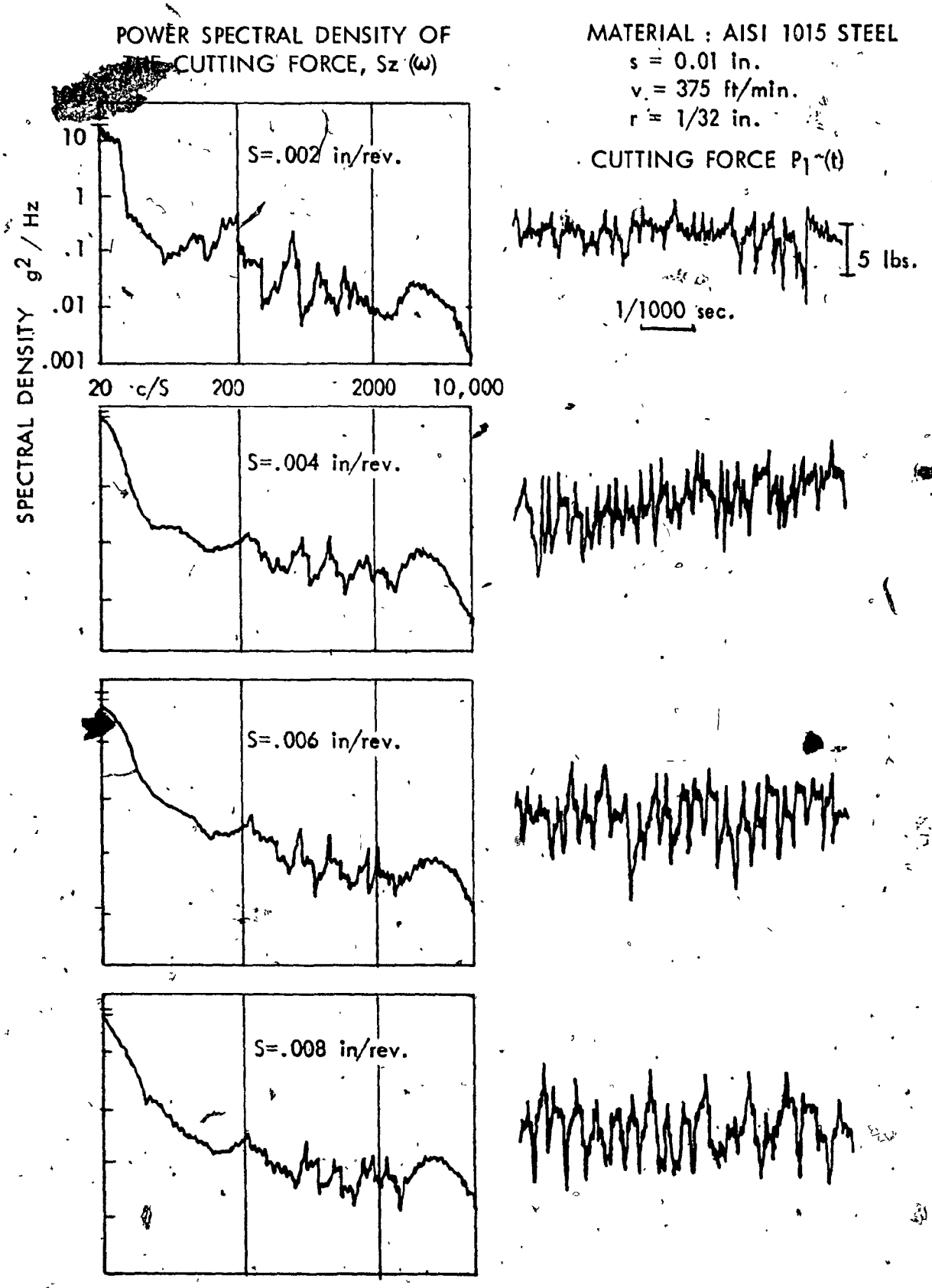

Figure 6.7 TYPICAL SPECTRAL DENSITY PLOTS OF THE CUTTING FORCES

MATERIAL : AISI 1015 STEEL
s = 0.01 in
v = 375 ft/min
r = 3/64 in.

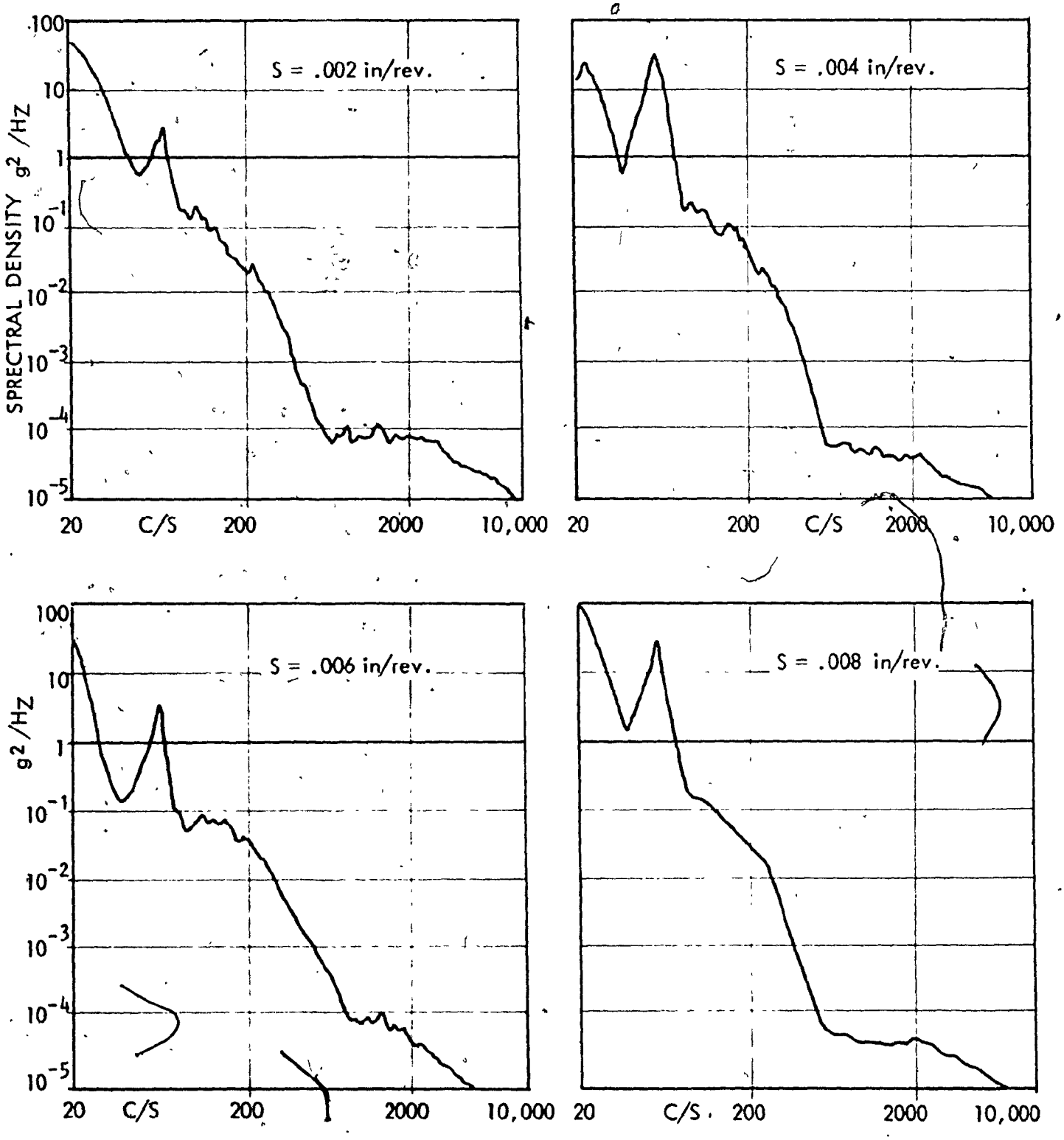

Figure 6.8 TYPICAL SPECTRAL DENSITY PLOTS OF THE SURFACE ROUGHNESS

MATERIAL: AISI 1015 STEEL
v : 375 ft/min.
s : 0.01 in
r : 1/32 in.

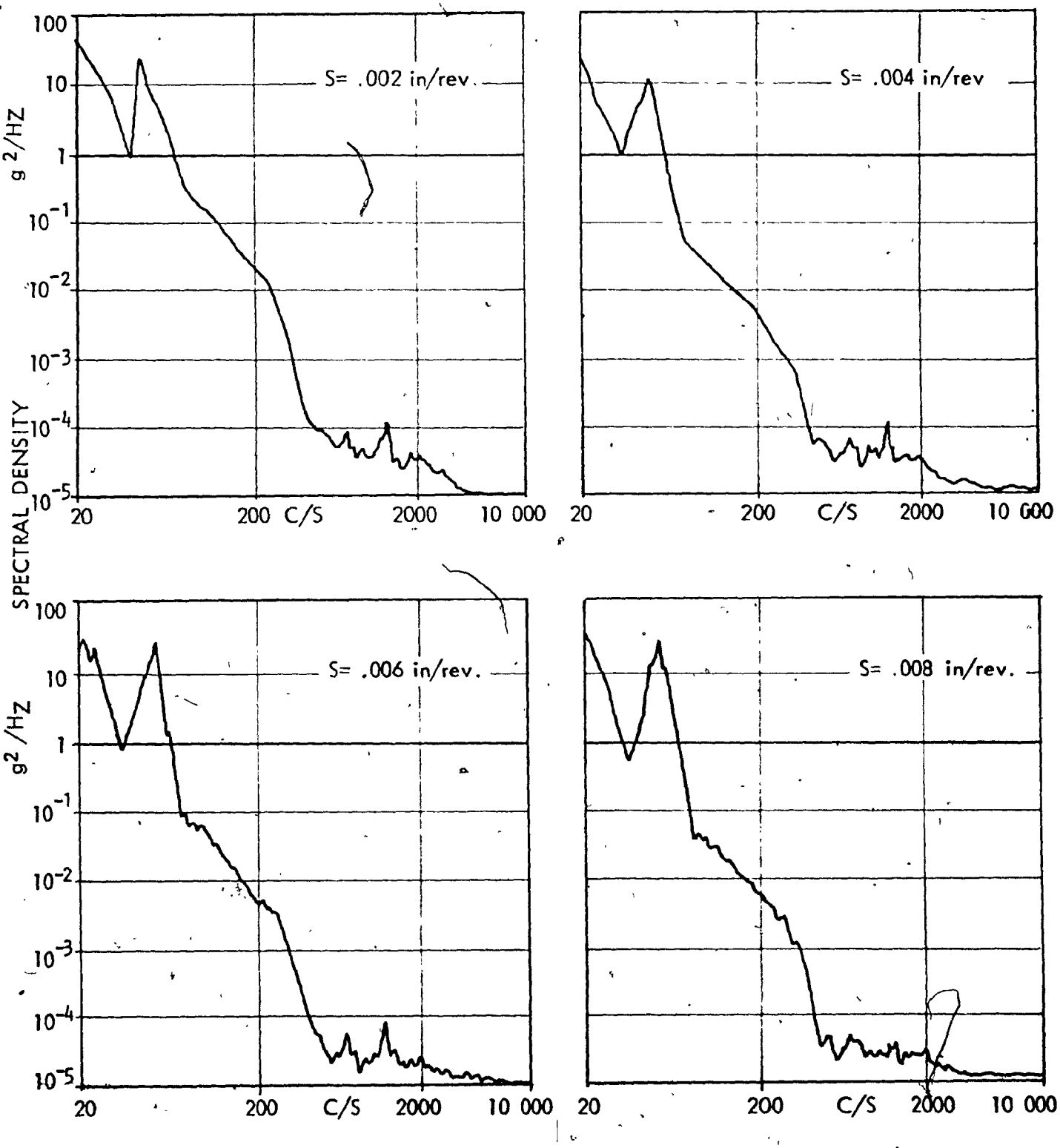

Figure 6.9 TYPICAL SPECTRAL DENSITY PLOTS OF THE SURFACE ROUGHNESS

spectrum over a wide frequency range. These plots also show that there are a number of frequencies below 50 Hz at which spectral density plots have large values. The reason for such high values of spectral density below 50 Hz may be attributed to the interaction between the cutting forces and the rotational frequencies of the system. The spectral density curves also indicated that the frequency components of the cutting forces are spread over a wide range. Hence by neglecting the power spectrum of the cutting forces below 50 Hz it will not introduce any appreciable error in finding the tool-workpiece response. The surface spectral plots, on the other hand, do not indicate any significant energy content for frequency values above 1 KHz. This is again due to the fact that the system characteristics between the tool and the workpiece act as a low pass filter, thus absorbing the higher frequency components.

6.3 Probability Density Analysis

Probability density analysis of the recorded signals of the cutting forces and surface roughnesses is performed to obtain further information on the statistical nature of the process involved. From the results of such analysis it may be possible to justify the assumptions of Gaussian distribution for the cutting forces and for the surface texture, the linear mathematical model of the machine-tool-workpiece system, etc.

The random signals of the cutting forces and surface

roughnesses were analyzed to obtain amplitude density characteristics using a Brüel and Kjaer Amplitude Distribution Analyzer model 161. A schematic of the set-up is shown in Figure 6.10(a) with the pictorial view in Figure 6.10(b). To verify whether the equipment was correctly calibrated, a sinusoidal signal whose probability density is known was fed through the probability density analyzer. The probability density thus obtained is shown in Figure 6.11 which indicates that the calibration of the equipment is correct.

The cutting force signals were analyzed and their probability density distribution is presented in Figure 6.12 and Figure 6.13. However, the surface roughness signals taped for one revolution of the workpiece were not of sufficient length for processing with this equipment. The processing time of the analyzer is such that it requires surface signals of longer durations. This was achieved by joining the open ends of the tape on which surface signals were recorded to make a closed loop. With such a loop running on the tape recorder, the analyzer could process the surface signals. Probability density plot of the surface roughness signals obtained is presented in Figure 6.14. The results of probability density analysis indicate that both the cutting forces and surface roughnesses have Gaussian distribution. This justifies the assumptions made regarding the statistical nature of the cutting forces and surface roughness in the analytical investigation

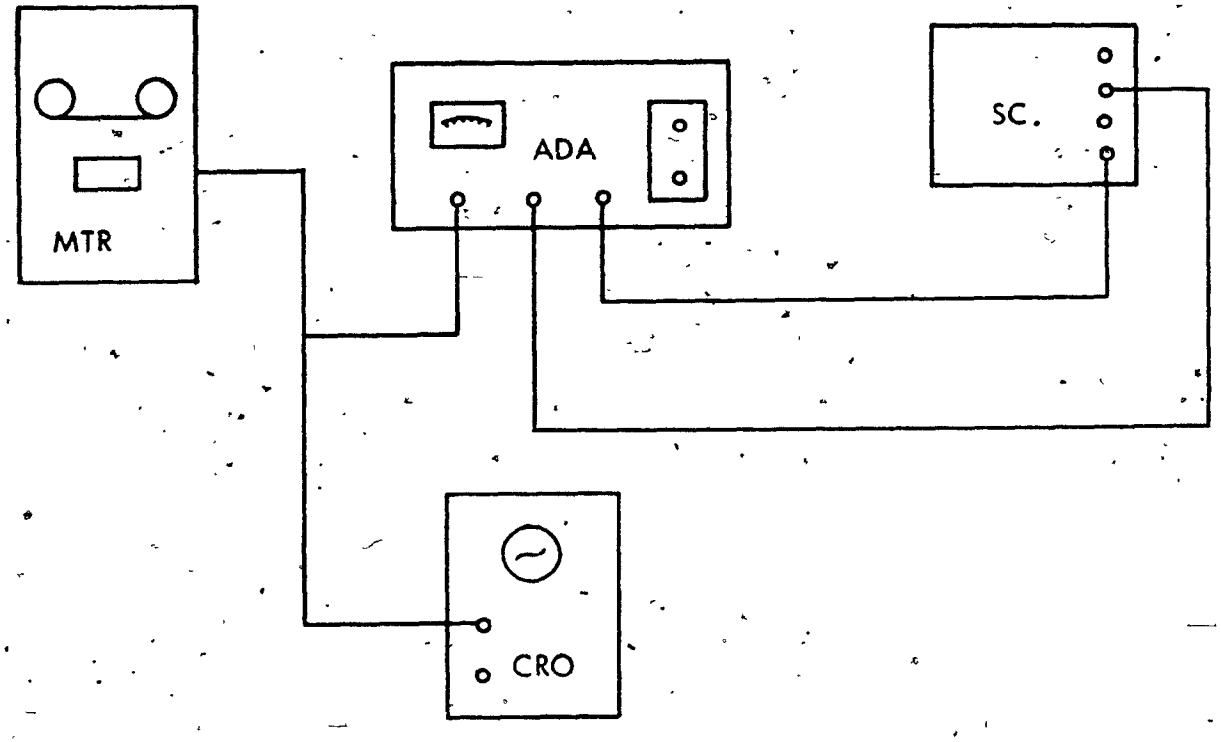

MTR : MAGNETIC TAPE RECORDER

ADA : AMPLITUDE DENSITY ANALYSER

SC : STRIP CHART

CRO : CATHODE RAY OSCILLOSCOPE

Figure 6.10(a) SCHEMATIC OF THE SET UP FOR A PROBABILITY DENSITY ANALYSIS

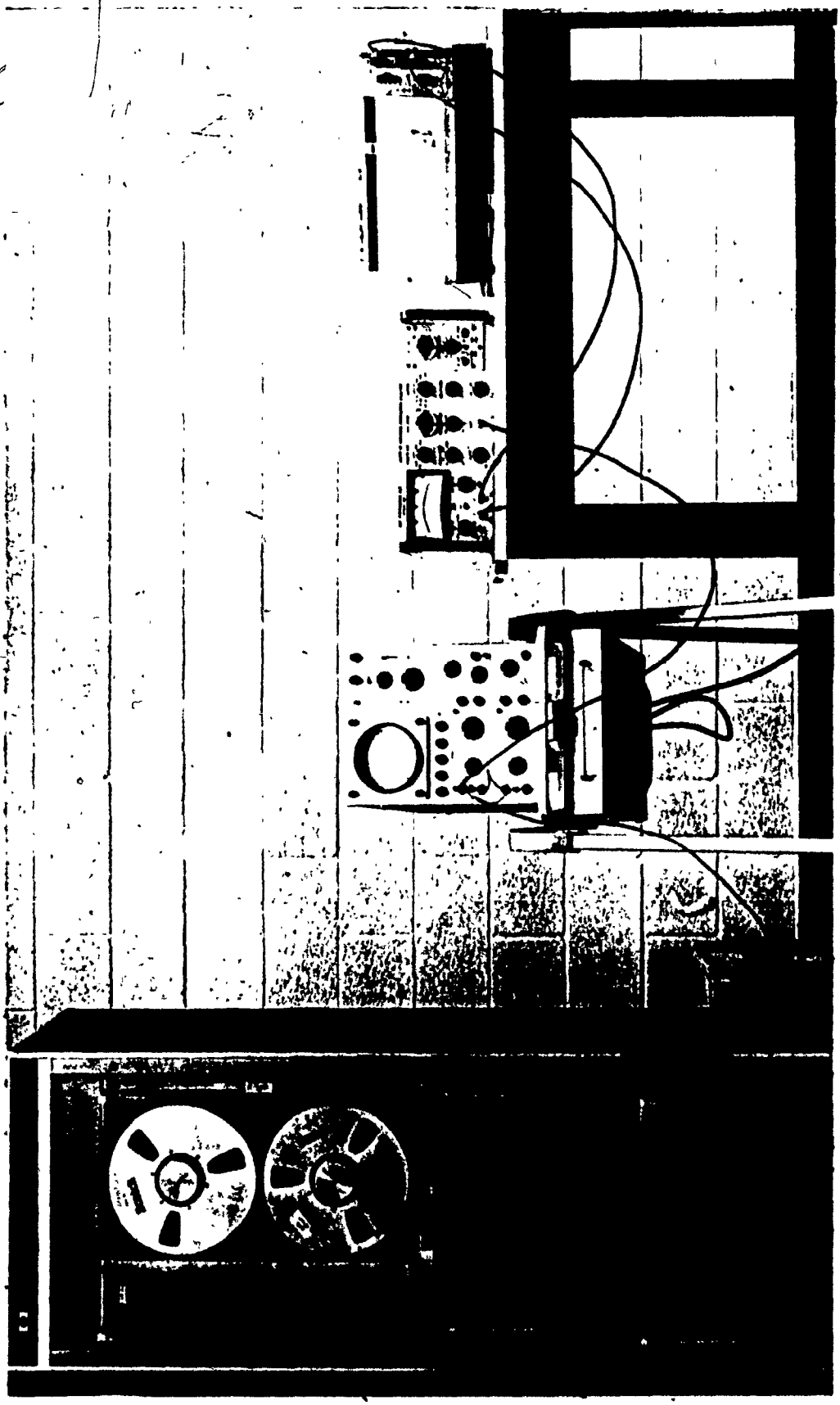

Figure 6.10(b) PICTORIAL VIEW OF THE EQUIPMENT USED FOR PROBABILITY DENSITY ANALYSIS

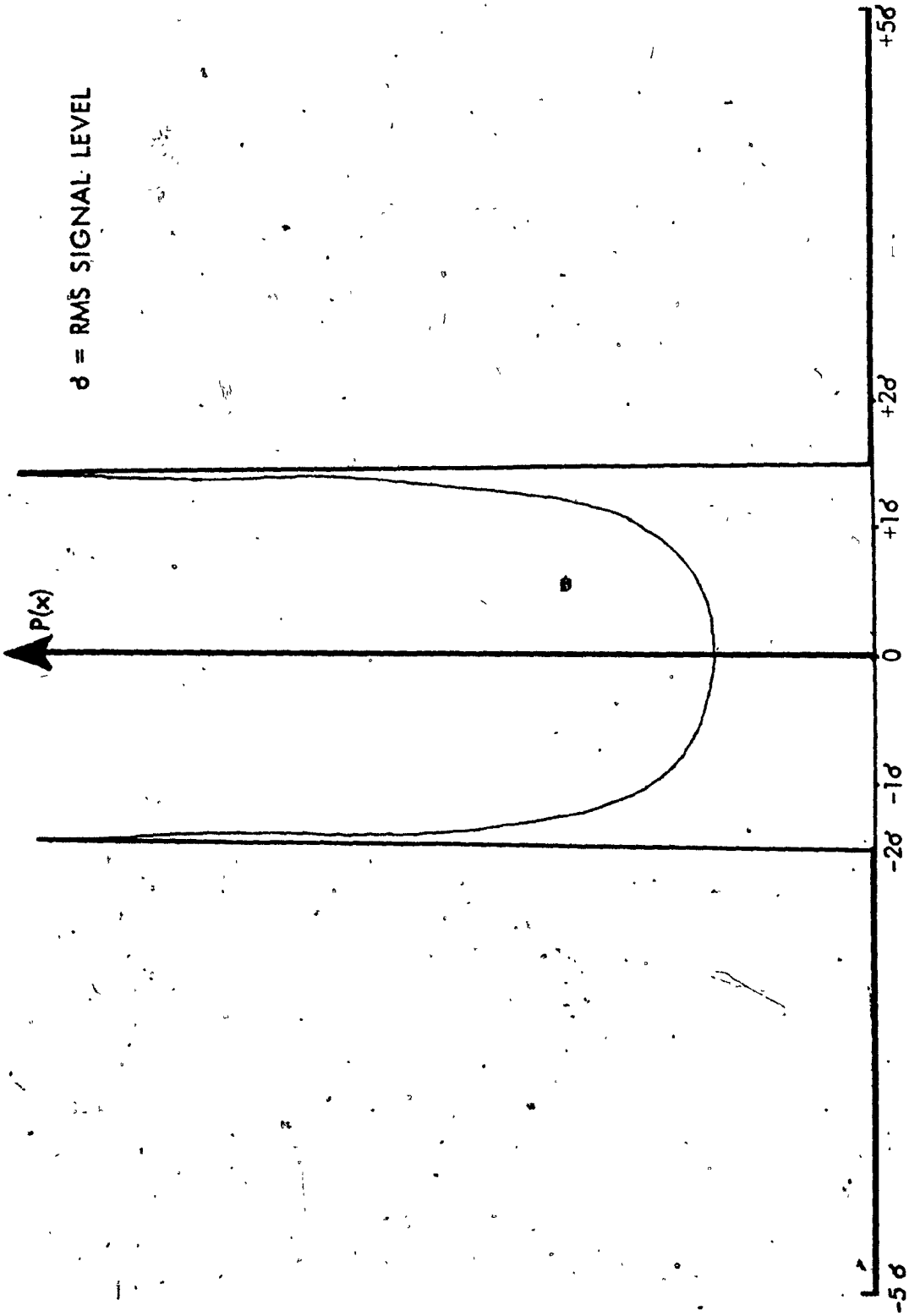

Figure 6.11 PROBABILITY DENSITY CURVE OF A KNOWN SINE SIGNAL

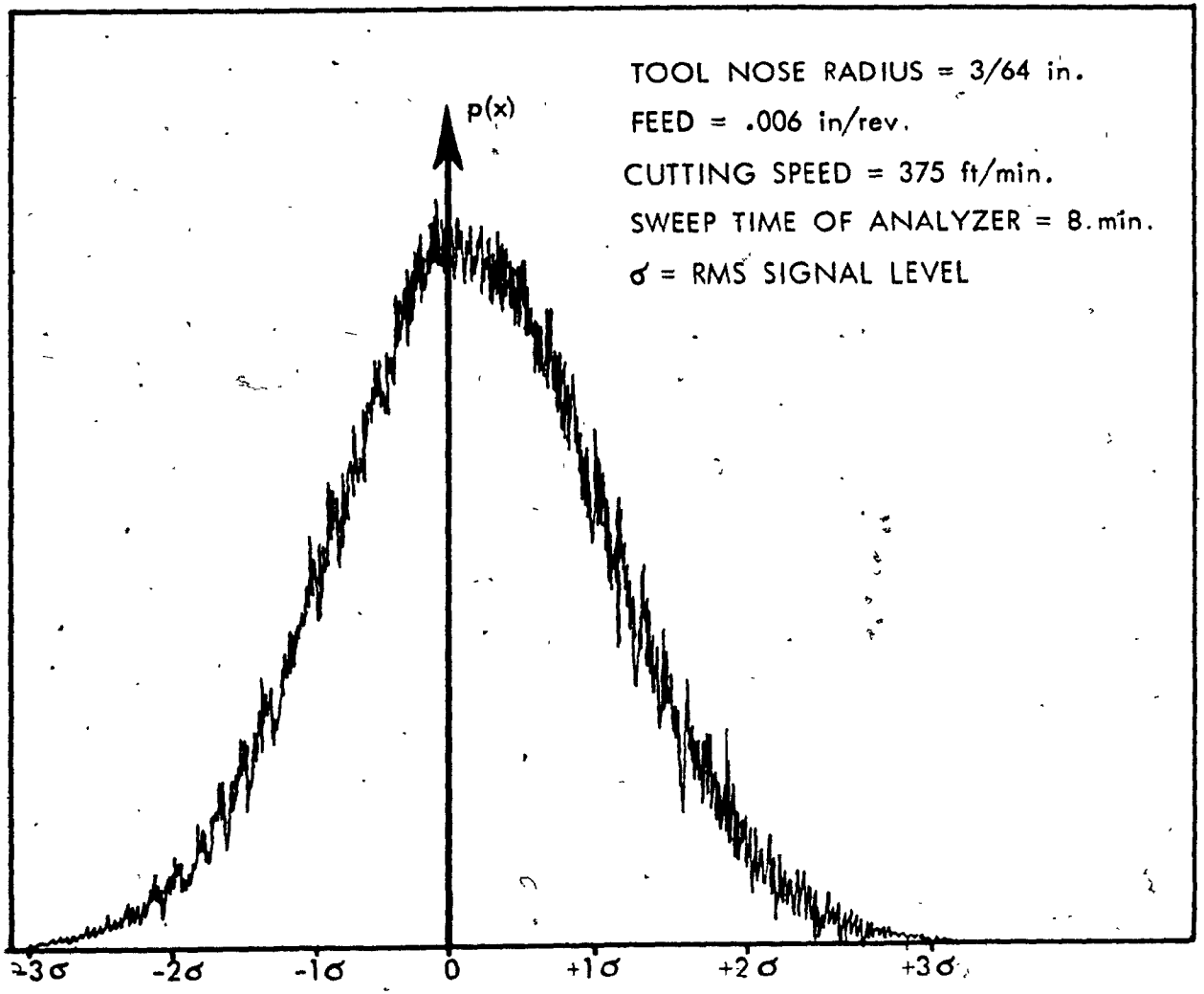

Figure 6.13 PROBABILITY DENSITY PLOT OF THE CUTTING FORCES

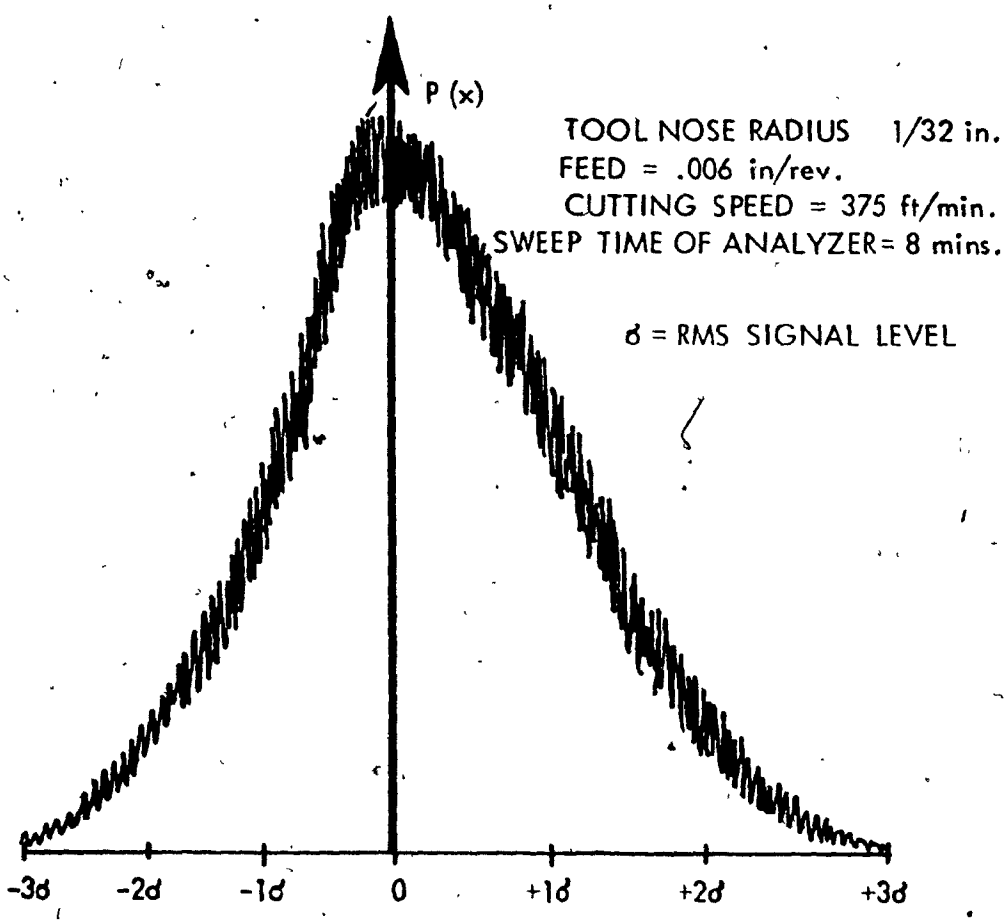

Figure 6.12 PROBABILITY DENSITY PLOT OF THE CUTTING FORCES

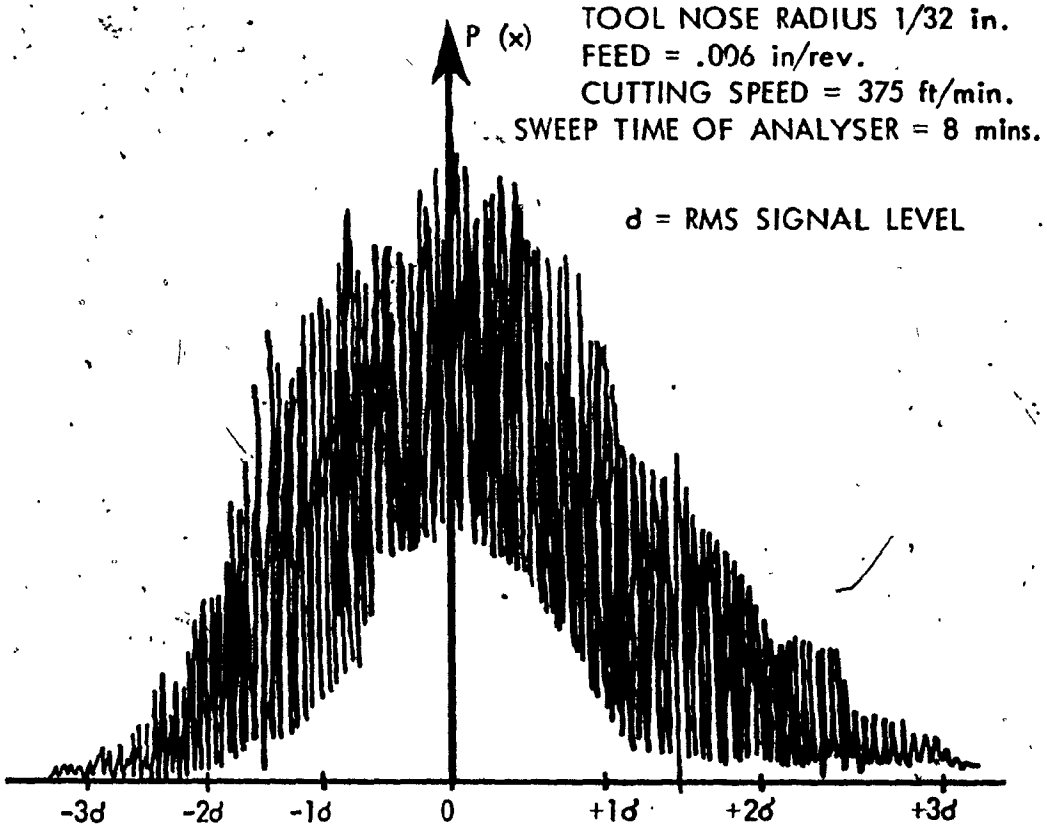

Figure 6.14 PROBABILITY DENSITY PLOT OF THE SURFACE ROUGHNESS

of the system.

Since the surface texture is found to be Gaussian, it is expected that the tool-workpiece response which is responsible for the surface texture formation will be also Gaussian. This shows that in a machine-tool-workpiece system the exciting forces and the tool-workpiece response are Gaussian. Hence it is consistent with the assumption of linear mathematical model of the machine-tool-workpiece system.

6.4 Computation of Total Surface Roughness

It is explained in Chapter 2 that a surface profile during a finish turning operation can be considered to consist of i) a basic or theoretical profile and ii) a random or fundamental profile superimposed on the theoretical profile.

The theoretical profile depends on the feed rate and tool nose radius and an expression is derived in equation (4.8) which states

$$\lambda_{Th} = S^2 / (18\sqrt{3})\, r$$

where λ_{Th} is the CLA value of the theoretical profile,

S is the feed rate, and

r is the tool nose radius.

Using this equation, the theoretical roughness of the surface for different feeds and tool nose radii were computed. Figure 6.15 shows the CLA-values of the theoretical roughness for different feeds and tool nose radii.

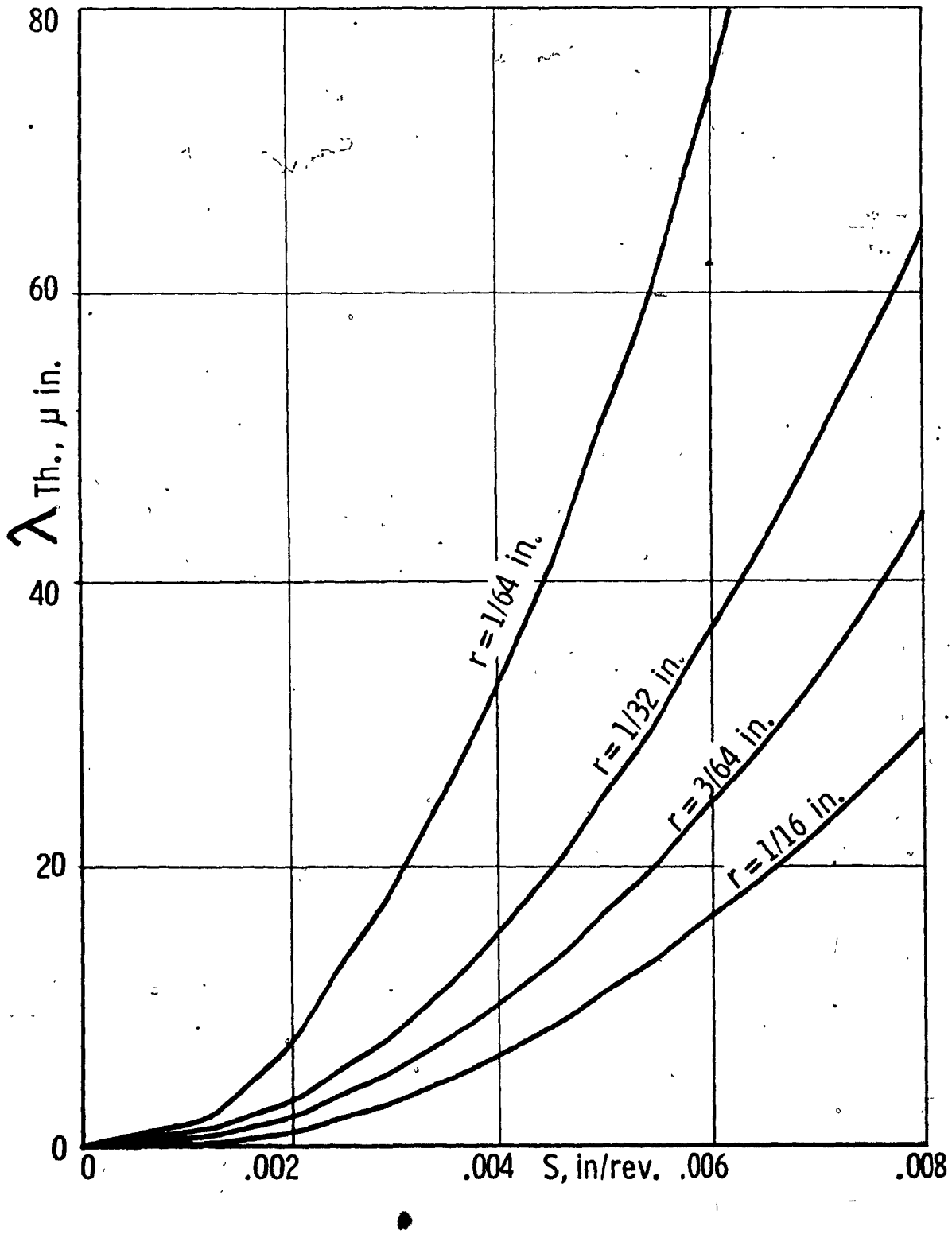

Figure 6.15 THEORETICAL ROUGHNESS OF A SURFACE FOR DIFFERENT FEEDS AND TOOL NOSE RADII

To compute σ_f of the random profile for applying in equation (4.11), it is necessary to find the mean square response $E[x^2]$ of the tool-workpiece system under the action of the random cutting forces presented in equation (3.45),

$$E[x^2] = \frac{S_o \pi}{\eta_5} [\eta_1 (\frac{B_o^2}{A_o}) + \eta_2 A_3 + \eta_3 A_1 + \eta_4 (\frac{B_3}{A_4})]$$

Here the response $E[x^2]$ is expressed in terms of constant spectral density S_o of the cutting forces whereas the experimental spectral density plots show a spectral density function varying with frequency. In order to evaluate the response of the tool-workpiece system, an equivalent constant spectral density S_o may be evaluated from the procedure described in Figure 6.16 and substituted for the frequency range that is of interest in this investigation. It can be shown that by considering the excitation in terms of constant spectral density instead of the variable spectral density as obtained for the cutting forces recorded, there will not be any appreciable change in the response characteristics of the tool-workpiece system. The principle of determining S_o is based on the estimation of a constant value of spectral density, such that the areas below and above this line are equal as indicated in Figure 6.16. Table 1 shows the values of the equivalent spectral density S_o for the different cutting conditions employed.

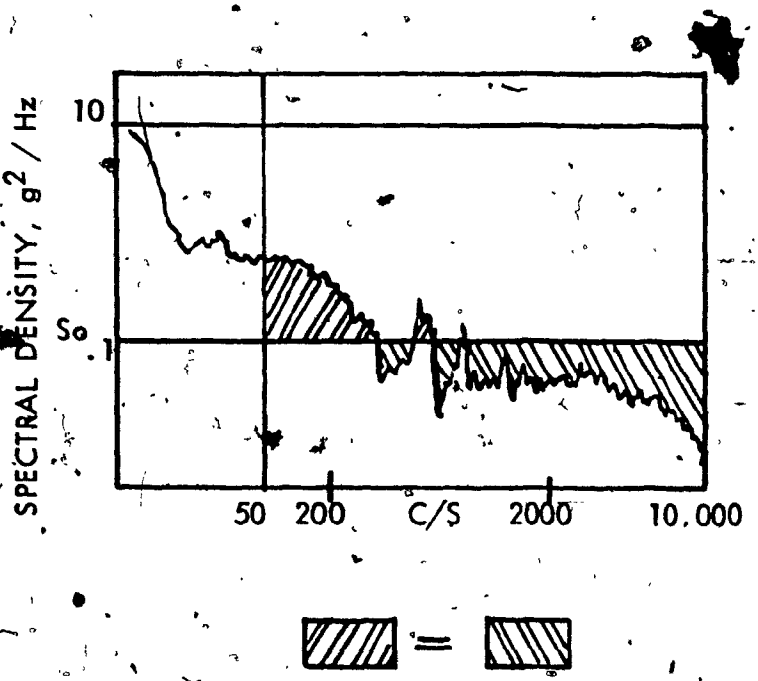

Figure 6.16 CONSTANT SPECTRAL DENSITY APPROXIMATION FROM THE MEASURED SPECTRAL DENSITY CURVE

The values of the constants A_o, A_1, A_3, A_4, B_o, B_3, n_1, n_2, n_3, n_4 and n_5 in equation (3.45) are evaluated with the following information available from the cutting tests.

workpiece diameter	2 in
equivalent length of spindle	15 in
length of workpiece	8 in
mass of the spindle with all the mountings (m_2)	0.36 lb sec^2/in
mass of the workpiece with the chuck (m_1)	0.18 lb sec^2/in
coefficient of damping (C)	275 lb sec/in
flexural rigidity of the spindle-workpiece unit (EI)	3390 $\times$ 10^6 lb in^2

The detailed calculation of the constants is explained in the Appendix II. The σ_f-values are then calculated from equation (4.11).

Figure 6.17 shows the calculated values of the fundamental roughness σ_f for different cutting conditions. Substituting the values of λ_{Th} from Figure 6.15 and σ_f from Figure 6.17 in equation (4.13), the total surface roughness is obtained. The detailed calculation is shown in Appendix II. Figure 6.18 shows a comparison between values of surface roughness from the tool-workpiece response obtained from the analytical procedure and the values measured experimentally with Talysurf 4 for different cutting conditions.

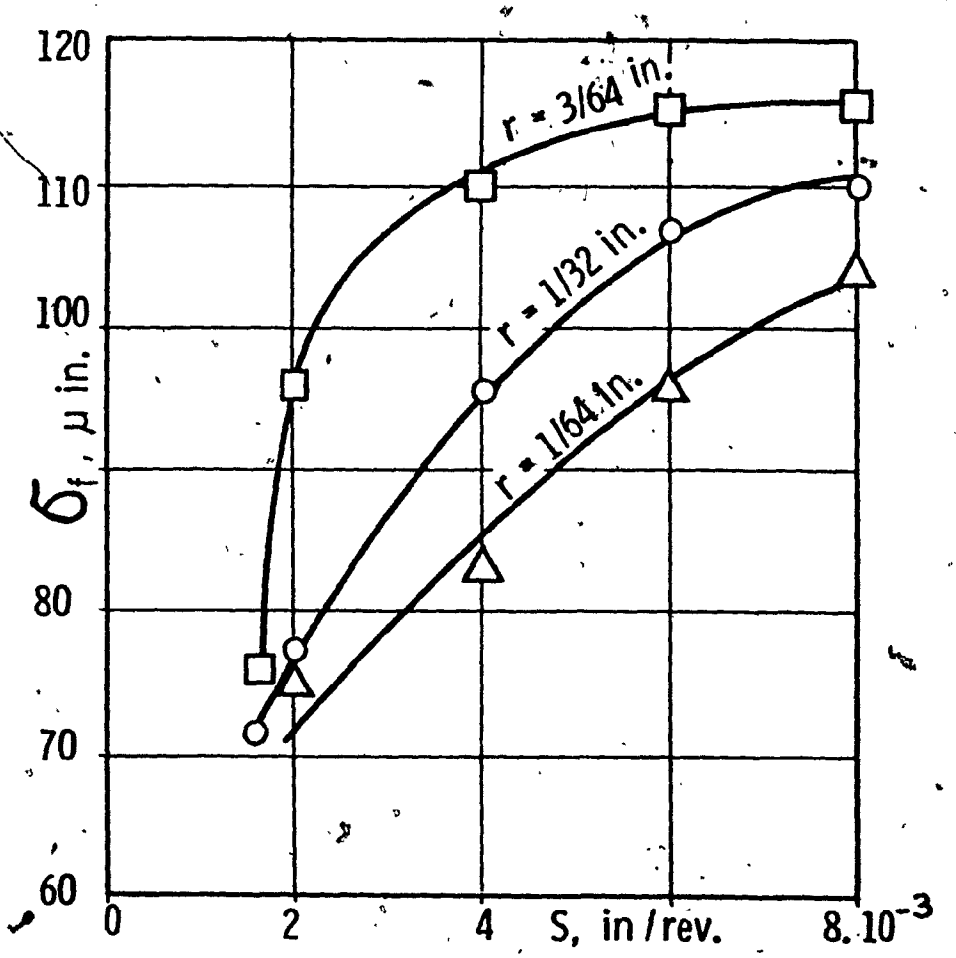

Figure 6.17 FUNDAMENTAL ROUGHNESS OF A SURFACE FOR DIFFERENT FEEDS AND TOOL NOSE RADII

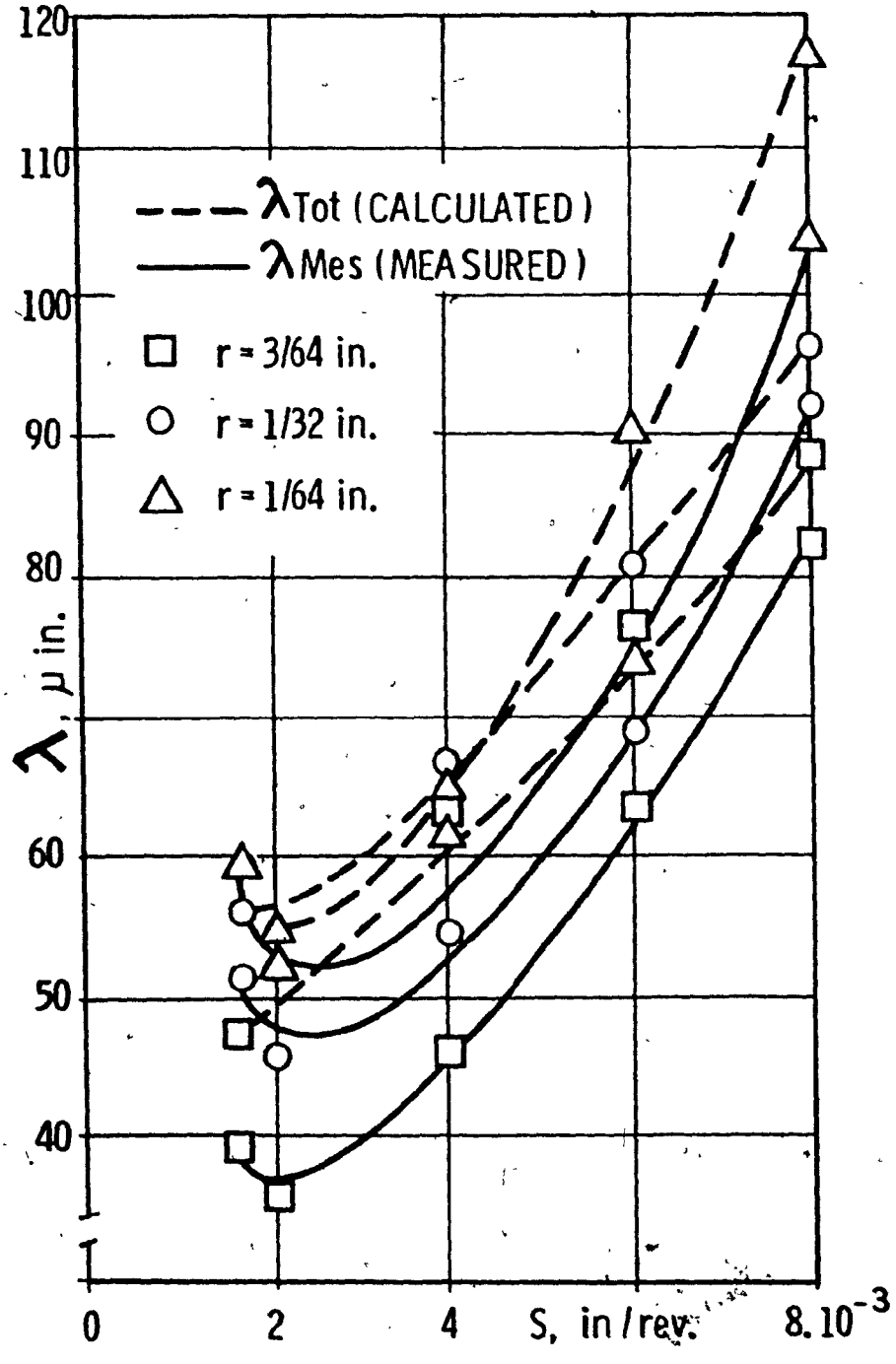

Figure 6.18 TOTAL SURFACE ROUGHNESS PROFILES-- EXPERIMENTALLY MEASURED AND ANALYTICALLY COMPUTED

The results of Figure 6.18 indicate that the analytically evaluated surface roughness values are approximately within 10% of the experimentally measured values. Hence it is reasonable to state that the surface roughness of a workpiece to be produced can be estimated beforehand from the knowledge of the tool-workpiece response and the cutting conditions.

CHAPTER 7

ESTIMATION OF SURFACE ROUGHNESS PARAMETERS FROM THE CUTTING FORCE FLUCTUATION CHARACTERISTICS

CHAPTER 7

ESTIMATION OF SURFACE ROUGHNESS PARAMETERS FROM THE CUTTING FORCE FLUCTUATION CHARACTERISTICS

7.I Background

In Chapter 4, an analytical procedure is presented for evaluating the response of the tool-workpiece system from the knowledge of probabilistic parameters of the random cutting forces and the system's physical parameters. This tool-workpiece response was then utilized for calculating the RMS- and the CLA-values of the surface roughness of the workpiece. But RMS- and CLA-values describe only the amplitude characteristics of the random surface profile. Such a description of the surface is insufficient when information on mechanical properties, namely, the wear resistance, the bearing strength and the lubricability of the surface is required.

An assessment of mechanical properties requires a surface characterization along its length, in addition to the standard amplitude description. A lengthwise description of a surface may be expressed in terms of the crest widths and valley spacings of the profile. An experimental determination of these stochastic "excursion" parameters from the vibratory response of the tool-workpiece system is difficult, because of the complexity in measuring the response close to the tool-workpiece interface. On the other hand, the

variation of the random cutting forces responsible for exciting the tool-workpiece system can be adequately measured with a dynamometer, as described in Chapter 5. With a knowledge of the cutting force fluctuations and the surface texture characteristics it may be possible to establish some relationships between the probabilistic excursion parameters of the cutting force and surface roughness. An estimate of the surface texture and its mechanical properties can then be directly obtained from the cutting force characteristics, which in turn depend primarily on the cutting conditions employed.

7.2 The Stochastic Excursions

An excursion is defined to be an event such that a random function Y(X) exceeds a certain fixed level $Y = Y_1$ during an interval λ. A typical signal is shown in Figure 7.1, where the interval λ is defined as the duration of the excursions. The interval Λ between the excursions is similarly defined. The interval λ is defined as the crest excursion and Λ as the valley excursion. Now, the stochastic parameters required to describe the texture may include the mean crest excursion or MCE, the root mean square crest excursion or RMSCE, the mean valley excursion or MVE, the root mean square valley excursion or RMSVE and the average wavelength of the random profile or AWL. If the probability density distributions of the duration λ as well as that of Λ are known, then the excursion parameters MCE, RMSCE, etc. may be calculated

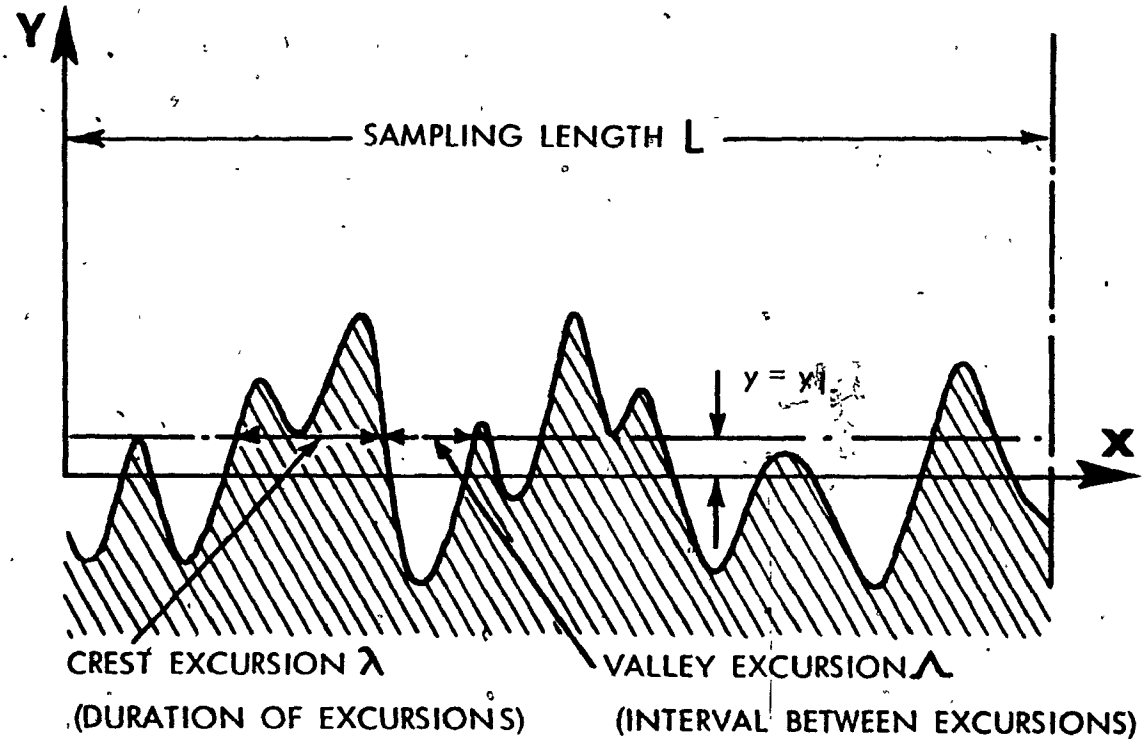

Figure 7.1 EXCURSION OF A RANDOM SIGNAL

by taking the first and the second moment of these probability densities.

It was mentioned that the mechanical properties such as the lubricability, the bearing strength, the wear and corrosion resistance depend to a large extent on the texture formation along the length of the machined surface. Lubricability of a surface depends on the capacity of the surface to hold lubricant in the valleys, and is evidently proportional to the parameters MVE and RMSVE. The bearing strength of a surface depends on the number and the width of the crests. Hence, it is dependent on MCE and RMSCE of the surface formed. Similarly, the number of crossings per unit length or the AWL could be related to the wear and corrosion resistance property of the exposed metal surface.

To describe accurately all the properties of a surface along its length, an infinite number of such excursion parameters may be required. However, for practical purposes, only a few of these parameters might be sufficient. In the present investigation, only MCE, RMSCE and AWL are employed for characterizing a surface along the length because of their generality and their relation with some of the mechanical properties mentioned earlier. Further, it may be shown that MVE and RMSVE can be derived from MCE, RMSCE, and AWL [31].

7.3 The Crest and the Valley Excursions of a Surface Profile

The information required for the proposed characteri-

zation along the length of the surface are the following probabilistic quantities:

a) the average number of crossings "ANC" per unit length of the surface undulations about a preselected level $Y = Y_1$ along the X-axis as illustrated in Figure 7.1,

b) the probability density $p_c(\lambda)$ of the crest excursions of the surface signal equal to or less than a λ-value that is specified, and

c) the probability density $p_v(\Lambda)$ of the valley excursions of the surface signal equal to or less than a Λ-value that is specified.

The probabilities $p_c(\lambda)$ and $p_v(\Lambda)$ mentioned in (b) and (c) above are computed about the preselected level $Y = Y_1$. It is reasonable to define the level Y_1 with respect to the CLA-value because the CLA-value is universally used in describing amplitude characteristics. This will enable description of the surface amplitude fluctuations in terms of the CLA-value and the excursion parameters with respect to the CLA-value. In general, the level Y_1 may be defined as

$$Y_1 = \nu[\text{CLA-level}] \tag{7.1}$$

where ν is a multiplication factor to determine the level Y_1 proportional to the CLA-level at which the excursion

parameters are calculated.

For a random signal that is stationary with a zero mean value and having a Gaussian distribution, the probability density discribution p(Y) is written in the form

$$p(Y) = \frac{1}{\sigma\sqrt{2\pi}} \exp(-Y^2/2\sigma^2) \qquad (7.2)$$

where

$$\sigma^2 = E[Y^2(X)] \qquad (7.3)$$

Here σ is the variance of Y(X) and E denotes the ensemble average. This assumption is justified for most real processes and is especially true in the case of cutting forces in finish turning and the surface texture produced.

If, for a random signal, E[Y(X)] is not equal to zero, the X-axis may be shifted to a new level along the Y-axis such that the new mean value is zero.

The mean slope η' (AMS) and the standard deviation σ' (RMSS) of the slope of the surface texture are defined respectively as

$$\begin{aligned} \eta' &= E[Y'(X)], \text{ and} \\ (\sigma')^2 &= E[\{Y'(X)\}^2] \end{aligned} \qquad (7.4)$$

where Y'(X) is the slope dY/dX of the function Y(X). The values of σ and σ' may be easily obtained for any given

random signal and are utilized later in the calculation of ANC, $P_c(\lambda)$ and $P_v(\Lambda)$.

The average number of crossings ANC per unit length of a signal about the level $Y = Y_1$ is given by the standard equation [31],

$$ANC = \frac{1}{2\pi\sigma}\,\sigma'\,\exp(-Y_1^2/2\sigma^2) \tag{7.5}$$

Then the average wavelength of crossing AWL is

$$AWL = \frac{1}{ANC} \tag{7.6}$$

The probability density of the duration of the surface excursions $p_c(\lambda)$ and the density of the interval between the excursions $p_v(\Lambda)$ about the level $Y = Y_1$ can be evaluated using a procedure developed by Tikhanov [36], later expanded by Sankar and Xistris [37], and utilized by Sankar and Osman [31] for a new approach to describe the quality of machined surfaces. For the purpose of clarification, the analytical method given by Sankar and Osman [31] is summarized here.

Let the crest excursion over the level Y_1 be started at the length coordinate $X = X_o$ and continue till $X = X_1$. Then

$$Y_o = Y(X)\Big|_{X = X_o} = Y(X_o) = Y_1 \tag{7.7}$$

and

$$Y'_o = \frac{d}{dX}Y(X)\Big|_{X = X_o} = Y'(X_o) > 0 \qquad (7.7)$$

Similarly,

$$Y_1 = Y(X_1) \text{ and } Y'_1 < 0 \text{ at } X = X_1$$

An approximate expression for the probability density $p_c(\lambda)$ may be written in terms of the random variables (Y_o, Y_1, Y'_o, Y'_1) as

$$p_c(\lambda) = \frac{1}{N_c(Y_1)} \int_0^{\infty} \int_0^{-\infty} Y'_o Y'_1 p_2(Y_o, Y_1, Y'_o, Y'_1) dY'_o dY'_1 \qquad (7.8)$$

Here the probability densities p_n for the signal $Y(X)$ are given by the general form

$$P_n(Y_1, Y_2, \ldots Y_n) = (2\pi)^{-\frac{n}{2}} D^{-\frac{1}{2}} \sigma^{-n} \exp\left[-\frac{1}{2D} \sum_{i,j=1}^{n} D_{ij} \frac{Y_i Y_j}{\sigma^2}\right] \qquad (7.9)$$

where D is the n-th order determinant

$$D = \begin{vmatrix} K_{11} & K_{12} & \cdots & K_{1n} \\ \vdots & & & \\ K_{n1} & K_{n2} & \cdots & K_{nn} \end{vmatrix}, \qquad (7.10)$$

and D_{ij} is the algebraic cofactor of the K_{ij} element of this determinant. Further, $K_{ij} = K(X_i - X_j)$ is the value of the

correlation coefficient for the random function Y(X) at values X_i and X_j. Using the general form (7.9), the probability density $p_2(Y_o, Y_1, Y_o', Y_1')$ in equation (7.8) can be written for the values of the function Y(X) and its derivatives at positions X_o and X_1 that are apart by the interval λ, equal to the crest width.

The correlation coefficients in the determinant (7.10) for the four random variables (Y_o, Y_1, Y_o', Y_1') may be expressed in terms of the following coefficients:

$$K = \frac{E[Y(X_o)Y(X_1)]}{\sigma^2}$$

$$K_1 = \frac{E[Y(X_o)Y'(X_1)]}{\sigma\sigma'} \qquad (7.11)$$

$$\text{and } K_2 = \frac{E[Y'(X_o)Y'(X_1)]}{\sigma'^2}$$

The determinant D for the variables then takes the symmetric form

$$D = \begin{vmatrix} 1 & K & 0 & K_1 \\ K & 1 & -K_1 & 0 \\ 0 & -K_1 & 1 & K_2 \\ K_1 & 0 & K_2 & 1 \end{vmatrix} \qquad (7.12)$$

It may be possible to consider the correlation coefficient $K(\tau)$ to be of the Gaussian form (valid for surface textures)

$$K(\tau) = \exp(-\alpha_1 \tau^2) \ , \qquad (7.13)$$

where α_1 is defined for the type of process Y(X) under consideration. The selection of such a $K(\tau)$ is quite valid in problems involving real and non-Markovian processes. It follows then from equation (7.13) that

$$\begin{aligned} \sigma_1' &= \sigma(2\alpha_1)^{\frac{1}{2}} \\ K_1 &= -\sqrt{2\alpha_1}\ \tau\ K(\tau) \qquad (7.14) \\ K_2 &= (1 - 2\alpha_1\tau^2)\ K(\tau) \end{aligned}$$

The D_{ij}'s in equation (7.12) may now be written in terms of K, K_1 and K_2.

Using the above results in equation (7.9), an expression for $p_2(Y_o, Y_1, \dot{Y}_o, \dot{Y}_1)$ may be obtained. Substituting this result in equation (7.8) and carrying out the integration, the probability density for the crest intercepts having a crest width less than or equal to λ about the level Y_1 may be obtained as

$$p_c(\lambda) = M(\bar{Y}_1, \lambda) \quad [a_0^2 + \sum_0^\infty \frac{a^2}{n!}\ \zeta_1^n] \ , \qquad (7.15)$$

where $\bar{Y}_1 = \frac{Y_1}{\sigma}$, and the function

$$M(\bar{y}_1,\lambda) = \frac{(2\alpha_1)}{(1-K^2)^{15}} D_{33} \exp\left[\bar{Y}_1^2 \left(\frac{1}{2} - \frac{D_{11}}{D}\right)\right]$$

with

$$\bar{Y}_1 = \frac{D_{34}}{D_{33}} .$$

The coefficients a_n are given by Sankar and Osman [31].

In the equation (7.15) for $p_c(\lambda)$, the summation need be taken only over the first six terms, say n=5, as an approximation.

The quantity $p_c(\lambda)$ represents the probability density of the surface signal excursion having an intercept or crest width less than or equal to a specified value λ about the level Y_1. Then, by definition,

$$MCE = E[\lambda] = \int_{-\infty}^{\infty} \lambda p_c(\lambda) d\lambda \qquad (7.16)$$

and

$$RMSCE = \{E[(\lambda-MCE)]\}^{\frac{1}{2}} \qquad (7.17)$$

Once the $p_c(\lambda)$ vs λ curve is available for different values of possible excursion intercepts, the parameters MCE and RMSCE can be computed using the moment formulae (7.16) and (7.17). MCE gives the mean crest intercepts at the level Y_1

for the surface sample and RMSCE gives the standard deviation of the crest excursions from the mean spacing of the surface texture.

A computer program based on the equations described is used for calculating the profile excursion parameters MCE, RMSCE, and AWL.

7.4 Computation of MCE, RMSCE, and AWL of the Cutting Forces and the Surface Profile

The analog signals of the cutting force and surface texture, obtained from the cutting test measurements, are recorded on magnetic tapes and are converted to a set of discrete data points for the purpose of analysis, by a sequence of programs running on EAI 690 hybrid computer and CDC 6400 digital computer. The acquisition program running on the hybrid computer samples the incoming analog signals, digitizes and stores these in a format for transmittal to the digital computer. When the signals are ready for processing, the conversion program is loaded into the digital section of the hybrid computer. The tape recorder with the signals stored in the magnetic tape was then connected to the analog/digital conversion channel. The hybrid computer then starts reading the analog/digital channel and stores it in a memory buffer in the digital section. When the memory buffer is full, the program automatically enters the output phase where the contents of

the memory buffer are transmitted over a specially designed telephone data link to a disc file in the digital computer. Data was transmitted in records of 18 data points at a rate of 30 characters/second.

These data points were then analysed by a computer program developed by Sankar and Osman [31] to calculate the various stochastic parameters. A flow chart of the analysis program for computation of these excursion parameters is given in Figure 7.2. Tables 2-5 (See Appendix III) show the listing of the excursion parameters of the cutting force and surface signals that were obtained from the cutting tests performed during the investigation. It can then be concluded from the results presented in the tables that the excursion properties of the force and the surface signals do not change significantly with an increase in the feed rate or in the tool nose radius. From the excursion analysis, the plots between the different stochastic excursion parameters of the force and the surface signals are obtained and are presented in Figures 7.3,7.4,7.5,7.6, and 7.7. They show a set of non-linear relationships but could be approximated to almost linear relationships as indicated by the broken lines in the figures. From these plots the following proportionality relations are derived as shown below:

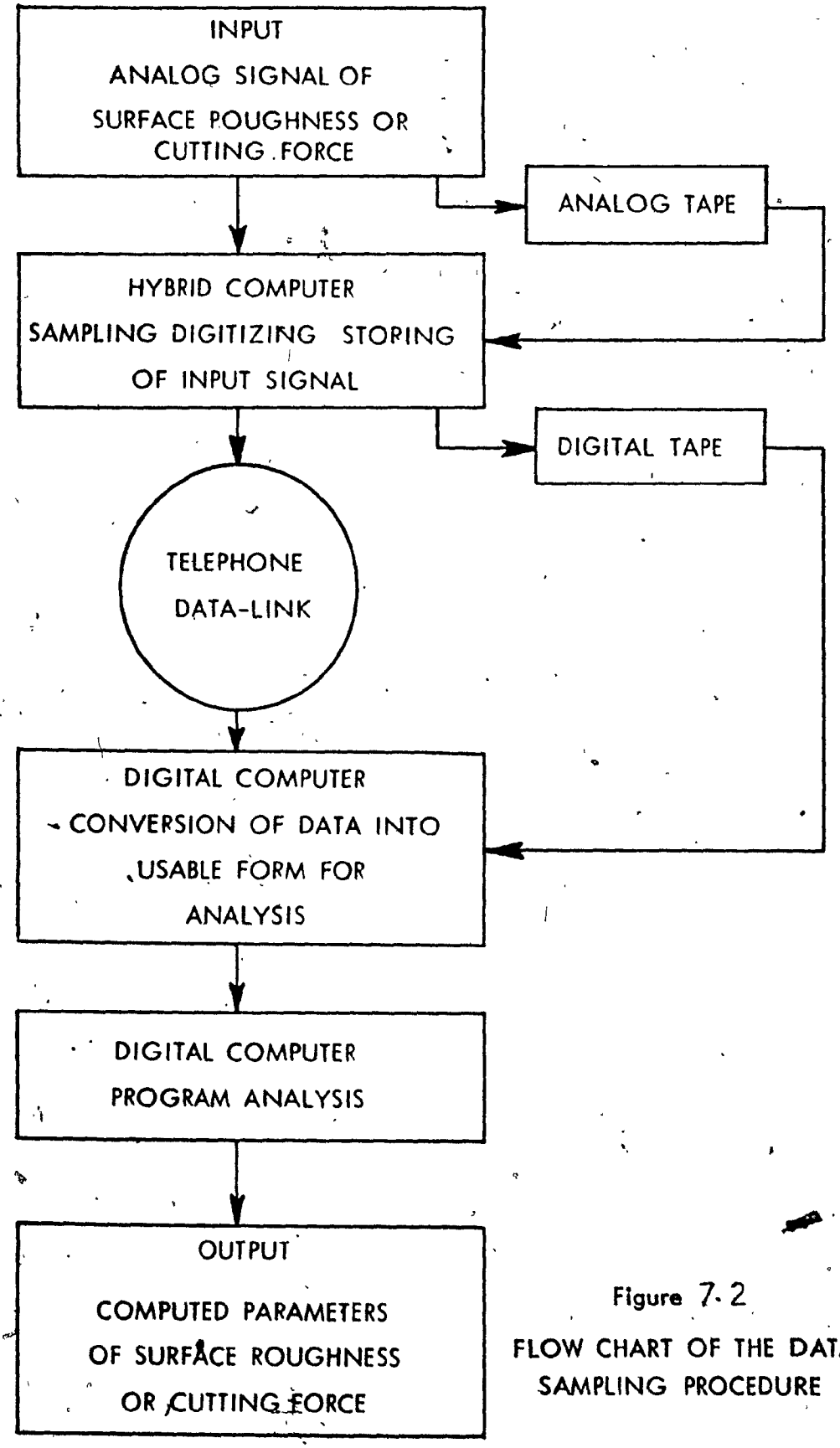

Figure 7.2

FLOW CHART OF THE DATA SAMPLING PROCEDURE

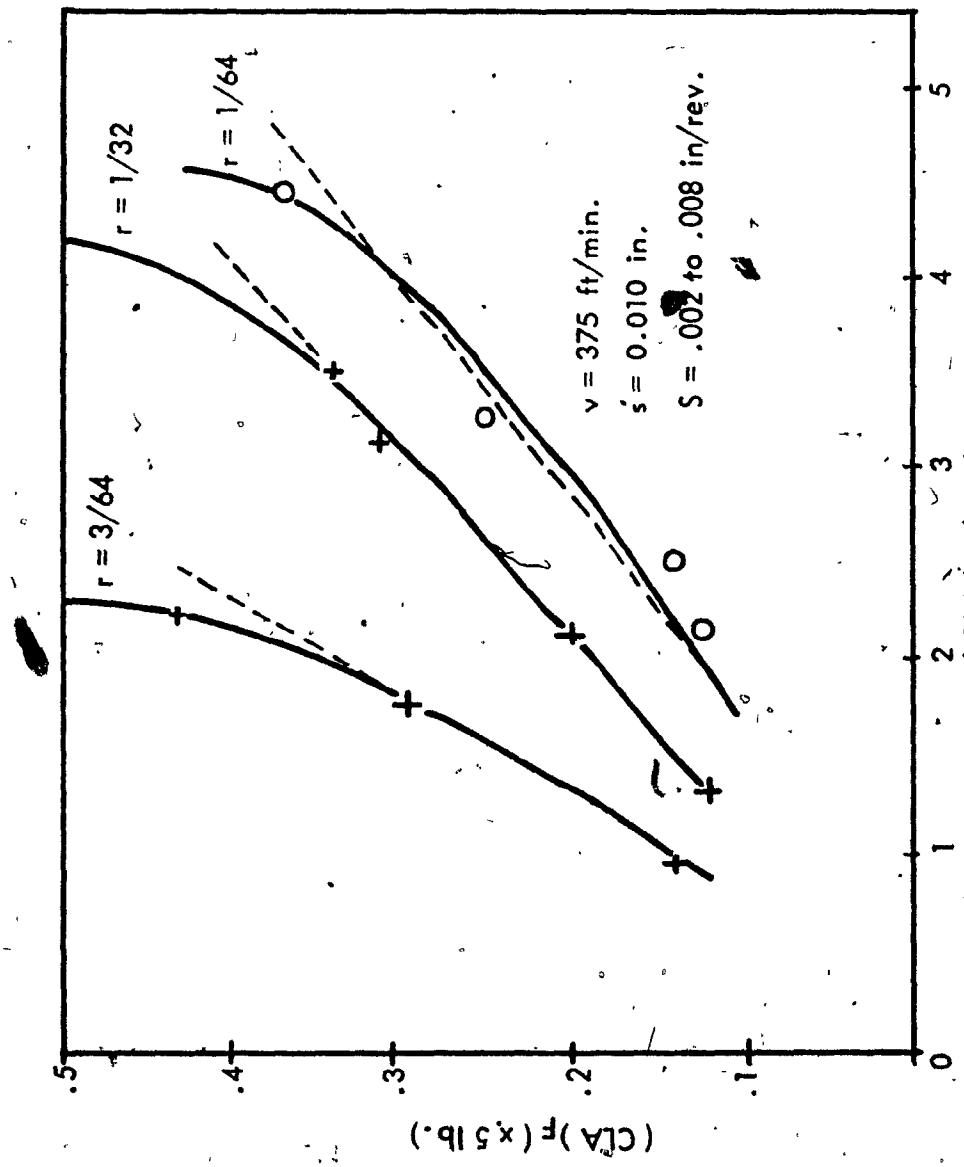

Figure 7.3 CLA-VALUES: THE CUTTING FORCES VS. THE SURFACE ROUGHNESS

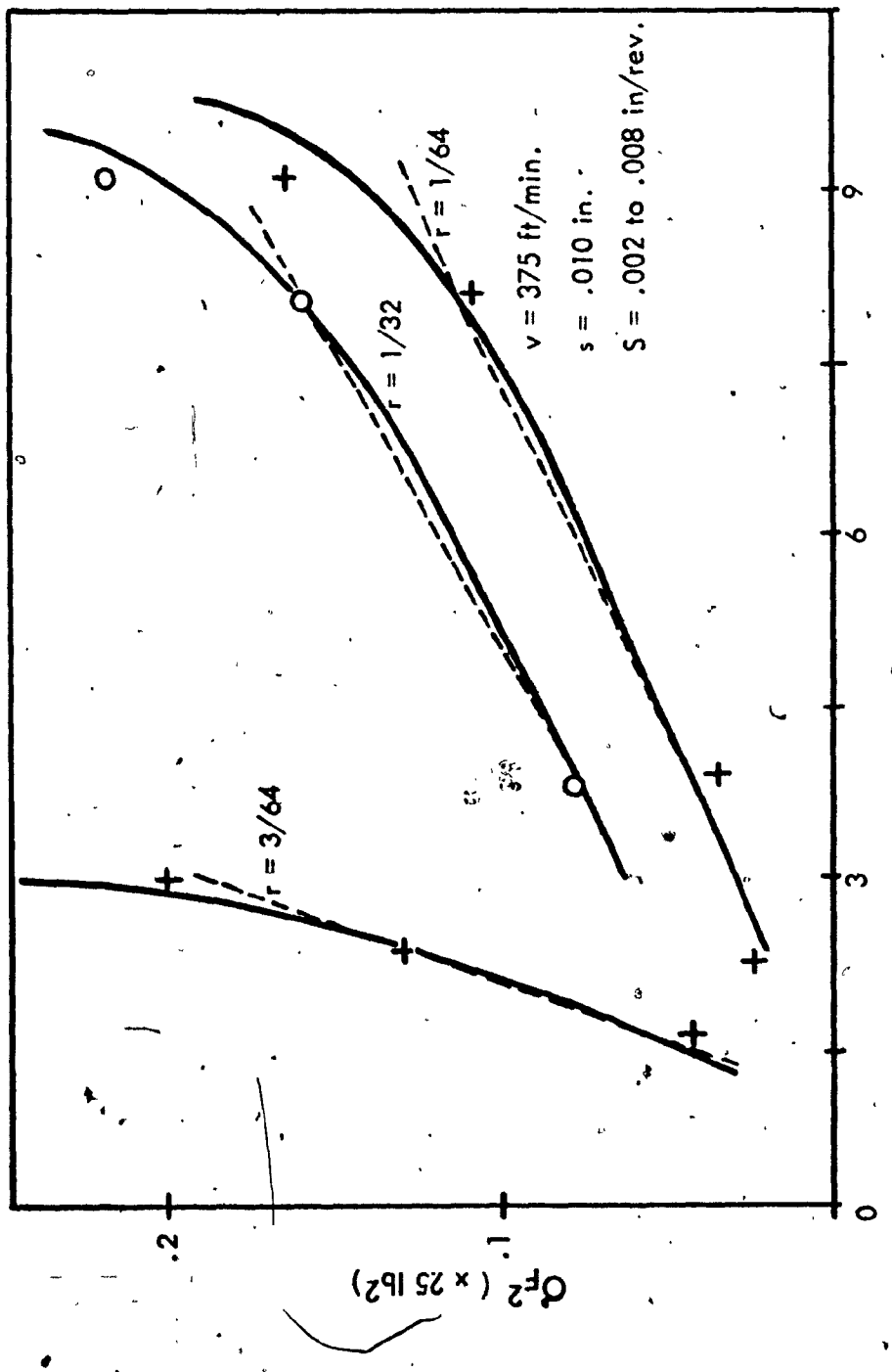

Figure 7.4 VARIANCE : CUTTING FORCES VS. THE SURFACE ROUGHNESS.

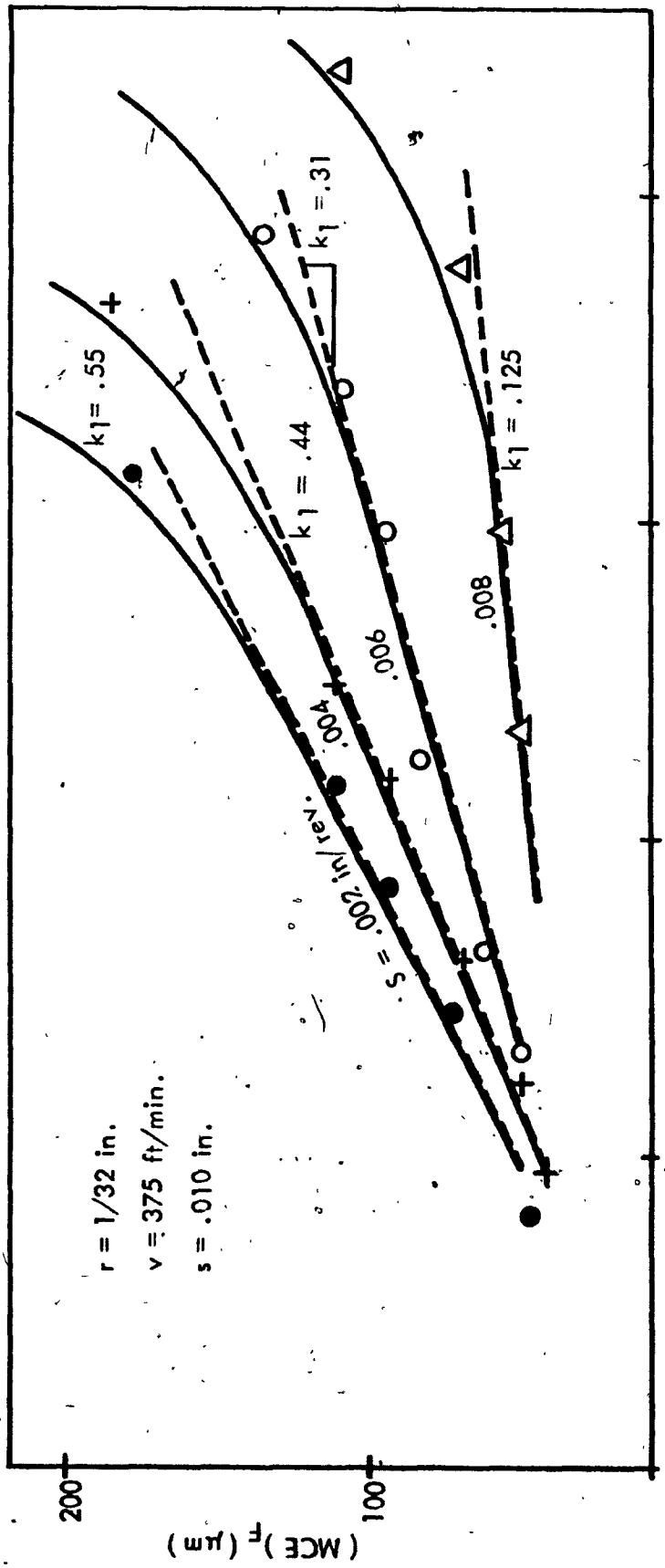

Figure 7.5 MEAN CREST EXCURSION: THE CUTTING FORCE SIGNAL VS. SURFACE ROUGHNESS SIGNAL.

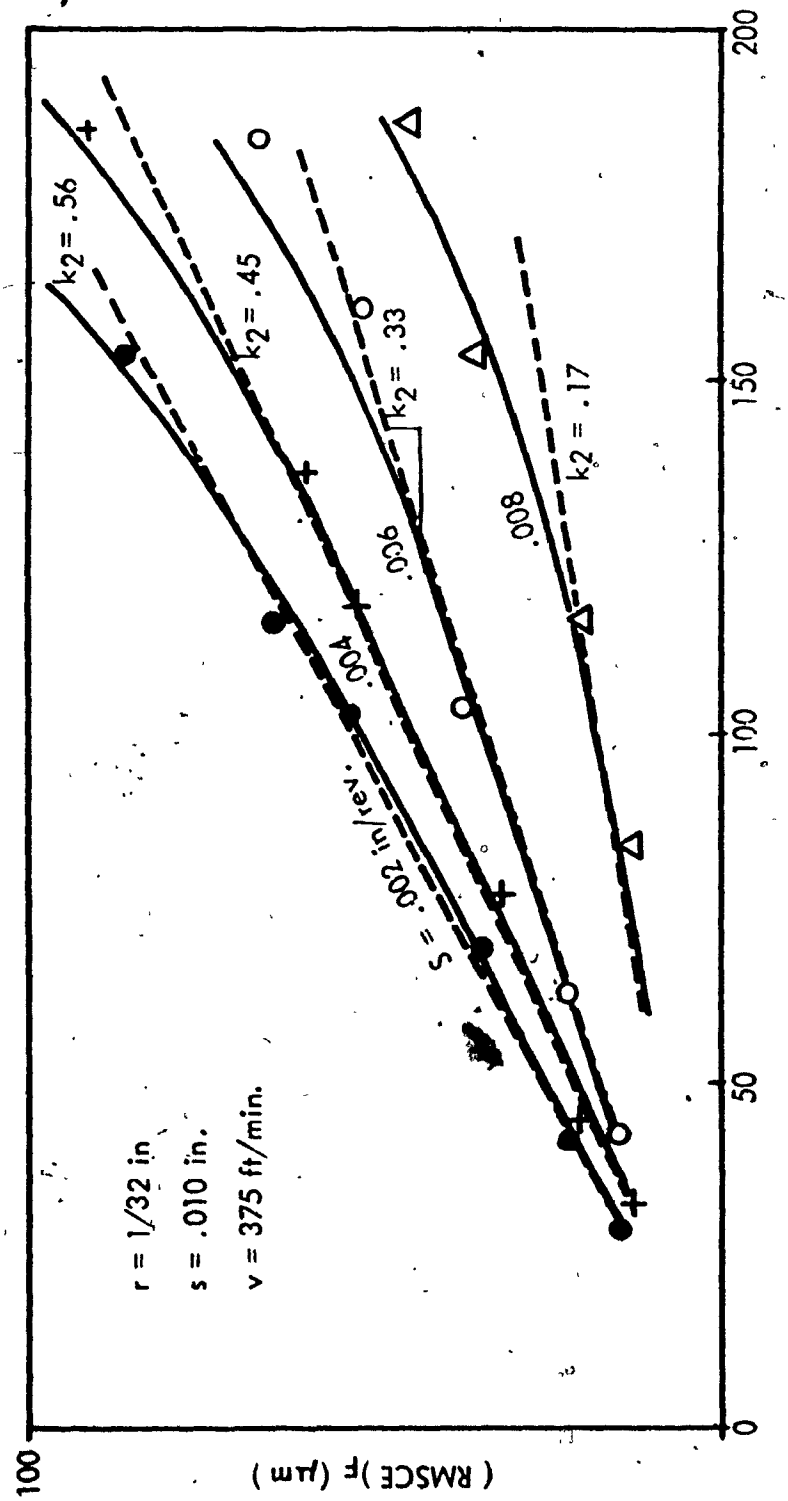

Figure 7.6 RMS CREST EXCURSION; THE CUTTING FORCE SIGNAL VS. SURFACE ROUGHNESS SIGNAL.

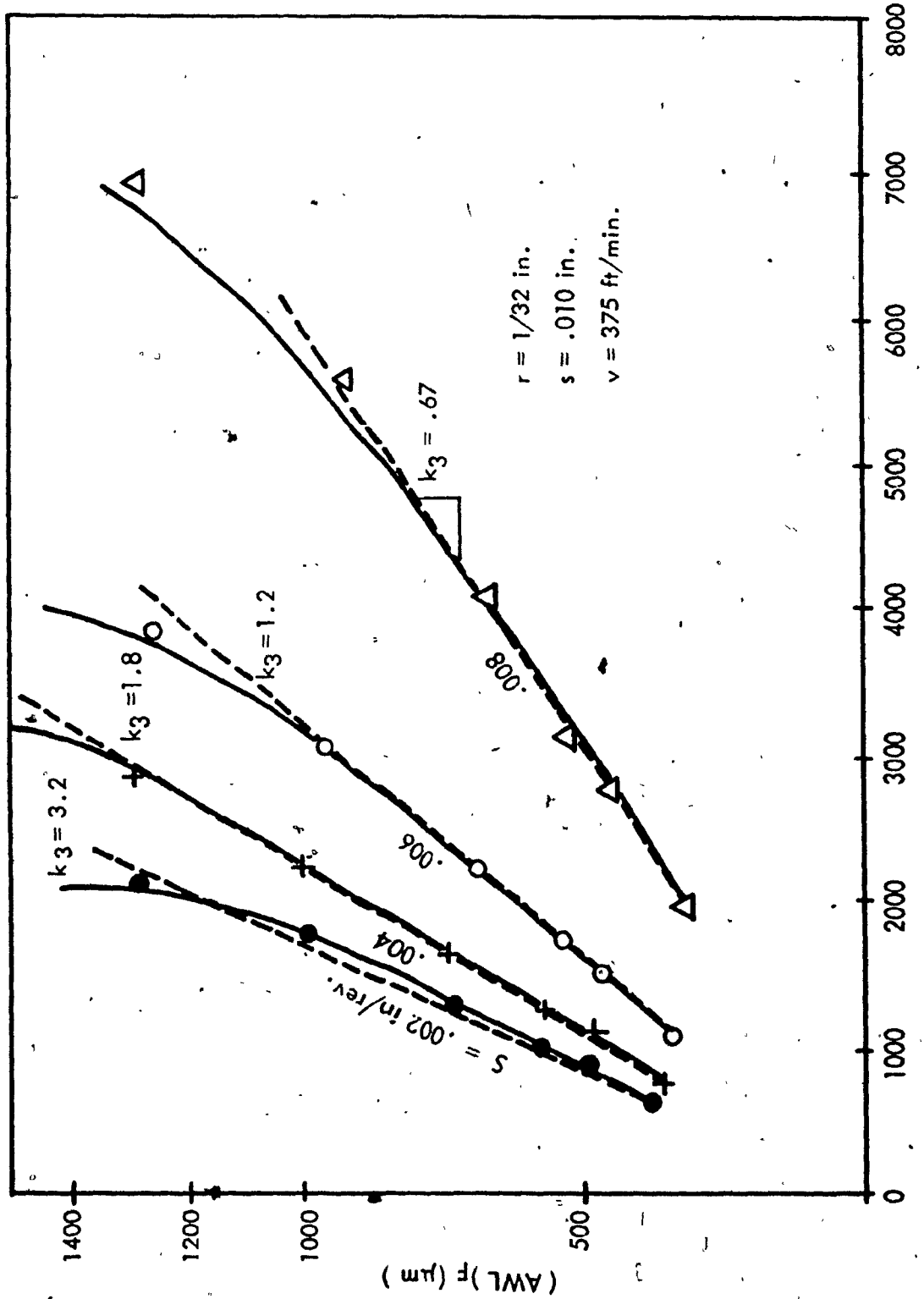

Figure 7.7 AVERAGE WAVE LENGTH OF CROSSING: FORCE AGAINST SURFACE ROUGHNESS.

$$(MCE)_F = k_1(MCE)_S$$

$$(RMSCE)_F = k_2(RMSCE)_S \qquad (7.18)$$

$$(AWL)_F = k_3(AWL)_S$$

where k_1, k_2 and k_3 are certain constants of proportionality and depend on the cutting conditions. From the plots between the excursion parameters of the surface roughness and those for the force fluctuations it may be possible to approximately estimate the values of the constants k_1, k_2, and k_3 for the cutting conditions employed. Such information is presented in Figure 7.8 where k_1, k_2, and k_3 are plotted against the feed rate for a specified tool nose radius.

With these relationships between the cutting force fluctuations and surface roughness it is now possible to select the necessary cutting conditions to produce a desired surface texture on a workpiece, by the following procedure.

Suppose the parameters governing the quality of the surface texture to be manufactured are specified. It is then necessary to determine the cutting force characteristics that would produce such surface texture. The information about the cutting force characteristics can be obtained from the plots 7.3, 7.4, 7.5, 7.6 and 7.7 that relate the stochastic cutting force parameters with the surface parameters. Knowing the cutting force characteristics, the values of the constants k_1, k_2 and k_3 can then be calculated using equation (7.18). With these

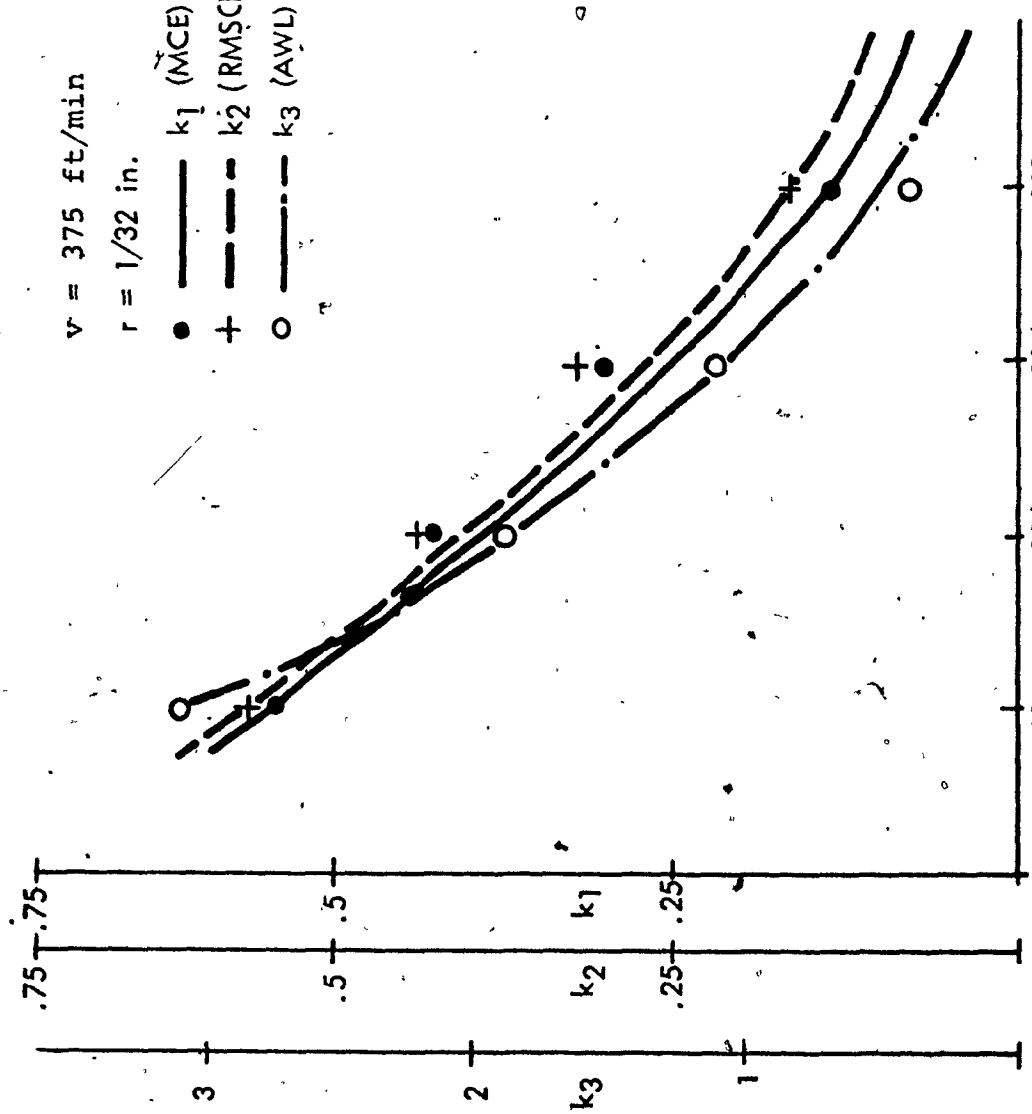

Figure 7.8 PLOT OF PROPORTIONALITY CONSTANT k_1, k_2 AND k_3 AGAINST FEED RATE FOR A 1/32" TOOL NOSE RADIUS.

values of k_1, k_2 and k_3, the approximate cutting conditions to be employed for the specified surface texture may be evaluated from the Figure 7.8.

7.5 Assessment of Surface Roughness from the Cutting Force Fluctuation Characteristics

From the experimental results available it may now be possible to establish definite relationships between the cutting force fluctuations and the resulting surface roughness.

In Chapter 3, an analytical expression for the mean square response of the machine tool system was obtained from the stationary solution of the probabilistic equations which describe the probability response of the system. The CLA-value of the surface roughness thus obtained agreed closely with the actual measured values in the case of finish turning. It was shown that a complex profile of a machined surface can not be fully described with a single parameter like CLA-value. Furthermore, CLA- and RMS-values give only the amplitude characteristics of the surface profile. Further, the mechanical properties such as the bearing capacity, the lubricability, the wear and corrosion resistance depend directly on the values of MCE, RMSCE, AWL etc.

Since it is difficult to measure the tool-workpiece response close to the cutting zone, the possibility of deducing the stochastic parameters MCE, RMSCE, and AWL of the surface roughness directly from the corresponding values of the cutting

force is explored in this section. Also, an attempt is made on the possibility of deducing the CLA-value and variance of the surface profile directly from the corresponding cutting force values. If direct empirical relationships between these quantities that describe the forces and surfaces are established, then the necessity of estimating the CLA-value from the stochastic response of the tool-workpiece system does not arise.

The CLA-values of the forces computed by the analysis program are plotted against the measured CLA-values of the machined surfaces as shown in Figure 7.3. They show that the CLA-value of the surface profile increases progressively with an increasing CLA-value of the force and then becomes asymptotically constant. This means that fluctuations of the cutting forces may continue to increase with variation in cutting conditions but the CLA-value of the surface would asymptotically approach a maximum value and stay at this constant level. The reason for this may be attributed to the elastoplastic strain energy consumed during the formation of the chip and the damping present in the machine tool system. The variance of the cutting force and that of the surface fluctuations are also plotted against each other and this is presented in Figure 7.4. This plot indicates a similar nonlinear relationship. From these plots it would then be possible to deduce directly the CLA-value

and variance of the surface roughness if the corresponding values for the force are known by experimental measurements for all cutting conditions employed.

CHAPTER 8

THE EFFECT OF CUTTING SPEED AND TOOL WEAR ON THE CUTTING FORCE FLUCTUATIONS AND SURFACE ROUGHNESS FORMATION IN FINISH TURNING

CHAPTER 8

THE EFFECT OF CUTTING SPEED AND TOOL WEAR ON THE CUTTING FORCE FLUCTUATIONS AND SURFACE ROUGHNESS FORMATION IN FINISH TURNING

8.1 Effect of Cutting Speed on Cutting Force Fluctuation and Surface Roughness Formation in Finish Turning

The cutting speed in a finish turning operation is chosen on the basis of the tool material and the workpiece material to be machined. Usually, a range for this cutting speed is specified at which a surface finish of reasonable quality and dimensional accuracy is obtained with a minimum tool wear. In the present investigation, a carbide tool was used to machine a workpiece of AISI 1015 steel. For this combination of tool and workpiece material, it has been found experimentally that a cutting speed of 300 - 400 ft/min. is to be used for a good quality finish.

To investigate the effect of the range of cutting speeds on the surface roughness, metal cutting experiments were carried out at two different cutting speeds — 375 and 300 ft/min, with similar feeds and tool nose radii. Surface roughness parameters obtained with 375 ft/min. cutting speed are shown in Figure 6.18 and Table 2 to 5 (Appendix III).

Similar analysis was carried out on the cutting force and surface roughness signals obtained with a 300 ft/min. cutting speed. The CLA-values of the surfaces computed analytically

from the cutting conditions and the tool-workpiece response are found to agree within 8% of the corresponding CLA-values calculated for cutting speed of 375 ft/min. The measured CLA-values at 300 ft/min. cutting speed were also found to agree within 10% of those measured during tests at 375 ft/min. This closeness of the CLA-values calculated at these two different speeds and their non-dependency on cutting speeds may be seen clearly from Figure 8.1. It was also found that there is negligible change in RMS-values of the cutting force and surface signals obtained at these two different cutting speeds.

In Chapter 7, an analysis of the cutting force and surface signals obtained at the cutting speed of 375 ft/min. is carried out to compute the excursion parameters. It was then undertaken to investigate whether there exists any significant variation in the excursion parameters of the cutting forces and the surface roughness profiles obtained at cutting speeds of 375 and 300 ft/min. For this purpose, the force and surface signals recorded for 300 ft/min. cutting speed tests were also analyzed with the analysis program described in Chapter 7. Results show that the excursion parameters of the cutting force and surface signals obtained with a 300 ft/min. cutting speed do not differ from those obtained for a 375 ft/min. cutting speed.

Since the amplitude characteristics and the excursion parameters of the cutting force and surface texture do not show

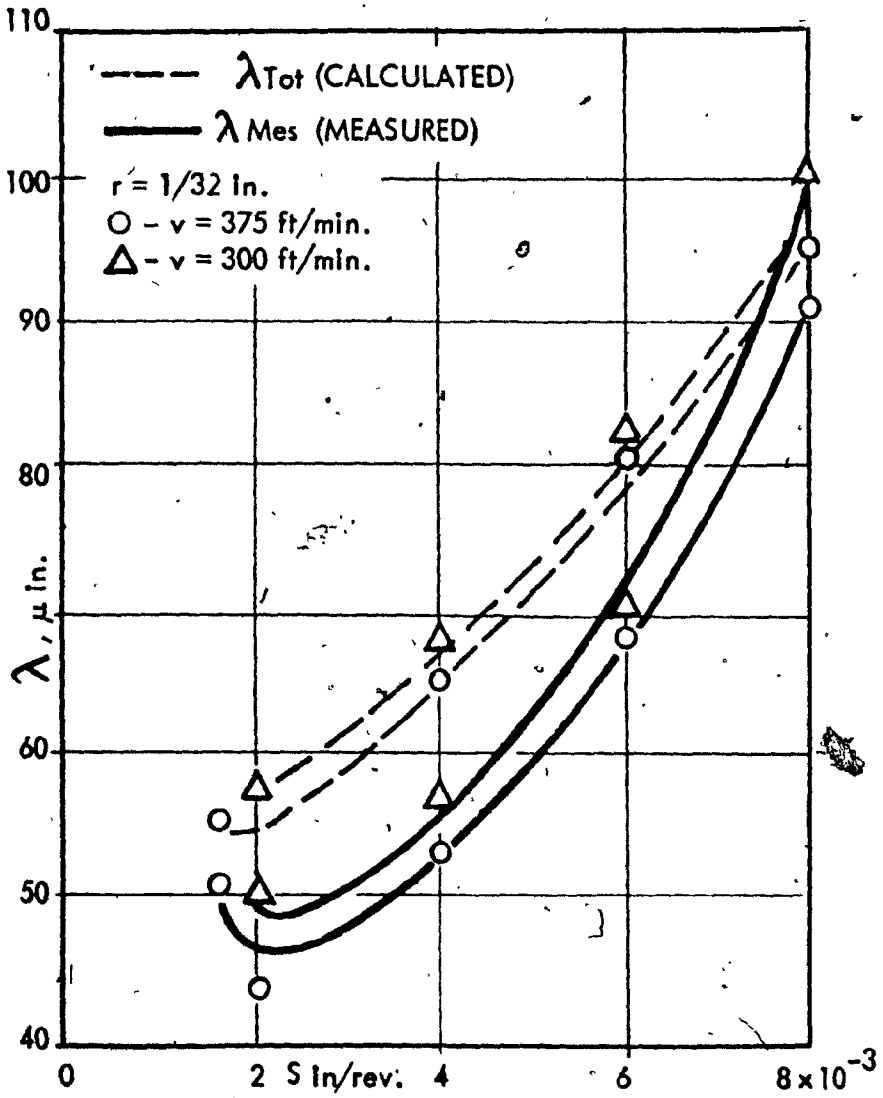

Figure 8.1 COMPUTED AND MEASURED SURFACE ROUGHNESS FOR DIFFERENT CUTTING SPEEDS.

any appreciable variation in the tests performed at two different cutting speeds, it is then reasonable to state that the cutting speed specified for a finishing operation do not affect the cutting force fluctuations and surface roughness characteristics.

8.2 The Effect of Tool Wear on the Cutting Force Fluctuations and the Formation of Surface Profiles in Finish Turning

In any metal cutting process, the tool undergoes gradual wearing after each cut. In a finishing operation, a tool is considered to be worn out when the CLA-value of the surface roughness of the machined component suddenly increases to a relatively high value under the same cutting conditions.

Investigations were carried out to find the effect of a limited tool wear, however small, during a finishing operation, on the cutting force fluctuations and the surface roughness characteristics. For this purpose, the finish machining tests that were performed and reported in earlier chapters were repeated a few times using the same tool and the same cutting conditions. The cutting force fluctuations and the surface profile parameters obtained for each test were compared with the results obtained from the initial cutting tests when the tool used was a freshly ground one.

The cutting force fluctuations and the surface roughnesses produced in each successive test, using tools with increasing wear, were recorded and analyzed. Results indicate that there

is no appreciable change in the amplitude characteristics and the excursion parameters of the cutting force and surface signals obtained each time. Hence, it can be argued that a limited tool wear, that is acceptable for finish machining, does not have any appreciable effect on the cutting force and the surface profile stochastic descriptions.

CHAPTER 9

DISCUSSION OF RESULTS, CONCLUSIONS AND RECOMMENDATIONS FOR FUTURE RESEARCH

CHAPTER 9

DISCUSSION OF RESULTS AND CONCLUSIONS

In this thesis, the influence of the random metal cutting forces on the quality of the machined surfaces in finish turning is investigated in detail through an analytical approach and supporting experimental observations. Direct relationships are established for defining stochastic character of the surface profile from a knowledge of the cutting force statistics.

It is attempted in this investigation to show that it is possible to have a reasonably good estimate of the surface texture from the dynamic response of the tool-workpiece system and the cutting conditions used. The dynamic response of the tool-workpiece system is responsible for the random or fundamental roughness and is computed from the probabilistic equations of motion of the machine-tool-workpiece system. On the other hand, cutting conditions such as feed, tool nose radius etc. affect the basic or theoretical roughness of the surface and this roughness component can be calculated using the empirical relationships given in Chapter 4. The total surface roughness so obtained describes the amplitude characteristics of the profile of the finished part. To describe a surface along its length direction, the stochastic excursion parameters are employed. Experiments were carried out to support the

validity of the mathematical model proposed and to establish approximate relationships between the cutting force fluctuation characteristics and the surface texture produced.

9.1 Discussions of Results

From the analytical results and the corresponding experimental investigation on the influence of the cutting forces on the character of the machined surfaces in finish turning, the following observations may be made:

The cutting forces exhibit random fluctuations and the degree of randomness increases with tool nose radius and feed. The dominant frequency components of the cutting forces are in the range of 600 to 3000 Hz with significant amplitudes identified in the frequency analysis diagram presented in Figure 6.2. The spectral density analysis of the cutting forces indicate a reasonably flat spectrum over the frequency range measured with fluctuation present up to 200 Hz. The spectral density varied from 1 g^2/Hz to .1 g^2/Hz in the frequency band of 50 to 200 Hz and from .1 g^2/Hz to .05 g^2/Hz between 200 to 3000 Hz. The probability density distribution of the cutting forces show clearly a Gaussian character. The surface texture measured on the test specimen shows dominant frequencies in the region 100 to 1000 Hz with the absence of any higher frequencies. The maximum spectral density variation was noted as 10 g^2/Hz to .0001 g^2/Hz in the frequency range of 100 to 1000 Hz. The amplitude density analysis of

the surface roughness also shows a Gaussian distribution.

The fundamental or the random component of the surface roughness calculated from the equations of motion of the tool-workpiece system gives an RMS-value of 70 to 75 μin at a feed of .002 in/rev and different tool nose radii. This RMS-value increased with increase in feed up to .006 in/rev and remained steady thereafter.

The CLA-values of the surface texture calculated from the fundamental roughness (given by the tool response) and the theoretical roughness (given by the cutting conditions) were found to be slightly higher than the CLA-values measured directly on the workpiece. The discrepancies between the analytical CLA-value and the experimental CLA-value were of the order 4 to 7 μin for all feed rates and tool nose radii employed. This indicates that a reasonable deduction of the quality of the surface can be made analytically if a knowledge of the cutting forces were available.

The plots describing the excursion parameters of the cutting force fluctuations against the corresponding parameters for the surface texture show approximately linear relationships. For mean crest excursion the linearity can be extended to a value of 140 μm MCE of the cutting forces or up to 250 μm of the surface undulation for 1/32 in tool nose radius and .002 in/rev feed. These results are not considerably altered by changes in feed and tool geometry. In the RMSCE plots such

linear approximations were valid up to 60 μm for cutting forces or 140 μm for surface texture.

The cutting forces in a metal cutting operation are mainly governed by the workpiece material and the cutting conditions employed. It may be interesting to observe whether a knowledge of the quality of the surface to be produced could be obtained directly from the cutting conditions used. This requires that the influence of the cutting conditions on the cutting forces be evaluated.

The cutting conditions in a turning operation are normally specified in terms of feed rate, tool geometry, cutting speed, etc. The cutting forces are expected to be considerably affected by a variation in any one of these cutting variables.

It was observed in the present investigation that the characteristics of the cutting force fluctuations in finish turning do vary considerably with the feed and the tool geometry. The variation in the cutting speed seemed to have negligible influence on the cutting force properties.

Results presented show that the CLA-values of the cutting forces increase with an increase in the tool nose radius or with an increase in the feed rate. On the other hand, the excursion properties of the cutting force signals do not change significantly with an increase in feed rate or in tool

nose radius. This indicates that for a particular workpiece material, the cutting conditions, namely, feed rate and tool geometry, affect the amplitude fluctuations of the cutting force but do not have appreciable influence on the excursion properties.

Results obtained for the surface roughnesses, also, show that the stochastic characteristics of a surface texture vary with the feed rate and the tool geometry. It is found that with an increasing feed rate, the CLA-values of the surface roughnesses also increase, whereas the CLA-values decrease with an increasing tool nose radius.

It is now proposed that similar exhaustive investigations be carried out for different machining processes under various cutting conditions and workpiece materials. From these experimental data, it may then be possible to establish a library of information on the cutting force fluctuation characteristics and the corresponding surface roughness parameters for specified cutting conditions. A quantitative analysis of this information will lead to a set of graphs as those presented in Figures 7.3 to 7.8 which would yield approximately the expected quality of the surface finish from the cutting conditions employed. Conversely, in order to obtain a surface finish of a specified quality, it would then be possible to recommend, through these libraries of plots, the appropriate cutting conditions to be employed for a given machining process and a specific workpiece material.

9.2 Conclusions

The following specific conclusions may be drawn from the experimental results for a finish turning:

i) The cutting forces in a finish turning operation are basically random in nature.

ii) The frequency range of the cutting forces is 1 KHz to 3 KHz.

iii) The surface texture produced is also random and its frequency range is much lower than that of the cutting forces and is of the order 200 Hz to 1kHz.

iv) The probability distribution of the cutting force and surface roughness amplitudes show that they are Gaussian in nature.

v) The spectral analysis of the cutting forces indicate that they are of wide band nature. Hence, the cutting forces may be represented as an almost white noise type of excitation in the mathematical model for the tool-workpiece system as proposed in Chapter 4.

vi) The results of excursion analysis of the force and surface signals indicate approximate linear relationships between the probabilistic parameters of the surface roughness and the cutting force fluctuations in a finish turning operation.

9.3 Limitations of the Present Work and Recommendations for Future Research

The basic purpose of this investigation is to understand the effect of cutting forces on the formation of surface texture during a metal cutting operation. It is shown how the tool workpiece response, which in turn depends on the dynamic nature of metal cutting forces, influences the surface texture of a workpiece. The tool-workpiece response is obtained from the probabilistic equations of motion of the machine-tool-workpiece system and is derived on the assumption that the random cutting forces are stationary with a Gaussian distribution. Such stochastic description for the cutting forces is justified only in the case of finish turning or grinding operation. But for rough turning processes and for milling, the cutting forces may be expected to be non-stationary and non-Gaussian. To apply the mathematical model developed here to all types of machining processes, it is necessary to solve for the response of the system under non-stationary, non-Gaussian forcing function. This will be mathematically complex.

It may also be noticed that, in the analytical approach, the machine-tool-workpiece is modelled as a two degree-of-freedom uncoupled system. Even though this might be an improvement over a single degree-of-freedom system and distinguishes the flexural action of the cutting forces from the

torsional action, it can be argued that a more effective mathematical model might be able to give accurate description of the responses in all the principal modes of vibration. On the contrary, the mathematical complexities introduced may not justify the improvement in the results based on a multi degree - of-freedom system. A further improvement to the two degree - of-freedom system proposed here may be in a better representation of the dimensions and rigidities of the spindle-workpiece unit and including the effect of tool mounting.

It is observed that the accuracy on the estimate of a surface texture obtained from the tool-workpiece response is within ±10% of the experimentally measured surface roughness. This accuracy could be improved if the transform characteristics of the system, especially at the tool-workpiece interface, are exactly known. In order to achieve this, a complete understanding of the complex thermodynamic process involved during shearing metal and a knowledge of the actual elastoplastic deformation process of the workpiece material are required. This information is not available at present.

A major approximation in the analytical investigation presented is the concept of representing the spectral density of the cutting forces by an equivalent constant white noise-spectral density that would produce a similar response of the system. Effectively, this is to say that the cutting forces are taken as a wide band random process with a delta

correlation. Although this can be interpreted as a limiting case for the cutting forces, the response of the system under the actual conditions can be evaluated using a similar procedure. It may be noted that the cutting tests results show a wide band spectrum for the cutting forces.

There were a few approximations involved in the finish turning experiments conducted in the laboratory due to equipment limitations. Some approximations were also involved in the computer analysis program for calculating the stochastic excursion parameters of the cutting forces and the corresponding surface texture for the experimental data. Because of the minor nature of these approximations, it is reasonable to expect that the results and conclusions reported in this thesis are valid.

A probable application of the results of this investigation lies in the area of control of machine tools in continuous production. If a continuous measurement of the machined surface is obtained through properly designed sensing devices and a corresponding data on the dynamic cutting forces were also continuously recorded, it would then be possible to vary the cutting conditions to produce a desired surface finish employing the information presented in this thesis.

An important future research in this area is to establish directly through detailed analytical and experimental studies the influence of the surface texture descriptors to the mech-

anical properties of the component. Such an investigation will extend the applicability of the results presented in this thesis to have an advanced knowledge of the functional integrity of the manufactured component.

REFERENCES

REFERENCES

1. Tlusty, J., "Die Berechnung des Rahmens der Werkzeugmaschine", Schwerindustrie der Tschechoslowakei, Vol. 1, No. 1, 1955, p. 8.

2. Tobias, S.A. and Fishwick, W., "Theory of Regenerative Machine Tool Chatter", Engineer, London, Vol. 205, 1 58, p. 199.

3. Cook, N.H., "Self-Excited Vibrations in Metal Cutting", Journal of Engineering for Industry, Trans. of the ASME, Series B, Vol. 81, 1959, p. 183.

4. Gurney, J.P. and Tobias, S.A., "A Graphical Analysis of Regenerative Machine Tool Instability", Journal of Engineering for Industry, Trans. of the ASME, Vol. 84, No. 1, 1962, p. 103.

5. Sweeney, G. and Tobias, S.A., "An Algebraic Method for the Determination of the Dynamic Stability of Machine Tools," Proceedings of the International Journal of Research in Production Engineering, Pittsburgh, 1963, p. 475.

6. Merritt, H.E., "Theory of Self-Excited Machine Tool Chatter", Journal of Engineering for Industry, Trans. of the ASME, Series B, 1965, p. 447.

7. Kimball, A.L. and Lovell, D.E. "Internal Friction in Solids", Trans. of the ASME, Vol. 48, 1926, p. 479.

8. Johnson, D.C., "Free Vibration of a Rotating Elastic Body", Aircraft Engineering, Vol. 24, 1952, p. 234.

9. Bishop, R.E.D., "The Vibration of Rotating Shafts", Journal of Mechanical Engineering Sciences, Vol. 1, No. 1, 1959.

10. Kimball, A.L. and Newkirk, B.L., "Internal Friction Theory of Shaft Whirling", General Electric Co. Review, Vol. 27, 1924.

11. Robertson, D., "The Whirling of Shafts", Engineer, London, Vol. 158, 1934, p. 228.

12. Bagci, C., "Torsional, Coupled Torsional and Lateral Vibrations of Shafts and Branched Systems on Non-Uniform Cross-sections by Matrix-Displacement — Direct Element Method", Proceedings of the Third World Congress for the Theory of Machines and Mechanisms, Jugoslavia, Vol.9, 1971.

13. Bickel, E., "Die Wechselnden Kräfte bei der Spanbildung", C.I.R.P. Annalen, 12(4), 1966, p. 206.

14. Field, C.F., "Cross-Correlation and Milling Machine Dynamics — A Case Study", International Journal of Machine Tool Design and Research, Vol. 9, 1969, p. 81.

15. Peklenik, J. and Kwiatkowski, W., "New Concepts in Investigating the Manufacturing Systems by Means of Random Process Analysis", Advances in Machine Tool Design and Research, 1966, p. 683.

16. Caughey, T.K. and Stumpf, H.J., "Transient Response of a Dynamic System under Random Excitations", Journal of Engineering for Industry, Trans. of the ASME, Vol. 83, 1961, p. 563.

17. Hu, P.Y., "Response of Linear Systems to Magnitude Limited Random Excitation", Journal of Engineering for Industry, Trans. of the ASME, 1969, p. 991.

18. Bhandari, R.G. and Sherer, R.E., "Random Vibrations in Discrete Non-Linear Dynamic Systems," Journal of Mechanical Engineering Sciences, Vol. 10, No. 3, 1968, p. 168.

19. Sankar, T.S. and Osman, M.O.M., "Flexural Stability of Machine Tool Spindles under Randomly Fluctuating Cutting Forces", Proceedings of the Third World Congress for the Theory of Machines and Mechanisms, Jugoslavia, Vol. 9, paper G-19, 1971, p. 269.

20. Roberts, J.B., "The Response of Linear Vibratory Systems to Random Impulses", Journal of Sound and Vibration, Vol. 2, 1965, p. 375.

21. Kwiatkowski, A.W. and Bennett, F.E., "Application of Random Force Excitation to the Determination of Receptances of Machine Tool Structures", Proceedings of the International Machine Tool Design and Research Conference, Sept. 1965.

22. Osman, M.O.M. and Sankar, T.S., "Short-Time Acceptance Test for Machine Tools based on the Random Nature of the Cutting Forces", Journal of Engineering for Industry, Trans. of the ASME, Series B, Vol. 94, No. 4, Nov. 1972, p. 1020.

23. Sokolowski, A.P., "Präzision in der Metallbearbeitung", VEB-Verlag Technik, Berlin, 1955.

24. Lambert, H.J., "Two Years of Finish Turning Research", Technological University, Delft, C.I.R.P. Annalen, Vol. 10, No. 4, 1961-62, p. 246.

25. Pesante, M., "Determination of Surface Roughness Typology by Means of Amplitude Density Curves", C.I.R.P. Annalen, Band XII, Heft 2, p. 61.

26. Peklenik, J., "Investigation of Surface Typology", Annals of C.I.R.P., Vol. 15, 1967, p. 381.

27. Nakamura, T., "The Analysis of Surface Roughness Curves (2nd report), Optical Correlators and their Utilization", J. Soc. Proc. Mech., Japan 25 (1959), No. 4, p. 110.

28. Onishy, Y., "New Theory Evaluating Surface Roughness and Its Application", Dissertation, Ehime University (1960), Japan.

29. Spragg, R.C. and Whitehouse, D.F., "A New Unified Approach to Surface Metrology", R.D. Rank Precision Industries Ltd., England, Proceedings of the Inst. of Mech. Engineers, Vol. 185, p. 697.

30. Peklenik, J., "Contribution to the Theory of Surface Characterization", Annals of CIRP, Vol. 12, 1964, p. 173.

31. Sankar, T.S. and Osman, M.O.M., "Profile Characterization of Manufactured Surfaces Using Random Excursion Techniques", submitted to ASME for publication.

32. Opitz, H. and E. Saljé, "Reibwertmessungen an Kunstoffgleitführungen für Werkzeugmaschinen", Industrie-Anzeiger, No. 63, 1952, p. 116.

33. James, H.M., Nichols, N.B. and Phillips, R.S., "Theory of Servomechanisms", M.I.T. Radiation Laboratory Series, Vol. 25, 1947, p. 333.

34. Osman, M.O.M. and Sankar, T.S., "Die Schnittflächenrauheit als Kurzprüfverfahren der Schlichtbarkeit beim Feindrehen, 1. Teil", TZ für Praktische Metallbearbeitung, Vol. 6, June 1970, p. 269.

35. Micheletti, B., vonTurkovich and Rossetto, S., "Three Force Component Piezo-Electric Dynamometer (ITM Mark 2)", International Journal of Machine Tool Design and Research, Vol. 10, 1970, p. 305.

36. Tikhonov, V.I., "The Distribution of the Duration of Excursions of Normal Fluctuations, Non-Linear Transformations of Stochastic Processes", Pergamon Press, 1965.

37. Sankar, T.S. and Xistris, G.D., "Failure Prediction Through the Theory of Stochastic Excursions of Extreme Vibration Amplitudes", Journal of Engineering for Industry, Trans ASME, Series B, Vol. 94, No. 1, 1972, p. 133.

APPENDIX I

CALCULATION OF THE EQUIVALENT VISCOUS DAMPING COEFFICIENT C OF THE TOOL-WORKPIECE SYSTEM

APPENDIX I

Equation (5.5) states

$$\zeta^2 = \frac{1}{4(\frac{\omega}{\omega_1})} \left[(\frac{X_o}{X})^2 - \{1 - (\frac{\omega}{\omega_1})^2\}^2 \right]$$

where ζ is the equivalent viscous damping ratio

ω is the exciting frequency

ω_1 is the undamped natural frequency

X_o is response amplitude at the ratio $\frac{\omega}{\omega_1} \simeq 0$

and X is response amplitude at the exciting frequency of ω.

So, to calculate ζ, the values of ω_1, ω, X and X_o are required. The undamped natural frequency ω_1 can be evaluated from the relationship shown in equation (5.4)

$$\omega_1 = \left(\frac{K_s}{m} \right)^{\frac{1}{2}}$$

where K_s is the static stiffness of the machine tool, and

m is the vibratory mass of the machine tool.

The static stiffness K_s is determined from the frequency response curve as illustrated in Figure 5.16 and found to be 14×10^5 lbs/in.

m is approximated as 210 lbs, which includes mass of the spindle, chuck and workpiece.

Using the values of K_s and m in the equation (5.4) the undamped natural frequency is found to be

$$\omega_1 = \left[\frac{(14 \times 105)}{\left(\frac{210}{386}\right)}\right]^{1/2}$$

$$= 1430 \text{ rad/sec.}$$

Now for an exciting frequency of 200 Hz, the response X from the Figure 5.16. is found to be 9×10^{-5} in and X_o is 4×10^{-5} in. Substituting the values of ω_1, ω, X and X_o in equation (5.5)

$$\zeta = \frac{1}{4\left(\frac{2\pi \times 200}{1430}\right)^2} \left[\left(\frac{4 \times 10^{-5}}{9 \times 10^{-5}}\right)^2 - \left(1 - \left(\frac{2\pi \times 200}{1430}\right)^2\right)^2\right]$$

$$= .14$$

Now, from the relationship

$$\zeta = \frac{c}{c_c}$$

$$= \frac{c}{2m\omega_1}$$

where c is equivalent viscous damping coefficient, and

c_c is equivalent critical viscous damping coefficient.

One can write

$$c = 2m\omega_1 \cdot \zeta$$

$$= 275 \text{ lb in/sec}$$

APPENDIX II

SAMPLE CALCULATION OF THE CLA-VALUE OF THE SURFACE FROM TOOL-WORKPIECE RESPONSE

APPENDIX II

As explained in Chapter 3, to calculate the RMS-value σ_f of surface, it is required to evaluate the mean square response $E[x^2]$ of the tool-workpiece system which in turn needs the value of the integral $\int_{-\infty}^{+\infty} |H(\omega)|^2 \, d\omega$.

Evaluation of $\int_{-\infty}^{+\infty} |H(\omega)|^2 d\omega$:

This integral is expressed in equation (3.44) in which the values of the coefficients A_o, A_1, etc., are calculated as shown below.

$$A_o = \frac{19260(EI)^2}{m_1 m_2 \ell^6} = 31 \times 10^6 \quad /sec^4$$

$$A_1 = \frac{174\ C \cdot EI}{m_1 m_2 \ell^3} + \frac{113\ C \cdot EI}{m_1 m_2 \ell^3} = 185 \times 10^{10} \quad /sec^3$$

$$A_2 = \frac{174\ EI}{m_2 \ell^3} + \frac{4C^2}{m_1 m_2} + \frac{113EI}{m_1 \ell^3} = 11.5 \times 10^8 \quad /sec^2$$

$$A_3 = \frac{C}{m_1} + \frac{C}{m_2} = 3.2 \times 10^8 \quad /sec$$

$$A_4 = 1$$

$$B_o = \frac{174\ EI}{m_2 \ell^3} = 7 \times 10^8 \quad /sec^2$$

$$B_1 = \frac{C}{m_2} = 1.6 \times 10^3 \quad /sec$$

$$B_2 = 1$$

$$B_3 = 0$$

Substituting the values of the coefficients in equation (3.44) it is found that

$$\int_{-\infty}^{+\infty} |H_1(\omega)|^2 \, d\omega = 41 \times 10^{-14} \text{ rad. sec}^3$$

Now, the values of σ_f can be calculated for different values of S_o from equation (4.11). The following table shows the values of σ_f obtained for different feeds and tool nose radius of 1/32 in.

Tool nose radius in.	Feeds in in/rev	S_o in g^2/CPS	$\{E[x^2]\}^{\frac{1}{2}}$ in.	k	σ_f in.
	.0017	.09	81×10^{-6}		73.2×10^{-6}
	.002	.12	86.2×10^{-6}		77×10^{-6}
1/32	.004	.18	112×10^{-6}	.85	96.7×10^{-6}
	.006	.25	123×10^{-6}		108.2×10^{-6}
	.008	.25	123×10^{-6}		110.1×10^{-6}

Table I

Calculation of CLA-value λ_{Tot} of the surface profile:

Knowing the σ_f and σ_{Th}, the CLA-value λ_{Tot} of the surface can be determined from the equation (4.13) for different cut-

ting conditions. A sample calculation for a tool with 1/32" tool nose radius and .0017 in/rev feed is shown below.

To compute λ_{Tot} from the equation

$$\lambda_{Tot} = [.865\ \lambda_{Th}^2 + .640\ \sigma_f^2]^{\frac{1}{2}}$$

the values of λ_{Th} and λ_f are to be obtained from the Figures 6.15 and 6.17 for 1/32 in. tool nose radius and .0017 in/rev feed. These values are found to be

$$\sigma_f = 73.2 \times 10^{-6} \text{ in.}$$

$$\lambda_{Th} = 3 \times 10^{-6} \text{ in.}$$

Substituting these values in the above equation

$$\lambda_{Tot} = [.865 \times (3.0 \times 10^{-6})^2 + .640 \times (73.2 \times 10^{-6})^2]^{\frac{1}{2}}$$

$$= .57 \times 10^{-6} \text{ in.}$$

Similarly, the values of λ_{Tot} for other cutting conditions are computed.

APPENDIX III

TABLES SHOWING CUTTING FORCE AND SURFACE ROUGHNESS STOCHASTIC PARAMETERS AT DIFFERENT LEVELS WITH RESPECT TO CLA-VALUE

r = 1/32 in.

FEED in/rev.	LEVEL	ANC (No. of crossing/ μm)		AWL (μm/crossing)		MCE (μm)		RMSCE (μm)		MVE (μm)		RMSVE (μm)	
		Force	Surface	Force	Surface	Force	Surface	Force	Surface	Force	Surface	Force	Surface
.002	MEAN	.00283	.00152	353.0	656.1	179.3	315.3	93.2	154.7	169.3	315.3	83.2	154.7
	CLA	.0020	.001135	485.4	880.7	111.6	213.6	61.0	116.1	71.3	141.2	86.0	163.6
	1.2CLA	.0018	.000997	558.4	1002.5	96.3	186.0	52.1	101.4	49.2	101.3	73.4	143.2
	1.5CLA	.0013	.000785	722.7	1272.4	72.1	142.8	33.7	69.4	16.7	41.6	39.8	88.3
	1.8CLA	.0010	.000587	990.6	1702.9	51.5	103.9	20.4	42.4	3.5	9.0	14.7	34.0
	2.0CLA	.00079	.000469	1261.9	2129.9	41.3	88.4	14.5	28.5	1.5	4.2	8.6	20.6

A-6

Table 2 · EXCURSION PARAMETERS OF CUTTING FORCE AND SURFACE ROUGHNESS SIGNALS AT DIFFERENT LEVELS WITH RESPECT TO THE CLA-VALUE FOR 1/32" TOOL NOSE RADIUS.

r = 1/32 in.

FEED in/rev.	LEVEL	ANC (No. of crossing/ μm)		AWL (μm/crossing)		MCE (μm)		RMSCE (μm)		MVE (μm)		RMSVE (μm)	
		Force	Surface	Force	Surface	Force	Surface	Force	Surface	Force	Surface	Force	Surface
.004	MEAN	.00283	.001258	352.4	794.5	179.5	380.5	93.1	187.4	169.5	380.5	83.1	187.4
	CLA	.0020	.00091	486.2	1091.5	110.0	249.8	60.4	136.9	69.6	159.3	84.9	192.6
	1.2CLA	.0017	.000796	560.1	1255.2	96.3	219.2	52.0	118.4	49.1	113.4	73.3	167.4
	1.5CLA	.0013	.000615	726.8	1623.4	71.3	162.8	33.2	76.2	15.9	38.1	38.6	90 4
	1.8CLA	.0010	.000449	999.3	2223.1	51.9	121.0	19.8	44.7	3.4	8.6	14.6	35.2
	2.0CLA	.0007	.000353	1276.0	2830.0	41.9	94.6	13.6	32.1	1.5	3.6	8.6	19.7

Table 3 EXCURSION PARAMETERS OF CUTTING FORCE AND SURFACE ROUGHNESS SIGNALS AT DIFFERENT LEVELS WITH RESPECT TO THE CLA-VALUE FOR 1/32" TOOL NOSE RADIUS.

r = 1/32 in.

FEED in/rev.	LEVEL	ANC (No. of crossing/ µm)		AWL (µm/crossing)		MCE (µm)		RMSCE (µm)		MVE (µm)		RMSVE (µm)	
		Force	Surface	Force	Surface	Force	Surface	Force	Surface	Force	Surface	Force	Surface
.005	MEAN	.00289	.000911	345.6	1096.9	166.5	528.9	81.4	258.5	166.5	528.9	81.4	258.5
	CLA	.0021	.000662	470.4	1509.6	109.2	342.8	59.9	188.3	70 3	217.5	84.1	264.5
	1.2CLA	.0018	.000575	538.7	1737.3	96.5	299.9	52.3	162.2	51.1	153.5	74.0	228.6
	1.5CLA	.0014	.000444	691.6	2250.2	72.2	224.9	34.4	104.7	18.3	52.3	41 7	124.4
	1.8CLA	.0010	.000323	938.5	3086.8	52.5	163.4	20.8	62.1	3.9	11.2	15 9	46.8
	2.0CLA	.0008	.000254	1186	3934.7	43.1	133.1	14.4	42.0	1.8	5.1	9.3	27.5

Table 4 EXCURSION PARAMETERS OF CUTTING FORCE AND SURFACE ROUGHNESS SIGNALS AT DIFFERENT LEVELS WITH RESPECT TO THE CLA-VALUE FOR 1/32" TOOL NOSE RADIUS.

$r = 1/32$ in.

FEED in/rev.	LEVEL	ANC (No. of crossing/ μm)		AWL (μm/crossing)		MCE (μm)		RMSCE (μm)		MVE (μm)		RMSVE (μm)	
		Force	Surface	Force	Surface	Force	Surface	Force	Surface	Force	Surface	Force	Surface
.008	MEAN	.00284	.000574	350.9	1739.3	167.3	731.2	82.8	410.6	167.3	731.2	82.8	410.6
	CLA	.00206	.000415	483.5	2408.3	110.1	541.5	60.3	297.2	70.0	341.1	84.9	418.0
	1.2CLA	.00179	.000359	556.8	2779.0	95.0	470.4	51.5	253.9	48.1	236.4	72.3	357.3
	1.5CLA	.001385	.000276	721.9	3617.1	71.1	349.8	33.2	161.7	16.0	75.9	38.7	186.9
	1.8CLA	.001008	.000200	991.6	4992.0	51.8	249.5	19.8	97.2	3.5	15.9	14.7	68.9
	2.0CLA	.000790	.000156	1265.2	6392.6	41.9	203.5	13.6	66.2	1.5	7.4	8.6	41.0

Table 5 EXCURSION PARAMETERS OF CUTTING FORCE AND SURFACE ROUGHNESS SIGNALS AT DIFFERENT LEVELS WITH RESPECT TO THE CLA-VALUE FOR 1/32" TOOL NOSE RADIUS.